THE ROLE OF PLEIOTROPHIN AND MICRORNA-150 IN FETAL LUNG DEVELOPMENT AND FUNCTIONS

By

TINGTING WENG

Bachelor of Sciences

University of Science & Technology of China

2003

Submitted to the Faculty of the Graduate College of the
Oklahoma State University in partial fulfillment of the
requirements for the Degree of
DOCTOR OF PHILOSOPHY
December, 2009

THE ROLE OF PLEIOTROPHIN AND MICRORNA-150 IN

FETAL LUNG DEVELOPMENT

AND FUNCTIONS

Dissertation Approved:

Dr. Lin Liu

Dissertation Adviser

Dr. Michael Davis

Dr. Lara Maxwell

Dr. Guolong Zhang

Dr. A. Gordon Emslie

Dean of the Graduate College

.

ACKNOWLEDGMENTS

This dissertation is the summary of my Ph.D. research. During my studies, I got a lot of help from various people and from the school. I have to say, without their help and support, I cannot get all these done.

First, I would like to convey my gratitude to my major advisor, Dr. Lin Liu. He gave me a great opportunity to pursue my research goals and provided constructive advice, which is helpful not only to my study but also to my life. His great personality, good research attitude, confidence and diligence also deeply influenced me. I would like to take this opportunity to convey my deep sense of appreciation for his constant encouragement and technical help, which enabled me to perform better and be more confident.

I would like to sincerely express my deep sense of gratitude to Drs. Michael Davis, Lara Maxwell, and Guolong Zhang for kindly being my committee members. Their gave me critical suggestions on my research project, which enabled me to better design new experiments and answer the biological questions in a better way. Their encouragement gave me confidence and a healthier attitude on the research.

I would like to convey my gratitude to Drs. Charlotte Ownby and Kenneth Clinkenbeard for their help and support for graduate students. They made a great effort on the presentation preparation and course selection. I really appreciate Drs. Ownby's affection and care for the international students. I also would like to thank Diana Moffeit and Paula Seales for their friendliness and wiliness to help whenever we needed.

I appreciate and thank Drs. Melanie Breshear and Nick Cross for their valuable suggestions on taking pictures and pathology studies.

I spent six years in a friendly but conscientious laboratory, which well prepared for my future career. I would like to specially thank Drs. Deming Gou and Nili Jin who had helped me in a great way during my early stages of research career. I owe my deep sense of gratitude to them for helping me to build up my characters, teaching me the right attitude of doing research, and imparting me the sense of cooperation and the importance of helping each others.

I thank my senior colleagues, Drs Jiwang Chen, Zhongming Chen, Pengcheng Wang, Li Gao, Honghao Zhang, Kexiong Zhang, Xi Dong, Chaoqun Huang for their help and suggestions on my research. They generously shared their experience which improved my techniques and quality of research. I want to convey my appreciation to Drs Narendranath Reddy Chintagari, Telugu Narasaraju and Narayanaperumal Jeya Parthasarathy for their critical suggestions and support. Narendranath is always willing to help others and never feels tired of that.

.

I appreciate and convey my heartfelt thanks to Yujie Guo, Yang Wang and Lijing Su for their help and care from the deep heart. Although younger than me, Yujie gave me the most support on my project and his valuable insights on experiment design extensively improved the quality of my studies. Yang's seriousness on the research deeply impressed me. Lijing is not only a lab colleague, but also one of my sisters and friends who help me in times of need. I also want to thank Manoj Bhaskaran, Pradyuamna Baviskar, and Amarjit Mishra for their help and encouragement in the lab. I have to say, they bring a lot of fun in the lab. Manoj always knows how to make the others happy and he was always willing to cheer us.

I would like to acknowledge Drs. Charmaine Naidoo, Zhixin Wang, Peng Sun and Hong Ma. As lab managers and technicians, they helped to keep the lab clean and well organized, and to order reagents and general lab supplies. Without their help, my research cannot go so smoothly. I would also want to thank Ms. Candice Marsh, Tisha Posey and Dr. Heidi Stricker for their support for the lab.

I would like to sincerely acknowledge Center for Veterinary Health Sciences for providing me the opportunities to pursue my Ph.D. study and to prepare my dream of being a research scientist. The center also offered me two student seed grants, which gave me the needed grant writing experience and enabled me to improve the quality of my research work. I also want to thank the American Heart Association for providing me with a two-year predoctoral fellowship.

I am lucky to have a lot of friends at University of Science and Technology of China and Oklahoma State Uinversity, who give me continuous support. They helped me to overcome the difficulties and to move on with more courage.

At last, I owe my deep sense of gratitude to my dear parents, Xinjun Weng and Miaoshi Shu, brothers Rongrong Weng, sister-in-laws Aihua Wang. They unselfishly gave all encouragement and support they could whenever I needed. They are the only ones who think about me more than themselves. They shared not only the happiness but also the pain with me. Any words are not enough to express my sincere appreciation to them. I could only say, without their encouragement and affection, I could not complete the current project.

TABLE OF CONTENTS

Chapter Page

LIST OF TABLES

Table Page

LIST OF FIGURES

ABBREVIATION

Actg2	γ-enteric muscle actin
Acvrl1	Activin A receptor type II-like-1
AD	adult
Adh1	alcohol dehydrogenase 1
Adh3	alcohol dehydrogenase-3
AEC I	alveolar epithelial type I cells
AEC II	alveolar epithelial type II cells
ALK	anaplastic lymphoma kinase
Aqp8	Aquaporin 8
Bmp4	bone morphogenetic protein 4
BzATP	3'-O-4-benzoylbenzoylATP
CC10	Clara cell 10KD protein
CFTR	cystic fibrosis conductance transmembrane regulator
ChIP	16 Chromatin Immunoprecipitation
CNND1	cyclin D1
csrp3	cysteine-rich protein 3
DAG	diacylglycerol
DGCR8	DiGeorge syndrome critical region gene-8
Dlk1	Delta-like homolog Drosophila 1
DMEM	Dulbecco's Modified Eagle Medium
DSFM	chemical defined serum-free medium
EB	ethidium bromide
ECM	extracellular matrix
EGF	epidermal growth factor
EMT	epithelial-mesenchymal transition
Eph	Ephrin
ESTs	expressed sequence tags
fAEC II	fetal alveolar epithelial type II cells
FGF10	fibroblast growth factor 10
FGFR2	fibroblast growth factor receptor 2
FGFs	Fibroblast growth factors
FL	Firefly luciferase
fzs	frizzleds
GDNF	glial cell-derived neutrophoic factor
GSK-3β	glycogen synthase kinase-3 beta
HBSS	Hanks' balanced salt solution

Hes	hairy and enhancer of split
HFH-4	HNF-3/forkhead homologue-4
hmg1	High-mobility group 1
HNF-3β	hepatocyte nuclear factor-3β
Hsd11b1	11-β Hydroxysteroid dehydrogenase type 1
IL-1β	interleukin-1beta
IP3	inositol trisphosphate
IPF	idiopathic pulmonary fibrosis
KGF	Keratinocyte growth factor
LAM	lymphangioleiomyomatosis
Lhx3	LIM homeodomain protein 3a
Ltbp1	Latent TGF-β-binding protein-1-like proteins
Ltbp2	Latent TGF-β-binding protein-2-like proteins
miRNA	MicroRNAs
Mist1	Intestine and stomach expression 1
MK	Midkine
MOI	Multiplicity of Infection
Myo1b	Myosin Ib
NB	and newborn
Nelf	nasal embryonic LHRH factor
Nf2	Merlin
P2XR	P2X receptors
P2YR	P2Y receptors
PC	phosphotidylcholine
PDGF	Platelet-derived growth factor
PG	phosphatidylglycerol
Pla2g1b	Phospholipase A2 group 1b
pri-miRNAs	miRNAs primary transcripts
PSMC	parabronchial smooth muscle cells
Ptc	Patched-1
ptgs2	Prostaglandin-endoperoxide synthase 2
PTN	Pleiotrophin
PTN-/-	PTN knockout
PTN+/+	PTN wild-type
RA	retinoid acid
RISC	RNA-induced silencing component
RL	*Renilla* luciferase
RPTPZ1 β/ζ	protein tyrosine phosphatase receptor β/ζ
SAM	significance analysis of microarray
Shh	Sonic Hedgehog
siRNA	small interfering RNA
SP-A	surfactant protein A
SP-B	surfactant protein B
SP-C	surfactant protein C
SP-D	surfactant protein D

Sycp1	synaptonemal complex protein 1
TBS	Tris-Buffered Saline
TGF-β	transforming growth factors
Tnni2	troponin I
Tnni3	cardiac troponin I
TTBS	Tris-buffered saline containing 0.05% Tween 20
TTF-1	thyroid transcription factor-1
VEGF	vascular endothelial growth factors
α-SMA	alpha smooth muscle actin

CHAPTER I

INTRODUCTION

1.1 Fetal lung development

1.1.1 Five stages of fetal lung development

Fetal lung development is a complex biological process which includes temporal and spatial regulation of multiple factors, such as growth factors, transcriptional factors and extracellular matrix (ECM). The development of the intimate relationship between airways and blood vessels is of crucial importance to the normal lung function. Morphologically, the rat lung development can be divided into 5 stages: Embryonic Stage (embryonic day 11.5 (E11.5) to E13), Pseudoglandular Stage (E13 to E18), Canalicular stage (E18 to E20), Sacular Stage (E20 to New born) and Alveolar Stage (New born to adult) (18; 25).

During the embryonic stage, the lung buds first originate as a diverticulum from the foregut endoderm and gradually grow into the surrounding mesoderm, which forms a bifurcate tube composed of highly columnar epithelium (18). After one or two generations of successive bifurcate division, the lung forms a tubulo-acinar gland.

The pseudoglandular stage in rat starts on embryonic day 13 and lasts for 5 days. This stage is marked with repeated dichotomous branching which establish almost all the geometric pattern of the conducting airways (13). The branching morphogenesis during this stage is achieved by inducing the bud from the outmost periphery of the epithelial tubes. As the lung originates, the pulmonary arteries bud off from the sixth pair of aortic arches and undergo the branching morphogenesis parallel to the airway tree (18). At this stage, the vascular system is separated from airway conducts by the mesenchyme and the capillaries are loosely lined into the surrounding mesenchyme.

After forming all the conducting airways, in the canalicular stage, several generations of more delicate primary and terminal bronchioles bud from the tips of the main bronchus. These primary bronchioles, together with their surrounding mesenchyme, represent the early acini for gas exchange. Simultaneously, the capillary networks readjust themselves and become more closely aligned with the distal cuboidal epithelium, where they form the early thin blood-gas barrier. However, during this stage, these acini do not have the ability to carry out gas exchange. Another marker of the canalicular stage is the development of the pulmonary epithelium. The columnar epithelial cells which are found typically in the peripheral airways become lowered in shape and change to cuboidal epithelial cells (79). The newly differentiated cells, known as alveolar epithelial type II cells (AEC II), are capable of secreting surfactant, which reduces the surface tension at the air-liquid interface.

The last two stages for the lung development are the saccular and alveolar stages. The beginning of the saccular stage is characterized by relatively thin-walled terminal saccules which are produced by the last generations of branching (18). During the saccular stage, the distal epithelium undergoes substantial enlargement, which results in a significant decrease in interstitial tissue. The epithelium and mesenchyme both become thinner and thinner, which causes the capillary network to further rearrange itself. The capillaries closely accompany the airway epithelium, which results in a significant increase of the saccule vascularity. The epithelial cells are further flattened and differentiated into alveolar epithelial type I cells (AEC I) (79; 140). The AEC I closely line along the capillary endothelial cells to form a thin blood-gas barrier in the intersaccular septa. More surfactants are secreted by AEC II cells. However, compared to the mature lung, the interstitial layer at this stage has much fewer extracellular fibers and the lung only forms less than 10% of the total alveoli (18; 26).

At birth, the lung develops functional sacs and acini which could support adaption to air breathing. However, the lung is not completely mature yet and still needs alveolarization to further increase the gas exchange area. One of the markers of the alveolar stage is repeated growth and separation of thousands of alveoli (19; 52). Elastin is continuously deposited underneath the epithelium to prepare for the generation of the secondary septa (18). The bulging of the new septa separates the original saccules and converts them into alveolar ducts, which gives rise to the new alveoli. The recurring alveolization dramatically increases the surface area for gas exchange. Simultaneously, the relatively thick septa are further attenuated and interstitial tissue is reduced. The capillaries are further rearranged and transformed into a single capillary network in the interalveolar septa, as observed in the mature lung. After completing alveolarization, the pulmonary system is more powerful for gas exchange.

The mouse and human lung development can also be divided into these five stages. The pseudoglandular stage starts from E14 to E16 in mouse and E42 to E112 in human. The

canalicular stage is from E16.5 to E17.5 in mouse and E112 to E186 in human. The saccular stage initiates on E17.5 and to birth in mouse and from E196 to E252 in human. The alveolar stage continues from term to ~P15 in mouse and to until 2 years in humans (74). However, some animals including rabbit, horse and sheep, complete the alveolarization and establish the majority of internal surface area before birth (31; 74).

1.1.2 Alveolar epithelium

The alveolar epithelium is the place where gas exchange occurs. AEC I and AEC II are the major components of distal airway epithelium and aid in the normal respiratory process.

AEC I are large squamous cells covering about 95% of the alveolar surface area. They form the gas-blood exchange barrier and function in gas exchange and fluid transport (49; 72). AEC II are cuboidal and are normally located in the corners of alveoli. They occupy less than 5% of the alveolar surface area (74). AEC I are terminally differentiated and are prone to damage. When this happens, AEC II act as progenitor cells, differentiate into type I cells, and repair the damaged alveolar epithelium. AEC II also synthesize and secrete pulmonary surfactant, a lipid-rich lipoprotein complex that spreads on the surface of alveoli to form a thin lining layer and reduces the surface tension. The surfactant facilitates the normal gas exchange process by reducing the force against lung inflation and keeping the alveoli from collapse. Insufficient amount of pulmonary surfactant leads to abnormal lung functions (43; 143).

Pulmonary surfactant is a heterogenous mixture containing 90-95% lipids and 5-10% proteins. The most abundant lipids are phospholipids, which contribute 80%. The other components of lipids include neutral and some other lipids. The most abundant phospholipids are phosphotidylcholine (PC) and phosphatidylglycerol (PG). PG is the last surfactant to be synthesized during development. The concentration of PG is normally assumed to be a marker of fetal lung maturity.

There are four surfactant proteins: surfactant protein A, B, C and D (SP-A, -B, -C and -D). SP-B and SP-C are hydrophobic proteins, and are packed into storage granules called lamellar bodies together with lipids before secretion (34; 124). The secretion of pulmonary surfactant are regulated by various molecules, such as intracellular Ca^{2+}, P2Y2 receptor agonists (ATP and UTP), adenosine, platelet activating factor, and IL-1 etc (4). SP-A and SP-D are hydrophilic proteins synthesized and secreted independent of lamellar bodies (4; 109). SP-A regulates surfactant secretion (138) and both SP-A and SP-D support alveolar immune defense (142). SP-B and SP-C are important for the dynamic properties of the pulmonary surfactant. Mice deficient of SP-B expression die as neonates because of respiratory failure (24). The mutation of SP-C is associated with interstitial lung disease (16).

1.1.3 Alveolar epithelial cell differentiation

The differentiation of AEC II and AEC I have crucial meanings for the normal lung function. In the pseudoglandular stage, some columnar epithelial cells begin to differentiate into ciliated cells with the expression of β-tubulin IV (100), and some other cells transform into shorter columnar cells containing large intracellular glycogen pools (17). These cells remain undifferentiated until the canalicular stage, when some of the distal epithelial cells become more cuboidal AEC II and begin to synthesize and secrete surfactant. AEC II have less glycogen pools and are characterized by the appearance of lamellar bodies (74). Soon after that, the overlying AEC II are induced to flatten and differentiate into AEC I.

Many transcription factors, including thyroid transcription factor-1 (TTF-1), hepatocyte nuclear factor (HNF)-3β and HNF-3/forkhead homologue-4 *(*HFH-4) have indispensable roles on the epithelial cell proliferation and differentiation. TTF-1, also known as Nkx2.1, is detected as early as E8-E8.5 in mouse endodermal cells and is identified as the earliest known marker of the lung. TTF-1 regulates the expression of all the surfactant protein genes, including SP-A, B, C and D. Mice deficient of TTF-1 have abnormal lungs which fail to express all the surfactant proteins and have significantly reduced collagen type IV and integrins (80).

HFH-4 is expressed in the epithelium during fetal lung development, and in basal and ciliated epithelial cells in the adult lung (129). HFH-4 induces the expression of β-tubulin IV in the pseudoglandular stage, and promotes the differentiation of ciliated epithelial cells.

HNF-3β is highly expressed in ciliated and columnar bronchial epithelial cells and AEC II during development. HNF-3β induces various lung epithelially restricted genes, including TTF-1 (46), SP-B (10) and CCSP (113; 114), in association with the differentiation of lung epithelial cells, including AEC II and Clara cells.

Other transcription factors, such as GATA-5, GATA-6, and Fox proteins are also important for the cell differentiation in the lung (70). The expression of these transcription factors decreases with the progression of development and is only restricted in subsets of Clara cells and AEC II at the late stage of development.

1.1.4 Epithelial-mesenchymal interactions

The interactive signaling between epithelial and mesenchymal cells is important for normal growth, morphogenesis, and cell differentiation in the developing lung. Removing the mesenchyme from the embryonic lung rudiment impairs the branching morphogenesis (35; 118). Lung mesenchyme has the capability to induce branching morphogenesis in non-lung epithelium such as salivary gland (57) and embryonic trachea, whose mesenchyme has been removed (2; 137). However, non-lung mesenchyme was only able to induce a bud in gut endoderm and these buds had no further branching (137). Besides its function in determining the epithelial patterning, mesenchyme can also dictate the differentiated phenotype of the epithelium (119).

The mesenchymal regulation of epithelium is mediated by many growth factors. These growth factors are precisely regulated in a temporal and spatial manner during fetal lung development. Fibroblast growth factors (FGFs) and their receptors are among the best characterized growth factors. They have crucial roles in branching morphogenesis, cell proliferation, differentiation, and migration (20). FGF10 is located in the mesenchyme around distal lung epithelial tips. It binds to the fibroblast growth factor receptor 2b (FGFR2b) on the epithelial cells and transmits a signal to induce the initiation of the lung bud (8; 44; 78; 94; 116; 134). Recombinant FGF10 alone can induce budding in the lung epithelial explants whose mesenchyme has been removed (8). Mice deficient of FGF10 or FGFR2b expression have severe abnormalities in lung development (28; 78). Both of these two mice show clear absence of lung, indicating that FGF10 and its receptors are crucial for the initiation of lung development. The expression of FGF10 and bud formation are regulated by retinoid acid as shown by the evidence that antagonist of retinoid acid completely prevents the formation of lung buds from foregut explants (29). Retinoid acid accelerates the development of the alveolar tree and promotes the expression of surfactant proteins and enzymes for the synthesis of surfactant lipids (68).

On the other hand, the pulmonary epithelial cells also influence mesenchymal and vascular cell proliferation and differentiation (100). The epithelial cells express and secrete vascular endothelial growth factors (VEGF). VEGF binds to its receptors, flk and flt in the progenitor cells of the mesenchyme, and at least in part, regulates pulmonary vasculogenesis (148). Similarly, Platelet-derived growth factor (PDGF), which is expressed in the epithelial cells, stimulates the differentiation and proliferation of myofibroblastes in the developing lung (12). Sonic Hedgehog (Shh) is a growth factor expressed in the developing epithelium, most abundantly in terminal buds. Its receptor Patched-1 (Ptc) is located in the mesenchymal cells. The interaction between Shh and Ptc is required for lung bud formation (7; 64; 131). Overexpression of Shh in AEC II with a surfactant protein C (SP-C) promoter disturbs the formation of alveoli by increasing the proliferation of mesenchymal cells, but not epithelial cells (7).

Other growth factors, such as transforming growth factors (TGF-β) and epidermal growth factor (EGF) are also involved in the epithelial-mesenchymal interactions and play essential roles in lung development (55).

1.1.5 Extracellular matrix proteins

Besides growth factors and transcriptional factors, extracellular matrix proteins play an important role in fetal lung development (14; 45; 108). The extracellular matrix proteins include intergrins, fibronectins, laminins, proteoglycans, and cadherins. Laminin is a glycoprotein which promotes the lung branching morphogenesis. Anti-laminin antibodies significantly reduce epithelial cell proliferation and the lung branching formation in fetal lung explant culture (115).

Integrins and fibronectins are essential for cell-cell and cell-extracellular matrix interactions. Fibronectins promotes branching morphogenesis and regulates the symmetry of the branching in cultured embryonic lung explants (108). Integrins and Cadherins are calcium-dependent cell surface glycoproteins responsible for cell-cell adhesion. The ligands of integrins include fibronectins, laminins and collagens. The binding of integrins to their ligands is crucial to regulate the cell proliferation, differentiation and migration, and to maintain the cell polarity during the development (120). Cadherins have several subtypes which are expressed in a spatial and temporal manner during fetal lung development. E-cadherins is expressed in epithelial cells. N-candherin is located in neural and muscle cells. VE-cadherin is present in the endothelial cells. These cadherins are responsible for the epithelial cell adhesion, thereby promoting the sheet and tube formation during branching morphogenesis (73).

1.2 Pleiotrophin

1.2.1 Introduction to Pleiotrophin

Pleiotrophin (PTN) is an 18 kDa heparin-binding cytokine and shares 50% sequence homology with midkine (76). PTN has two beta-sheet domains that bind to heparin and extracellular matrix with high affinity (77). The amino acid sequence of PTN is highly conserved among different organisms (63).

PTN was first identified as a growth factor from bovine uterus (77) and as a neurite outgrowth promoting factor in the neonatal rat brain (106). In comparison with midkine, which is regulated by retinoid acid (51), PTN does not respond to retinoid acid but could be upregulated by PDGF in primary hepatic stellate cells (5). The mRNA expression of PTN is significantly upregulated in some organs in midkine deficient mice, suggesting that PTN and midkine have functional redundancy (40). In fact, PTN and midkine do share multiple functions. They both regulate the neurite outgrowth, play important role in neural development and cancer development, enhance the proliferation, migration, inhibit the apoptosis of various cells, and have important roles in epithelial-mesenchymal interactions during organogenesis (50; 87).

1.2.2 The expression and multiple roles of Pleiotrophin

PTN is expressed in a temporal and cell-type-specific manner in order to precisely restrict its functional activities at the right time and the right site. The expression level of PTN is regulated during development. During the mouse embryogenesis, PTN is highly expressed in central and peripheral nervous systems, in organs undergoing branching morphogenesis (including salivary gland, lung and kidney), digestive and skeletal systems, sense organ and facial processes and limbs (81). The expression of PTN is detected as early as embryonic day 9 and peaks in the late stage of embryogenesis (shortly after birth) (63; 132). PTN is mainly located in the basement membrane of the developing epithelium and in mesenchymal tissues undergoing remodeling,

suggesting that it may regulate cell differentiation and play an important role in mesenchymal-epithelial interactions. In the adult stage, PTN expression is mainly restricted in central nervous system (63; 89).

PTN is highly expressed in the fetal bone cartilage and plays an important role in the bone formation and remodeling (127). During the early stage of osteogenic differentiation, PTN is synthesized by osteocytes and located at sites of new bone formation (47; 127). Exogenous PTN, but not midkine, promotes the chondrogenesis in micromass culture of chicken limb bud mesenchymal cells (32). As a growth factor that stimulates the proliferation and differentiation of osteoblastic MC3T3-EL cells, PTN promotes the bone morphogenetic protein (BMP)-induced osteogenesis at a high concentration. However, PTN has an opposite effect at a low concentration (62; 112). Targeted overexpression of PTN in mice promotes the bone growth and maturation during the early stage of bone development. However, the effect is diminished with advanced age and the generated bones are more brittle compared to the wild type (62).

PTN plays an important role in kidney development. The lung and kidney development involves repeated branching morphogenesis and prominent interactions between mesenchyme and epithelium. In the embryonic kidney, PTN is present in the basement membrane surrounding the developing ureteric bud. Recombinant human PTN increases the branching morphogenesis of cultured uteric bud in the presence of glial cell-derived neutrophoic factor (GDNF) (110). In the absence of GDNF, PTN still has the ability to induce the branching morphogenesis of uteric cells (110). These studies suggest that PTN is one of the key modulators of branching morphogenesis in kidney and maybe in other organisms.

PTN is up-regulated in the injured rat brain cells and plays an role in new tissue formation during the recovery from injury (146). After ischemia exposure, dramatically higher PTN levels have been observed in macrophages, endothelial cells and astrocytes in the mouse brain, especially in the areas with high neovasculogenesis activity, suggesting that PTN may have an important role in the neurovascular formation during development. PTN upregulation is also observed in dermis after an incisional wound in rat skin (30). Additionally, local delivery of PTN in the dog fibrin glue after angioplasty injury significantly increases the rates of re-endothelialization. This effect is mainly due to the stimulation of endothelial cell angiogenesis and promotion of smooth muscle cell proliferation (15). All these studies suggest that PTN plays essential roles in injury repair by promoting tissue regeneration, cell proliferation and differentiation.

The PTN level is much lower in the adult tissue than that in the fetal tissue. However, PTN is overexpressed in a number of cancers, such as human breast cancer (37; 107; 136), melanocytic tumor (117; 144), and glioblastoma (65; 85; 102; 149). As a heparin-binding cytokine, PTN acts as a growth factor to promote cell growth in cells transformed by the v-sis oncogene (77). The function of PTN in tumor angiogenesis has been addressed to some extent. SW-13 cells

transformed by PTN amino acid residues exhibit a much higher growth rate and higher density of microvessels (150). The nude mice injected with PTN transformed NIH 3T3 cells have a higher degree of tumor angiogenesis (22). This effect could be blocked by a dominant negative PTN (151). PTN also increases the endothelial cell proliferation and tube formation, suggesting an important role of PTN as an angiogenic factor during the tumor formation (146). These studies strongly suggest that PTN is a potential target for cancer therapy. Elucidating the function and regulatory pathway of PTN may contribute to the establishment of a new cancer treatment method.

PTN also functions as a mitogen for endothelial cells (30; 146), epithelial cells and different fibroblast cell lines (77). The function of PTN can be extended to some other aspects, such as regulating the long-term potentiation by controlling the neurite cell outgrowth (3).

1.2.3 PTN regulatory pathways

PTN signals through three cell surface receptors, syndecan-3, anaplastic lymphoma kinase (ALK) and protein tyrosine phosphatase receptor (RPTPβ/ζ) (87).

Syndecan-3 belongs to the syndecan family and is a transmembrane protein. Its extracellular domain contains 3 glycosaminoglycan attachment sites (21). The binding of PTN with syndecan-3 induces neurite outgrowth of embryonic neurons (105). Heparitinase, which cleaves heparin sulfate chain and disrupts the binding of PTN, inhibits PTN-induced neurite outgrowth. Anit-syndecan-3 antibodies have a similar effect. Additionally, overexpression of syndecan-3 in N18 neuroblastoma cells significantly increases the PTN-induced neurite outgrowth. The PTN/syndecan-3 pathway is possibly mediated by the c-Src which binds to the intracellulcar domain of syndecan-3 and subsequently alters the activity of cortactin (53).

ALK is a receptor tyrosine kinase highly expressed in the developing nervous systems and some tumor cells (48; 82). It shows a similar expression pattern as PTN in different cell lines (125). Upon the binding with PTN, ALK phosphorylates Ras protein or Akt, and thus activates the Ras-MAPK or the PI_3K-Akt signaling pathway. This sequentially, stimulates cell proliferation and mitogenesis, and inhibits apoptosis (102; 125). However，a recent study has shown that ALK does not directly bind with PTN, but is one of the substrates of RPTPβ/ζ (99).

RPTPβ/ζ is a transmembrane tyrosine phosphatase, which is composed of a cytosoplasmic portion carrying protein tyrosine phosphatase activity, a transmembrane region, and an extracellular domain containing chondroitin sulfate for ligand binding (38). The extracellular part of RPTPβ/ζ also possesses a carbonic anhydrase-like domain, a fibronectin III-like domain, and a glycine-serine rich domain (38). These domains interact with the adhesion molecules and mediate the cell-cell adhesion. PTN is identified as the first natural ligand for the transmembrane

tyrosine phosphatase receptors. It binds to the chondroitin sulfate portion of RPTPβ/ζ with high affinity (69).

In the absence of PTN, β-catenin is associated with E-cadherin. In U373-MG glioblastoma cells, the binding of PTN with RPTPβ/ζ results in the dimerization and inactivation of the receptor and thus significantly increases the tyrosine phosphorylation of β-catenin (75; 97). Phosphorylated β-catenin rapidly dissociates from E-cadherin and accumulates in the cytoplasm. The disassociation of β-catenin from E-cadherin disrupts the cell-cell adhesion and possibly promotes the cell migration. Since β-catenin is the central component of Wnt signaling pathway, it may be a link between PTN and Wnt signaling pathways. However, how these two pathways are associated and whether PTN/ RPTPβ/ζ pathway has a role in fetal lung development are unknown.

Other downstream targets of the PTN/RPTPβ/ζ include β-adducin (92; 93). Recently, the Src family member, Fyn has been identified as another substrate of the PTN/RPTPβ/ζ signaling pathway (91). RPTPβ/ζ is broadly expressed in almost all of human breast cancer cells lines, and it plays an important role in the adhesion and migration of tumor cells (98). Since the PTN pathway through ALK is also mediated through RPTPβ/ζ, the signal through RPTPβ/ζ may be the main regulatory pathway for PTN to regulate cell growth, proliferation, migration, and mesenchymal-epithelial transition (97).

1.2.4 PTN knockout mouse

At least two groups of PTN knockout mice have been generated to investigate the function of PTN. PTN deficient mice are anatomically normal. However, these mice exhibit enhanced hippocampal long-term potentiation (3). Deficiency of PTN results in increased proliferation rate of neuronal stem cells in the adult mouse cerebral cortex (41). This is consistent with the observation that exogenous PTN reduces the neuronal stem cell proliferation through inhibiting the expression of FGF-2 and promotes the cell differentiation (41).

Similarly, midkine knockout mice do not have significant abnormalities (88). However, it shows deficiency in memory due to decreased expression of calretinin in the hippocampus of infant mice (88). Additionally, midkine knockout mice result in decreased neutrophil infiltration after ischemic renal injury (111). Interestingly, midkine knockout mice have increased PTN expression in many organs, including eye, heart, bladder etc., suggesting they may have redundant roles (40).

The few abnormalities shown by PTN or midkine knockout mice seem to be inconsistent with their crucial roles in the proliferation, differentiation and migration of various cells. This may be partly due to the functional redundancy between PTN and midkine. Lack of PTN expression might somehow be compensated by midkine. To test this possibility, some research groups have

produced PTN and midkine double knockout mice. These mice have reduced expression of beta-tectorin and serious auditory deficits (154). Additionally, they have significantly reduced reproduction abilities and exhibit infertility in most female mice (86).

Transgenic mice overexpressing PTN show abnormalities in brain and bone formation and remodeling. PTN overexpressing mice are morphologically normal, but have attenuated hippocampal long term potential (96). Specifically overexpressing PTN in osteoclasts under the control of human osteocalcin promoter increases bone mass in female mice, but not male mice (39; 71). These mice also have advanced bone growth during the early developing stage, damaged fracture healing, and delayed callus formation (62).

PTN also has a high expression during the late stages of fetal lung development. However, its role in the lung development has never been studied. Additionally, PTN expression in the lung is not dependent on midkine expression (40), suggesting that PTN and midkine may have distinct roles in the lung.

1.3 Wnt signaling pathway

Wnt is a family of growth factors which play important roles in cell proliferation and cell fate determination. Wnt has as many as 19 isoforms which bind to frizzled receptors (fzs) and trigger at least three intracellular signaling pathways. One of the most important pathways of Wnt signaling is the canonical signaling pathway through β-catenin. Wnt regulates lung morphogenesis through the canonical β-catenin/LEF-TCF pathway (33; 95; 141). The binding of Wnt to frizzleds inhibits the activity of glycogen synthase kinase (GSK-3) and thus stabilizes β-catenin in the cytoplasm. β-catenin accumulates in the cytoplasm and translocates into the nucleus, where it binds to TCF/LEF transcription factors to stimulate the transcription of its downstream genes, such as N-myc, bone morphogenetic protein 4 (Bmp4), FGF etc (121). Current studies of Wnt signaling in the developing lung reveal essential roles of Wnt in normal lung development.

1.3.1 Wnt and β-catenin expression during fetal lung development

The expression of Wnts and β-catenin are precisely regulated during fetal lung development. *In situ* hybridization reveals that Wnt2 is highly expressed in the fetal lung, and its expression is restricted to mesenchymal cells (60). In fetal E12.5 to E16.5 mouse lung, Wnt11 expression is observed in epithelial and mesenchymal cells (56), while Wnt7b is only localized in distal and proximal bronchial epithelial cells (135). Wnt5a expression is barely detectable in E12 mouse lung, and reached a high level in E16 in both epithelial and mesenchymal cells. In E18, Wnt5a is mainly localized in airway epithelial cells (61). Wnt3a expression is mainly in AEC II and some ciliated airway epithelial cells in the adult human lung (54).

β-catenin is expressed in the airway and alveolar epithelial cells during fetal lung development. β-catenin nuclear expression is especially high in pre-alveolar acini budding from respiratory airways (33). From E14.5 to E17.5, cytoplasmic and nuclear expression of β-catenin is also found in the primordial and alveolar epithelial cells, and adjacent mesenchymal cells, indicating that the β-catenin signaling may be activated in these cells (33). The cytoplasmic and nuclear β-catenin level decreases in the mesenchyme after E13.5 (128). TCF and LEF have very similar expression pattern as β-catenin during fetal lung development (128). TCF1 protein is present in both epithelial and surrounding mesenchymal cells from E10.5 to E17.5. LEF1 protein expression is high in adjacent mesenchyme but low in proximal epithelium. TCF3 and TCF4 protein are almost expressed in all kinds of cells, including proximal and distal alveolar epithelial cells, and mesenchymal cells from E11.5 to E17.5 (128).

The mesenchymal localization of Wnt ligands and epithelial localization of β-catenin suggest the possible role of Wnt signaling in epithelial-mesenchymal interactions, which is crucial for normal lung morphogenesis, growth, and cell fate determination. Since β-catenin nuclear localization is mainly observed in developing epithelial cells, Wnt canonical signaling may mediate the epithelial proliferation or differentiation.

1.3.2 Wnt signaling in lung morphogenesis

Recently, the transgenic and knockout mice studies have revealed some important roles of Wnt signaling on lung morphogenesis. Wnt5a conditional knockout is fatal and results in abnormal distal lung morphogenesis, which is characterized by the hypercellular and thicker intersaccular walls (61). However, Wnt5a knockout does not affect vascular distribution and maturation.

The lungs from Wnt7b null mice exhibit a smaller and collapsed appearance and fail to inflate properly which causes the death of these mice shortly after birth (122). Wnt7b knockout lung has other defects, such as hypoplasia, which is shown by extremely thin distal mesenchyme. Additionally, smooth muscle α-actin (α-SMA) expression is abnormal in Wnt7b knockout mice. Since smooth muscle cells are differentiated from mesenchymal cells, these studies indicate that Wnt7b affects the lung morphogenesis possible through the regulation of mesenchyme cells.

Specifically silencing β-catenin in the embryonic mesenchyme leads to shortened trachea, decreased branching, and reduced peripheral mesenchyme (27). However, the sub-epithelial mesenchyme is not affected. On the other hand, overexpression of β-catenin in alveolar type II cells using SP-C promoter destroys the normal lung morphogenesis, arrests the differentiation of peripheral airways, and leaves the lung containing mainly conducting airways (84). Consistently, hyperactivating β-catenin in epithelial cells of the developing lung causes enlarged air space, atypical expression of alveolar type II cells, and epithelial cell dysplasia. This

effect is possibly through the downregulation of Foxa2 expression in the epithelium (83). However, further work may be required to elucidate the molecular mechanism of this process.

1.3.3 Wnt signaling in cell differentiation and proliferation

The action of Wnt signaling on the lung morphology is mainly achieved by the regulation of proliferation, differentiation and apoptosis of the lung cells. The regulation of the lung cell proliferation by Wnt signaling is well coupled with cell differentiation. The signals that increase the proliferation of progenitor cells normally arrest the further differentiation of these cells.

Wnt7b knockout mice did not show abnormal differentiation of some epithelial cells including Clara cells, and alveolar type II cells. However, the alveolar type I cell differentiation is delayed in Wnt7b knockout mice, suggesting that Wnt7b may be important for the late epithelial cell differentiation. Wnt7b knockout significantly reduces the proliferation of mesenchymal cells on E12.5 but not on E14.5. However, the proliferation of epithelial cells is not affected (103; 122). These results indicate that Wnt7b is a regulator for mesenchymal cell proliferation in the early developing lung. Besides that, apoptosis increases significantly in the vascular smooth muscle and epithelium following the deprivation of Wnt7b.

Interestingly, hyperactivation of β-catenin specifically in lung endoderm leads to increased amplification of distal lung progenitor cells and lacking of fully differentiated lung cell types (90). Activation of β-catenin signaling only in epithelial cells causes ectopic differentiation of AEC II (83). Additionally, conditional knockout β-catenin in mesenchyme increases the proliferation of Fgf10 expression in parabronchial smooth muscle cells (PSMC). However, the differentiation of this group of cells is not affected (27). All these results indicate that β-catenin signaling is essential for normal epithelial differentiation.

Conditional knockout of Wnt5a caused a significant increase in lung cell proliferation without interfering with cell differentiation (61).

1.3.4 Wnt signaling in lung diseases

The dysregulation of Wnt signaling in adult lung causes many diseases such as lung cancer, fibrosis, and inflammation (101). Hyperactivation of β-catenin caused by mutations of β-catenin, adenomatous polyposis coli (APC) and axin in lung epithelium induces lung tumors (83). β-catenin are highly overexpressed and activated in many lung cancer cells . Drugs targeting wnt/β-catenin have become a novel therapeutic strategy for cancer. Fibrosis is a crucial process during tissue repairing after an injury. Hyperactivation of wnt signaling pathway causes abnormal cell proliferation and differentiation during pulmonary fibrosis, and also overexpresses fibrosis regulators such as metalloproteinase matrilysin (101).

In summary, Wnt is important for cell proliferation and differentiation during fetal lung development, although how Wnt proteins regulate the lung development is still not clear. Wnt7b

promoter is regulated by TTF-1 (135), a known transcription factor regulating multiple epithelium cell differentiation in the developing lung. This finding suggests a possible molecular mechanism of TTF-1 in regulating the lung epithelium differentiation.

1.4 P2X7 receptors and microRNAs

Purinergic receptors are composed of P2X receptors (P2XR) and P2Y receptors (P2YR). P2XR are expressed in many cells including neuron, glia, bone, epithelial and endothelial cells (104). P2XRs are plasma membrane ligand-gated ion channels activated by purine nucleotides including ATP, while P2YRs are G-protein-coupled receptors which mediate slow responses through G-proteins (1). In mammalian cells, P2XRs are encoded by 7 genes which either comprise seven functional homomeric assemblies (P2X1-P2X7) or form functional heteromeric assemblies (P2X 1/2,1/4,1/5,2/3,2/6,4/6,4/7 etc) (139). Generally, P2XR assemblies contain three glycosylated subunits, and each has two transmembrane-spanning domains. These six transmembrane-spanning domains are closely associated to form the ion channel (139). The binding of ATP causes P2XR to open within milliseconds and stimulate cell depolarization by an influx of cationic ions, including Na^+, K^+, Ca^{2+} ions, and, in some cases, large ions such as Cl^- ions. The moderate influx of Ca^{2+} activates a cascade of intracellular signaling molecules, which subsequently regulates a series of cellular processes. However, high ATP doses and sustained stimulation of P2XR may result in irreversible cell damage and lead to necrosis or apoptosis.

P2X7R is quite different from other P2XRs. Structurally it has an unusually long C-terminus. It can form a large non-selective pore permeable to larger molecular weight species (123). The activation of P2X7R needs at least 10-fold higher concentration of ATP. This high concentration of ATP is normally achieved during a massive lysis of host cells or pathogen defense. 3'-O-(4-benzoyl) benzoylATP (BzATP), which has around 10-fold more activities than ATP, is the most potent known agonist for P2X7R. High doses of BzATP and sustained stimulations of P2X7R also lead to membrane blebbing and programmed cell death (130).

P2X7R was initially identified in immune systems as an ion-channel receptor which is non-selectively permeable to large molecules and mediates the programmed cell death (36; 126). Stimulation of P2X7R leads to the secretion of IL-1beta from macrophages, and consequently initiates the pro-inflammatory response (23; 67). P2X7R is involved in pathological conditions, such as pain, inflammation, apoptosis, neurodegenerative conditions, and Alzheimer disease (9; 42). Recently, P2X7R has been used as a therapeutic target for pharmacological intervention.

MicroRNAs (miRNA) are small non-coding RNAs that can either cleave specific mRNAs or inhibit mRNA translation through complementary base pairing (6). MiRNAs naturally exist in organisms. They regulate diverse cellular processes such as proliferation, differentiation, apoptosis, and exocytosis.

The processing of miRNAs includes several steps. MiRNAs are first transcribed as pri-miRNAs from the genomic DNA. The production of mature miRNA is a two-step process, which requires both Drosha and Dicer 33. Drosha is a nuclear RNase III endonuclease. Drosha-DGCR8 complex (DiGeorge syndrome critical region gene-8) cleaves the pri-miRNA and releases the loop structure from the primary transcript to generate the pre-miRNAs (58). The pre-miRNAs are ~70 nt long and contain a stem-loop structure (59).They contains 2-nt overhangs at their 3' ends. They first bind to Exportin 5-RanGTP, and are exported out of the nucleus. In the cytoplasm, the pre-miRNAs are further cleaved by Dicer to yield the mature miRNAs (11; 66; 147).

The function of miRNAs is mostly through the reduction of their target proteins. miR-150 and miR-186 are identified to target P2X7R protein in HeLa and primary human ectocervical-vaginal epithelial cells and disrupt P2X7R expression (153). MiR-150 is highly expressed in the tumour cells surrounding the proliferation centres in the bone marrow and lymphoid tissues (133). MiR-150 is also present in mature B and T cells and blocks B cell development by decreasing the expression of c-Myb (145; 152). The functions of miR-150 and miR-186 in the lung have not been studied yet.

1.5 Purposes

Mammalian lung development is a complex biological process which is temporally and spatially regulated by growth factors, hormones, and extracellular matrix proteins. Abnormal changes of these molecules often lead to impaired lung development and thus pulmonary diseases such as pulmonary hypoplasia and neonatal respiratory distress syndrome (43; 143).

The first part (Chapter 2) of the dissertation research focuses on the DNA Microarray to identify genes that are differentially expressed during fetal lung development. Such studies lead to the discovery that PTN is highly expressed at the late stage of fetal lung development. Chapter 3 investigates the role of PTN in fetal lung epithelial cell proliferation and differentiation and its regulatory pathway in *in vitro* cell and organ cultures. Chapter 4 further studies physiological functions of PTN in lung development using PTN knockout mice. The secretion of lung surfactant into alveolar space is crucial for the preparation for extrautero life. Thus the regulation of surfactant secretion is an important aspect of lung development. Chapter 5 examines how microRNA-150 regulates surfactant secretion via P2X7R. Finally, chapter 6 deals with a technical aspect of real-time PCR, a byproduct derived from this dissertation research.

PTN is a growth factor differentially expressed during fetal lung development. The elucidation of the role of PTN in fetal lung development and its regulatory pathway may offer opportunities in the development of new therapeutic strategies and drugs to resolve the disorders associated with fetal lung development. Successful differentiation of AEC II and AEC I has crucial functions to surfactant secretion during lung development. Insufficient amount of pulmonary surfactant leads to abnormal lung function, including respiratory distress syndrome. P2X7R, as a non-selective ion

channel specifically expressed in AEC I, may play an important role in surfactant secretion. Elucidation of the regulation of P2X7R will open a new area for developing therapeutic strategies to treat lung diseases.

1.6 References

1. Abbracchio MP and Burnstock G. Purinoceptors: are there families of P2X and P2Y purinoceptors? *Pharmacol Ther* 64: 445-475, 1994.

2. ALESCIO T and CASSINI A. Induction in vitro of tracheal buds by pulmonary mesenchyme grafted on tracheal epithelium. *J Exp Zool* 150: 83-94, 1962.

3. Amet LE, Lauri SE, Hienola A, Croll SD, Lu Y, Levorse JM, Prabhakaran B, Taira T, Rauvala H and Vogt TF. Enhanced hippocampal long-term potentiation in mice lacking heparin-binding growth-associated molecule. *Mol Cell Neurosci* 17: 1014-1024, 2001.

4. Andreeva AV, Kutuzov MA and Voyno-Yasenetskaya TA. Regulation of surfactant secretion in alveolar type II cells. *Am J Physiol Lung Cell Mol Physiol* 293: L259-L271, 2007.

5. Antoine M, Tag CG, Wirz W, Borkham-Kamphorst E, Sawitza I, Gressner AM and Kiefer P. Upregulation of pleiotrophin expression in rat hepatic stellate cells by PDGF and hypoxia: implications for its role in experimental biliary liver fibrogenesis. *Biochem Biophys Res Commun* 337: 1153-1164, 2005.

6. Bartel DP. MicroRNAs: genomics, biogenesis, mechanism, and function. *Cell* 116: 281-297, 2004.

7. Bellusci S, Furuta Y, Rush MG, Henderson R, Winnier G and Hogan BL. Involvement of Sonic hedgehog (Shh) in mouse embryonic lung growth and morphogenesis. *Development* 124: 53-63, 1997.

8. Bellusci S, Grindley J, Emoto H, Itoh N and Hogan BL. Fibroblast growth factor 10 (FGF10) and branching morphogenesis in the embryonic mouse lung. *Development* 124: 4867-4878, 1997.

9. Bernardino L, Balosso S, Ravizza T, Marchi N, Ku G, Randle JC, Malva JO and Vezzani A. Inflammatory events in hippocampal slice cultures prime neuronal susceptibility to excitotoxic injury: a crucial role of P2X7 receptor-mediated IL-1beta release. *J Neurochem* 106: 271-280, 2008.

10. Bohinski RJ, Di LR and Whitsett JA. The lung-specific surfactant protein B gene promoter is a target for thyroid transcription factor 1 and hepatocyte nuclear factor 3, indicating common factors for organ-specific gene expression along the foregut axis. *Mol Cell Biol* 14: 5671-5681, 1994.

11. Bohnsack MT, Czaplinski K and Gorlich D. Exportin 5 is a RanGTP-dependent dsRNA-binding protein that mediates nuclear export of pre-miRNAs. *RNA* 10: 185-191, 2004.

12. Bostrom H, Willetts K, Pekny M, Leveen P, Lindahl P, Hedstrand H, Pekna M, Hellstrom M, Gebre-Medhin S, Schalling M, Nilsson M, Kurland S, Tornell J, Heath JK and Betsholtz C. PDGF-A signaling is a critical event in lung alveolar myofibroblast development and alveogenesis. *Cell* 85: 863-873, 1996.

13. Boyden EA. Development of the pulmonary airways. *Minn Med* 54: 894-897, 1971.

14. Boyer B and Thiery JP. Epithelial cell adhesion mechanisms. *J Membr Biol* 112: 97-108, 1989.

15. Brewster L, Brey EM, Addis M, Xue L, Husak V, Ellinger J, Haudenschild CC and Greisler HP. Improving endothelial healing with novel chimeric mitogens. *Am J Surg* 192: 589-593, 2006.

16. Bridges JP, Wert SE, Nogee LM and Weaver TE. Expression of a human surfactant protein C mutation associated with interstitial lung disease disrupts lung development in transgenic mice. *J Biol Chem* 278: 52739-52746, 2003.

17. Brody JS and Williams MC. Pulmonary alveolar epithelial cell differentiation. *Annu Rev Physiol* 54: 351-371, 1992.

18. Burri PH. Fetal and postnatal development of the lung. *Annu Rev Physiol* 46: 617-628, 1984.

19. Burri PH, Dbaly J and Weibel ER. The postnatal growth of the rat lung. I. Morphometry. *Anat Rec* 178: 711-730, 1974.

20. Cardoso WV. Molecular regulation of lung development. *Annu Rev Physiol* 63: 471-494, 2001.

21. Carey DJ, Evans DM, Stahl RC, Asundi VK, Conner KJ, Garbes P and Cizmeci-Smith G. Molecular cloning and characterization of N-syndecan, a novel transmembrane heparan sulfate proteoglycan. *J Cell Biol* 117: 191-201, 1992.

22. Chauhan AK, Li YS and Deuel TF. Pleiotrophin transforms NIH 3T3 cells and induces tumors in nude mice. *Proc Natl Acad Sci U S A* 90: 679-682, 1993.

23. Chen L and Brosnan CF. Regulation of immune response by P2X7 receptor. *Crit Rev Immunol* 26: 499-513, 2006.

24. Clark JC, Wert SE, Bachurski CJ, Stahlman MT, Stripp BR, Weaver TE and Whitsett JA. Targeted disruption of the surfactant protein B gene disrupts surfactant homeostasis, causing respiratory failure in newborn mice. *Proc Natl Acad Sci U S A* 92: 7794-7798, 1995.

25. Copland I and Post M. Lung development and fetal lung growth. *Paediatr Respir Rev* 5 Suppl A: S259-S264, 2004.

26. Davies G and Reid L. Growth of the alveoli and pulmonary arteries in childhood. *Thorax* 25: 669-681, 1970.

27. De Langhe SP, Carraro G, Tefft D, Li C, Xu X, Chai Y, Minoo P, Hajihosseini MK, Drouin J, Kaartinen V and Bellusci S. Formation and differentiation of multiple mesenchymal lineages during lung development is regulated by beta-catenin signaling. *PLoS One* 3: e1516, 2008.

28. De ML, Spencer-Dene B, Revest JM, Hajihosseini M, Rosewell I and Dickson C. An important role for the IIIb isoform of fibroblast growth factor receptor 2 (FGFR2) in mesenchymal-epithelial signalling during mouse organogenesis. *Development* 127: 483-492, 2000.

29. Desai TJ, Malpel S, Flentke GR, Smith SM and Cardoso WV. Retinoic acid selectively regulates Fgf10 expression and maintains cell identity in the prospective lung field of the developing foregut. *Dev Biol* 273: 402-415, 2004.

30. Deuel TF, Zhang N, Yeh HJ, Silos-Santiago I and Wang ZY. Pleiotrophin: a cytokine with diverse functions and a novel signaling pathway. *Arch Biochem Biophys* 397: 162-171, 2002.

31. Docimo SG, Crone RK, Davies P, Reid L, Retik AB and Mandell J. Pulmonary development in the fetal lamb: morphometric study of the alveolar phase. *Anat Rec* 229: 495-498, 1991.

32. Dreyfus J, Brunet-de CN, Duprez D, Raulais D and Vigny M. HB-GAM/pleiotrophin but not RIHB/midkine enhances chondrogenesis in micromass culture. *Exp Cell Res* 241: 171-180, 1998.

33. Eberhart CG and Argani P. Wnt signaling in human development: beta-catenin nuclear translocation in fetal lung, kidney, placenta, capillaries, adrenal, and cartilage. *Pediatr Dev Pathol* 4: 351-357, 2001.

34. Foster CD, Zhang PX, Gonzales LW and Guttentag SH. In vitro surfactant protein B deficiency inhibits lamellar body formation. *Am J Respir Cell Mol Biol* 29: 259-266, 2003.

35. Gabrielli MG, Materazzi G, Bondi AM and Menghi G. Developmental expression of glycocomponents in the chick chorioallantoic membrane. *Anat Embryol (Berl)* 207: 63-71, 2003.

36. Garcia-Marcos M, Pochet S, Marino A and Dehaye JP. P2X7 and phospholipid signalling: the search of the "missing link" in epithelial cells. *Cell Signal* 18: 2098-2104, 2006.

37. Garver RI, Jr., Radford DM, Donis-Keller H, Wick MR and Milner PG. Midkine and pleiotrophin expression in normal and malignant breast tissue. *Cancer* 74: 1584-1590, 1994.

38. Gebbink MF, Zondag GC, Wubbolts RW, Beijersbergen RL, van E, I and Moolenaar WH. Cell-cell adhesion mediated by a receptor-like protein tyrosine phosphatase. *J Biol Chem* 268: 16101-16104, 1993.

39. Hashimoto-Gotoh T, Ohnishi H, Tsujimura A, Tsunezuka H, Imai K, Masuda H and Nakamura T. Bone mass increase specific to the female in a line of transgenic mice

overexpressing human osteoblast stimulating factor-1. *J Bone Miner Metab* 22: 278-282, 2004.

40. Herradon G, Ezquerra L, Nguyen T, Silos-Santiago I and Deuel TF. Midkine regulates pleiotrophin organ-specific gene expression: evidence for transcriptional regulation and functional redundancy within the pleiotrophin/midkine developmental gene family. *Biochem Biophys Res Commun* 333: 714-721, 2005.

41. Hienola A, Pekkanen M, Raulo E, Vanttola P and Rauvala H. HB-GAM inhibits proliferation and enhances differentiation of neural stem cells. *Mol Cell Neurosci* 26: 75-88, 2004.

42. Hughes JP, Hatcher JP and Chessell IP. The role of P2X(7) in pain and inflammation. *Purinergic Signal* 3: 163-169, 2007.

43. Hutchison AA. Respiratory disorders of the neonate. *Curr Opin Pediatr* 6: 142-153, 1994.

44. Hyatt BA, Shangguan X and Shannon JM. FGF-10 induces SP-C and Bmp4 and regulates proximal-distal patterning in embryonic tracheal epithelium. *Am J Physiol Lung Cell Mol Physiol* 287: L1116-L1126, 2004.

45. Hynes RO. Integrins: bidirectional, allosteric signaling machines. *Cell* 110: 673-687, 2002.

46. Ikeda K, Shaw-White JR, Wert SE and Whitsett JA. Hepatocyte nuclear factor 3 activates transcription of thyroid transcription factor 1 in respiratory epithelial cells. *Mol Cell Biol* 16: 3626-3636, 1996.

47. Imai S, Kaksonen M, Raulo E, Kinnunen T, Fages C, Meng X, Lakso M and Rauvala H. Osteoblast recruitment and bone formation enhanced by cell matrix-associated heparin-binding growth-associated molecule (HB-GAM). *J Cell Biol* 143: 1113-1128, 1998.

48. Iwahara T, Fujimoto J, Wen D, Cupples R, Bucay N, Arakawa T, Mori S, Ratzkin B and Yamamoto T. Molecular characterization of ALK, a receptor tyrosine kinase expressed specifically in the nervous system. *Oncogene* 14: 439-449, 1997.

49. Johnson MD, Widdicombe JH, Allen L, Barbry P and Dobbs LG. Alveolar epithelial type I cells contain transport proteins and transport sodium, supporting an active role for type I cells in regulation of lung liquid homeostasis. *Proc Natl Acad Sci U S A* 99: 1966-1971, 2002.

50. Kadomatsu K and Muramatsu T. Midkine and pleiotrophin in neural development and cancer. *Cancer Lett* 204: 127-143, 2004.

51. Kadomatsu K, Tomomura M and Muramatsu T. cDNA cloning and sequencing of a new gene intensely expressed in early differentiation stages of embryonal carcinoma cells and in mid-gestation period of mouse embryogenesis. *Biochem Biophys Res Commun* 151: 1312-1318, 1988.

52. Kauffman SL, Burri PH and Weibel ER. The postnatal growth of the rat lung. II. Autoradiography. *Anat Rec* 180: 63-76, 1974.

53. Kinnunen T, Kaksonen M, Saarinen J, Kalkkinen N, Peng HB and Rauvala H. Cortactin-Src kinase signaling pathway is involved in N-syndecan-dependent neurite outgrowth. *J Biol Chem* 273: 10702-10708, 1998.

54. Konigshoff M, Balsara N, Pfaff EM, Kramer M, Chrobak I, Seeger W and Eickelberg O. Functional Wnt signaling is increased in idiopathic pulmonary fibrosis. *PLoS One* 3: e2142, 2008.

55. Kumar VH and Ryan RM. Growth factors in the fetal and neonatal lung. *Front Biosci* 9: 464-480, 2004.

56. Lako M, Strachan T, Bullen P, Wilson DI, Robson SC and Lindsay S. Isolation, characterisation and embryonic expression of WNT11, a gene which maps to 11q13.5 and has possible roles in the development of skeleton, kidney and lung. *Gene* 219: 101-110, 1998.

57. Lawson KA. Mesenchyme specificity in rodent salivary gland development: the response of salivary epithelium to lung mesenchyme in vitro. *J Embryol Exp Morphol* 32: 469-493, 1974.

58. Lee Y, Ahn C, Han J, Choi H, Kim J, Yim J, Lee J, Provost P, Radmark O, Kim S and Kim VN. The nuclear RNase III Drosha initiates microRNA processing. *Nature* 425: 415-419, 2003.

59. Lee Y, Jeon K, Lee JT, Kim S and Kim VN. MicroRNA maturation: stepwise processing and subcellular localization. *EMBO J* 21: 4663-4670, 2002.

60. Levay-Young BK and Navre M. Growth and developmental regulation of wnt-2 (irp) gene in mesenchymal cells of fetal lung. *Am J Physiol* 262: L672-L683, 1992.

61. Li C, Xiao J, Hormi K, Borok Z and Minoo P. Wnt5a participates in distal lung morphogenesis. *Dev Biol* 248: 68-81, 2002.

62. Li G, Bunn JR, Mushipe MT, He Q and Chen X. Effects of pleiotrophin (PTN) over-expression on mouse long bone development, fracture healing and bone repair. *Calcif Tissue Int* 76: 299-306, 2005.

63. Li YS, Milner PG, Chauhan AK, Watson MA, Hoffman RM, Kodner CM, Milbrandt J and Deuel TF. Cloning and expression of a developmentally regulated protein that induces mitogenic and neurite outgrowth activity. *Science* 250: 1690-1694, 1990.

64. Litingtung Y, Lei L, Westphal H and Chiang C. Sonic hedgehog is essential to foregut development. *Nat Genet* 20: 58-61, 1998.

65. Lu KV, Jong KA, Kim GY, Singh J, Dia EQ, Yoshimoto K, Wang MY, Cloughesy TF, Nelson SF and Mischel PS. Differential induction of glioblastoma migration and growth by two forms of pleiotrophin. *J Biol Chem* 280: 26953-26964, 2005.

66. Lund E, Guttinger S, Calado A, Dahlberg JE and Kutay U. Nuclear export of microRNA precursors. *Science* 303: 95-98, 2004.

67. MacKenzie A, Wilson HL, Kiss-Toth E, Dower SK, North RA and Surprenant A. Rapid secretion of interleukin-1beta by microvesicle shedding. *Immunity* 15: 825-835, 2001.

68. Maden M. Retinoids in lung development and regeneration. *Curr Top Dev Biol* 61: 153-189, 2004.

69. Maeda N, Nishiwaki T, Shintani T, Hamanaka H and Noda M. 6B4 proteoglycan/phosphacan, an extracellular variant of receptor-like protein-tyrosine phosphatase zeta/RPTPbeta, binds pleiotrophin/heparin-binding growth-associated molecule (HB-GAM). *J Biol Chem* 271: 21446-21452, 1996.

70. Maeda Y, Dave V and Whitsett JA. Transcriptional control of lung morphogenesis. *Physiol Rev* 87: 219-244, 2007.

71. Masuda H, Tsujimura A, Yoshioka M, Arai Y, Kuboki Y, Mukai T, Nakamura T, Tsuji H, Nakagawa M and Hashimoto-Gotoh T. Bone mass loss due to estrogen deficiency is compensated in transgenic mice overexpressing human osteoblast stimulating factor-1. *Biochem Biophys Res Commun* 238: 528-533, 1997.

72. Matthay MA, Folkesson HG and Clerici C. Lung epithelial fluid transport and the resolution of pulmonary edema. *Physiol Rev* 82: 569-600, 2002.

73. McGowan SE. Extracellular matrix and the regulation of lung development and repair. *FASEB J* 6: 2895-2904, 1992.

74. McGowan SE and Synder JM. Development of Alveoli. In: The lung: development, aging and the environment., edited by Harding R, Pinkerton KE and Plopper CG. Academic Press, 2004, p. 55-73.

75. Meng K, Rodriguez-Pena A, Dimitrov T, Chen W, Yamin M, Noda M and Deuel TF. Pleiotrophin signals increased tyrosine phosphorylation of beta beta-catenin through inactivation of the intrinsic catalytic activity of the receptor-type protein tyrosine phosphatase beta/zeta. *Proc Natl Acad Sci U S A* 97: 2603-2608, 2000.

76. Merenmies J and Rauvala H. Molecular cloning of the 18-kDa growth-associated protein of developing brain. *J Biol Chem* 265: 16721-16724, 1990.

77. Milner PG, Li YS, Hoffman RM, Kodner CM, Siegel NR and Deuel TF. A novel 17 kD heparin-binding growth factor (HBGF-8) in bovine uterus: purification and N-terminal amino acid sequence. *Biochem Biophys Res Commun* 165: 1096-1103, 1989.

78. Min H, Danilenko DM, Scully SA, Bolon B, Ring BD, Tarpley JE, DeRose M and Simonet WS. Fgf-10 is required for both limb and lung development and exhibits striking functional similarity to Drosophila branchless. *Genes Dev* 12: 3156-3161, 1998.

79. Minoo P. Transcriptional regulation of lung development: emergence of specificity. *Respir Res* 1: 109-115, 2000.

80. Minoo P, Su G, Drum H, Bringas P and Kimura S. Defects in tracheoesophageal and lung morphogenesis in Nkx2.1(-/-) mouse embryos. *Dev Biol* 209: 60-71, 1999.

81. Mitsiadis TA, Salmivirta M, Muramatsu T, Muramatsu H, Rauvala H, Lehtonen E, Jalkanen M and Thesleff I. Expression of the heparin-binding cytokines, midkine (MK) and HB-GAM (pleiotrophin) is associated with epithelial-mesenchymal interactions during fetal development and organogenesis. *Development* 121: 37-51, 1995.

82. Morris SW, Naeve C, Mathew P, James PL, Kirstein MN, Cui X and Witte DP. ALK, the chromosome 2 gene locus altered by the t(2;5) in non-Hodgkin's lymphoma, encodes a novel neural receptor tyrosine kinase that is highly related to leukocyte tyrosine kinase (LTK). *Oncogene* 14: 2175-2188, 1997.

83. Mucenski ML, Nation JM, Thitoff AR, Besnard V, Xu Y, Wert SE, Harada N, Taketo MM, Stahlman MT and Whitsett JA. Beta-catenin regulates differentiation of respiratory epithelial cells in vivo. *Am J Physiol Lung Cell Mol Physiol* 289: L971-L979, 2005.

84. Mucenski ML, Wert SE, Nation JM, Loudy DE, Huelsken J, Birchmeier W, Morrisey EE and Whitsett JA. beta-Catenin is required for specification of proximal/distal cell fate during lung morphogenesis. *J Biol Chem* 278: 40231-40238, 2003.

85. Muller S, Kunkel P, Lamszus K, Ulbricht U, Lorente GA, Nelson AM, von SD, Chin DJ, Lohr SC, Westphal M and Melcher T. A role for receptor tyrosine phosphatase zeta in glioma cell migration. *Oncogene* 22: 6661-6668, 2003.

86. Muramatsu H, Zou P, Kurosawa N, Ichihara-Tanaka K, Maruyama K, Inoh K, Sakai T, Chen L, Sato M and Muramatsu T. Female infertility in mice deficient in midkine and pleiotrophin, which form a distinct family of growth factors. *Genes Cells* 11: 1405-1417, 2006.

87. Muramatsu T. Midkine and pleiotrophin: two related proteins involved in development, survival, inflammation and tumorigenesis. *J Biochem* 132: 359-371, 2002.

88. Nakamura E, Kadomatsu K, Yuasa S, Muramatsu H, Mamiya T, Nabeshima T, Fan QW, Ishiguro K, Igakura T, Matsubara S, Kaname T, Horiba M, Saito H and Muramatsu T. Disruption of the midkine gene (Mdk) resulted in altered expression of a calcium binding protein in the hippocampus of infant mice and their abnormal behaviour. *Genes Cells* 3: 811-822, 1998.

89. Neame PJ, Treep JT and Young CN. An 18-kDa glycoprotein from bovine nasal cartilage. Isolation and primary structure of small, cartilage-derived glycoprotein. *J Biol Chem* 265: 9628-9633, 1990.

90. Okubo T and Hogan BL. Hyperactive Wnt signaling changes the developmental potential of embryonic lung endoderm. *J Biol* 3: 11, 2004.

91. Pariser H, Ezquerra L, Herradon G, Perez-Pinera P and Deuel TF. Fyn is a downstream target of the pleiotrophin/receptor protein tyrosine phosphatase beta/zeta-signaling pathway: regulation of tyrosine phosphorylation of Fyn by pleiotrophin. *Biochem Biophys Res Commun* 332: 664-669, 2005.

92. Pariser H, Herradon G, Ezquerra L, Perez-Pinera P and Deuel TF. Pleiotrophin regulates serine phosphorylation and the cellular distribution of beta-adducin through activation of protein kinase C. *Proc Natl Acad Sci U S A* 102: 12407-12412, 2005.

93. Pariser H, Perez-Pinera P, Ezquerra L, Herradon G and Deuel TF. Pleiotrophin stimulates tyrosine phosphorylation of beta-adducin through inactivation of the transmembrane receptor protein tyrosine phosphatase beta/zeta. *Biochem Biophys Res Commun* 335: 232-239, 2005.

94. Park WY, Miranda B, Lebeche D, Hashimoto G and Cardoso WV. FGF-10 is a chemotactic factor for distal epithelial buds during lung development. *Dev Biol* 201: 125-134, 1998.

95. Pauling MH and Vu TH. Mechanisms and regulation of lung vascular development. *Curr Top Dev Biol* 64: 73-99, 2004.

96. Pavlov I, Voikar V, Kaksonen M, Lauri SE, Hienola A, Taira T and Rauvala H. Role of heparin-binding growth-associated molecule (HB-GAM) in hippocampal LTP and spatial learning revealed by studies on overexpressing and knockout mice. *Mol Cell Neurosci* 20: 330-342, 2002.

97. Perez-Pinera P, Alcantara S, Dimitrov T, Vega JA and Deuel TF. Pleiotrophin disrupts calcium-dependent homophilic cell-cell adhesion and initiates an epithelial-mesenchymal transition. *Proc Natl Acad Sci U S A* 103: 17795-17800, 2006.

98. Perez-Pinera P, Garcia-Suarez O, Menendez-Rodriguez P, Mortimer J, Chang Y, Astudillo A and Deuel TF. The receptor protein tyrosine phosphatase (RPTP)beta/zeta is expressed in different subtypes of human breast cancer. *Biochem Biophys Res Commun* 362: 5-10, 2007.

99. Perez-Pinera P, Zhang W, Chang Y, Vega JA and Deuel TF. Anaplastic lymphoma kinase is activated through the pleiotrophin/receptor protein-tyrosine phosphatase beta/zeta signaling pathway: an alternative mechanism of receptor tyrosine kinase activation. *J Biol Chem* 282: 28683-28690, 2007.

100. Perl AK and Whitsett JA. Molecular mechanisms controlling lung morphogenesis. *Clin Genet* 56: 14-27, 1999.

101. Pongracz JE and Stockley RA. Wnt signalling in lung development and diseases. *Respir Res* 7: 15, 2006.

102. Powers C, Aigner A, Stoica GE, McDonnell K and Wellstein A. Pleiotrophin signaling through anaplastic lymphoma kinase is rate-limiting for glioblastoma growth. *J Biol Chem* 277: 14153-14158, 2002.

103. Rajagopal J, Carroll TJ, Guseh JS, Bores SA, Blank LJ, Anderson WJ, Yu J, Zhou Q, McMahon AP and Melton DA. Wnt7b stimulates embryonic lung growth by coordinately increasing the replication of epithelium and mesenchyme. *Development* 135: 1625-1634, 2008.

104. Ralevic V and Burnstock G. Receptors for purines and pyrimidines. *Pharmacol Rev* 50: 413-492, 1998.

105. Raulo E, Chernousov MA, Carey DJ, Nolo R and Rauvala H. Isolation of a neuronal cell surface receptor of heparin binding growth-associated molecule (HB-GAM). Identification as N-syndecan (syndecan-3). *J Biol Chem* 269: 12999-13004, 1994.

106. Rauvala H. An 18-kd heparin-binding protein of developing brain that is distinct from fibroblast growth factors. *EMBO J* 8: 2933-2941, 1989.

107. Riegel AT and Wellstein A. The potential role of the heparin-binding growth factor pleiotrophin in breast cancer. *Breast Cancer Res Treat* 31: 309-314, 1994.

108. Roman J. Fibronectin and fibronectin receptors in lung development. *Exp Lung Res* 23: 147-159, 1997.

109. Rooney SA. Regulation of surfactant secretion. *Comp Biochem Physiol A Mol Integr Physiol* 129: 233-243, 2001.

110. Sakurai H, Bush KT and Nigam SK. Identification of pleiotrophin as a mesenchymal factor involved in ureteric bud branching morphogenesis. *Development* 128: 3283-3293, 2001.

111. Sato W, Kadomatsu K, Yuzawa Y, Muramatsu H, Hotta N, Matsuo S and Muramatsu T. Midkine is involved in neutrophil infiltration into the tubulointerstitium in ischemic renal injury. *J Immunol* 167: 3463-3469, 2001.

112. Sato Y, Takita H, Ohata N, Tamura M and Kuboki Y. Pleiotrophin regulates bone morphogenetic protein (BMP)-induced ectopic osteogenesis. *J Biochem* 131: 877-886, 2002.

113. Sawaya PL and Luse DS. Two members of the HNF-3 family have opposite effects on a lung transcriptional element; HNF-3 alpha stimulates and HNF-3 beta inhibits activity of region I from the Clara cell secretory protein (CCSP) promoter. *J Biol Chem* 269: 22211-22216, 1994.

114. Sawaya PL, Stripp BR, Whitsett JA and Luse DS. The lung-specific CC10 gene is regulated by transcription factors from the AP-1, octamer, and hepatocyte nuclear factor 3 families. *Mol Cell Biol* 13: 3860-3871, 1993.

115. Schuger L, O'Shea S, Rheinheimer J and Varani J. Laminin in lung development: effects of anti-laminin antibody in murine lung morphogenesis. *Dev Biol* 137: 26-32, 1990.

116. Sekine K, Ohuchi H, Fujiwara M, Yamasaki M, Yoshizawa T, Sato T, Yagishita N, Matsui D, Koga Y, Itoh N and Kato S. Fgf10 is essential for limb and lung formation. *Nat Genet* 21: 138-141, 1999.

117. Seykora JT, Jih D, Elenitsas R, Horng WH and Elder DE. Gene expression profiling of melanocytic lesions. *Am J Dermatopathol* 25: 6-11, 2003.

118. Shannon JM and Hyatt BA. Epithelial-mesenchymal interactions in the developing lung. *Annu Rev Physiol* 66: 625-645, 2004.

119. Shannon JM, Nielsen LD, Gebb SA and Randell SH. Mesenchyme specifies epithelial differentiation in reciprocal recombinants of embryonic lung and trachea. *Dev Dyn* 212: 482-494, 1998.

120. Sheppard D. Functions of pulmonary epithelial integrins: from development to disease. *Physiol Rev* 83: 673-686, 2003.

121. Shu W, Guttentag S, Wang Z, Andl T, Ballard P, Lu MM, Piccolo S, Birchmeier W, Whitsett JA, Millar SE and Morrisey EE. Wnt/beta-catenin signaling acts upstream of N-myc, BMP4, and FGF signaling to regulate proximal-distal patterning in the lung. *Dev Biol* 283: 226-239, 2005.

122. Shu W, Jiang YQ, Lu MM and Morrisey EE. Wnt7b regulates mesenchymal proliferation and vascular development in the lung. *Development* 129: 4831-4842, 2002.

123. Smart ML, Gu B, Panchal RG, Wiley J, Cromer B, Williams DA and Petrou S. P2X7 receptor cell surface expression and cytolytic pore formation are regulated by a distal C-terminal region. *J Biol Chem* 278: 8853-8860, 2003.

124. Stahlman MT, Gray MP, Falconieri MW, Whitsett JA and Weaver TE. Lamellar body formation in normal and surfactant protein B-deficient fetal mice. *Lab Invest* 80: 395-403, 2000.

125. Stoica GE, Kuo A, Aigner A, Sunitha I, Souttou B, Malerczyk C, Caughey DJ, Wen D, Karavanov A, Riegel AT and Wellstein A. Identification of anaplastic lymphoma kinase as a receptor for the growth factor pleiotrophin. *J Biol Chem* 276: 16772-16779, 2001.

126. Surprenant A, Rassendren F, Kawashima E, North RA and Buell G. The cytolytic P2Z receptor for extracellular ATP identified as a P2X receptor (P2X7). *Science* 272: 735-738, 1996.

127. Tare RS, Oreffo RO, Clarke NM and Roach HI. Pleiotrophin/Osteoblast-stimulating factor 1: dissecting its diverse functions in bone formation. *J Bone Miner Res* 17: 2009-2020, 2002.

128. Tebar M, Destree O, de Vree WJ and Ten Have-Opbroek AA. Expression of Tcf/Lef and sFrp and localization of beta-catenin in the developing mouse lung. *Mech Dev* 109: 437-440, 2001.

129. Tichelaar JW, Wert SE, Costa RH, Kimura S and Whitsett JA. HNF-3/forkhead homologue-4 (HFH-4) is expressed in ciliated epithelial cells in the developing mouse lung. *J Histochem Cytochem* 47: 823-832, 1999.

130. Tsukimoto M, Harada H, Ikari A and Takagi K. Involvement of chloride in apoptotic cell death induced by activation of ATP-sensitive P2X7 purinoceptor. *J Biol Chem* 280: 2653-2658, 2005.

131. Urase K, Mukasa T, Igarashi H, Ishii Y, Yasugi S, Momoi MY and Momoi T. Spatial expression of Sonic hedgehog in the lung epithelium during branching morphogenesis. *Biochem Biophys Res Commun* 225: 161-166, 1996.

132. Vanderwinden JM, Mailleux P, Schiffmann SN and Vanderhaeghen JJ. Cellular distribution of the new growth factor pleiotrophin (HB-GAM) mRNA in developing and adult rat tissues. *Anat Embryol (Berl)* 186: 387-406, 1992.

133. Wang M, Tan LP, Dijkstra MK, van LK, Robertus JL, Harms G, Blokzijl T, Kooistra K, van T'veer MB, Rosati S, Visser L, Jongen-Lavrencic M, Kluin PM and van den BA. miRNA analysis in B-cell chronic lymphocytic leukaemia: proliferation centres characterized by low miR-150 and high BIC/miR-155 expression. *J Pathol* 215: 13-20, 2008.

134. Weaver M, Dunn NR and Hogan BL. Bmp4 and Fgf10 play opposing roles during lung bud morphogenesis. *Development* 127: 2695-2704, 2000.

135. Weidenfeld J, Shu W, Zhang L, Millar SE and Morrisey EE. The WNT7b promoter is regulated by TTF-1, GATA6, and Foxa2 in lung epithelium. *J Biol Chem* 277: 21061-21070, 2002.

136. Wellstein A, Fang WJ, Khatri A, Lu Y, Swain SS, Dickson RB, Sasse J, Riegel AT and Lippman ME. A heparin-binding growth factor secreted from breast cancer cells homologous to a developmentally regulated cytokine. *J Biol Chem* 267: 2582-2587, 1992.

137. Wessells NK. Mammalian lung development: interactions in formation and morphogenesis of tracheal buds. *J Exp Zool* 175: 455-466, 1970.

138. White MK and Strayer DS. Surfactant protein A regulates pulmonary surfactant secretion via activation of phosphatidylinositol 3-kinase in type II alveolar cells. *Exp Cell Res* 255: 67-76, 2000.

139. Wildman SS and King BF. P2X receptors: epithelial ion channels and regulators of salt and water transport. *Nephron Physiol* 108: 60-67, 2008.

140. Williams MC. Alveolar type I cells: molecular phenotype and development. *Annu Rev Physiol* 65: 669-695, 2003.

141. Wodarz A and Nusse R. Mechanisms of Wnt signaling in development. *Annu Rev Cell Dev Biol* 14: 59-88, 1998.

142. Wright JR. Immunoregulatory functions of surfactant proteins. *Nat Rev Immunol* 5: 58-68, 2005.

143. Wright JR and Clements JA. Metabolism and turnover of lung surfactant. *Am Rev Respir Dis* 136: 426-444, 1987.

144. Wu H, Barusevicius A, Babb J, Klein-Szanto A, Godwin A, Elenitsas R, Gelfand JM, Lessin S and Seykora JT. Pleiotrophin expression correlates with melanocytic tumor progression and metastatic potential. *J Cutan Pathol* 32: 125-130, 2005.

145. Xiao C, Calado DP, Galler G, Thai TH, Patterson HC, Wang J, Rajewsky N, Bender TP and Rajewsky K. MiR-150 controls B cell differentiation by targeting the transcription factor c-Myb. *Cell* 131: 146-159, 2007.

146. Yeh HJ, He YY, Xu J, Hsu CY and Deuel TF. Upregulation of pleiotrophin gene expression in developing microvasculature, macrophages, and astrocytes after acute ischemic brain injury. *J Neurosci* 18: 3699-3707, 1998.

147. Yi R, Qin Y, Macara IG and Cullen BR. Exportin-5 mediates the nuclear export of pre-microRNAs and short hairpin RNAs. *Genes Dev* 17: 3011-3016, 2003.

148. Zeng X, Wert SE, Federici R, Peters KG and Whitsett JA. VEGF enhances pulmonary vasculogenesis and disrupts lung morphogenesis in vivo. *Dev Dyn* 211: 215-227, 1998.

149. Zhang L, Mabuchi T, Satoh E, Maeda S, Nukui H and Naganuma H. Overexpression of heparin-binding growth-associated molecule in malignant glioma cells. *Neurol Med Chir (Tokyo)* 44: 637-643, 2004.

150. Zhang N, Zhong R, Perez-Pinera P, Herradon G, Ezquerra L, Wang ZY and Deuel TF. Identification of the angiogenesis signaling domain in pleiotrophin defines a mechanism of the angiogenic switch. *Biochem Biophys Res Commun* 343: 653-658, 2006.

151. Zhang N, Zhong R, Wang ZY and Deuel TF. Human breast cancer growth inhibited in vivo by a dominant negative pleiotrophin mutant. *J Biol Chem* 272: 16733-16736, 1997.

152. Zhou B, Wang S, Mayr C, Bartel DP and Lodish HF. miR-150, a microRNA expressed in mature B and T cells, blocks early B cell development when expressed prematurely. *Proc Natl Acad Sci U S A* 104: 7080-7085, 2007.

153. Zhou L, Qi X, Potashkin JA, bdul-Karim FW and Gorodeski GI. MicroRNAs miR-186 and miR-150 down-regulate expression of the pro-apoptotic purinergic P2X7 receptor by activation of instability sites at the 3'-untranslated region of the gene that decrease steady-state levels of the transcript. *J Biol Chem* 283: 28274-28286, 2008.

154. Zou P, Muramatsu H, Sone M, Hayashi H, Nakashima T and Muramatsu T. Mice doubly deficient in the midkine and pleiotrophin genes exhibit deficits in the expression of beta-tectorin gene and in auditory response. *Lab Invest* 86: 645-653, 2006.

CHAPTER II

GENE EXPRESSION PROFILING IDENTIFIES REGULATOR PATHWAYS INVOLVED IN THE LATE STAGE OF RAT FETAL LUNG DEVELOPMENT

2.1 Abstract

Fetal lung development is a complex biological process that involves temporal and spatial regulations of many genes. To understand the molecular mechanisms of this process, we investigated gene expression profiles of fetal lungs on gestational *days 18, 19, 20*, and *21*, as well as newborn and adult rat lungs. For this analysis, we used an in-house rat DNA microarray containing 6,000 known genes and 4,000 expressed sequence tags (ESTs). Of these, 1,512 genes passed the statistical significance analysis of microarray (SAM) test; an at least twofold change was shown for 583 genes (402 known genes and 181 ESTs) between at least two time points. *K*-means cluster analysis revealed seven major expression patterns. In one of the clusters, gene expression increased from *day 18* to *day 20* and then decreased. In this cluster, which contained 10 known genes and 5 ESTs, 8 genes are associated with development. These genes can be integrated into regulatory pathways, including growth factors, plasma membrane receptors, adhesion molecules, intracellular signaling molecules, and transcription factors. Comparing the expression changes between adjacent time points, real-time PCR analysis of these 10 genes showed an 88% consistency with the microarray data. The mRNA of LIM homeodomain protein 3a (Lhx3), a transcription factor, was enriched in fetal type II cells. In contrast, pleiotrophin, a growth factor, had a much higher expression in fetal lung tissues than in fetal type II cells. Immunohistochemistry revealed that Lhx3 was localized in fetal lung epithelial cells and pleiotrophin in the mesenchymal cells adjacent to the developing epithelium and blood vessel. Using GenMAPP, we identified four regulatory pathways: transforming growth factor-β signaling, inflammatory response, cell cycle, and G protein signaling. We also identified two metabolic pathways: glycolysis-gluconeogenesis and proteasome degradation. Our results may provide new insights into the complex regulatory pathways that control fetal lung development.

Key Words: DNA microarray; cell differentiation

.

2.2 Introduction

Fetal Development of the pulmonary system is a complex and important morphogenetic process. The lung is among the last of the fetal organs to mature functionally. Development of this complex air-exchange interface can be divided into five stages (6). In the embryonic stage (*days 0–13*), the lung originates as an outpouch from the ventral wall in the primitive esophagus and grows caudally into the splanchnic mesoderm to form the right and left buds. The terminal buds then dichotomously divide until the lung forms a glandlike structure. During the pseudoglandular stage (*days 13–18*), the bronchial buds repeatedly branch into the mesenchymal tissue to form the conductive airways of the lung. At this stage, there is little lumen in the epithelial tubes. In the canalicular stage (*days 18–20*), the lung grows considerably, with multiple generations of bronchioles. Capillaries are closely arranged with the terminal and respiratory bronchioles. The columnar epithelial cells undergo morphological changes to become cuboidal epithelial cells. In the saccular stage (*day 20* to full term), the terminals of bronchioles become saccular, with the formation of alveolar ducts and air sacs. Capillaries bulge into terminal sacs to establish blood-air barriers. In the alveolar stage (from full term to adult), the alveolar-capillary barrier becomes progressively thinner, with an increasing capacity for gas exchange. The number and size of capillaries and alveoli increase markedly.

Coordinated regulation of signaling molecules and their pathways is required for fetal lung development (7, 41, 63, 80). These molecules include, for example, retinoic acid, fibroblast growth factors, transforming growth factors (TGF), and sonic hedgehog. Complex interactions occur between epithelial, mesenchymal, and extracellular matrix components. Through temporal and spatial regulations of these molecules and their interactions, the stem cells proliferate and differentiate into ≥ 40 distinct cell lineages, resulting in formation of the whole lung tissue.

DNA microarray has been used for gene expression profiling of pulmonary diseases, including lung cancers (3), emphysema (16), and hyperoxia or ventilator-induced lung injury (35, 53). This approach has been used previously to study mouse fetal lung development (2, 38). However, DNA microarray analysis of rat fetal lung development has not been reported. Gene expression in response to hypoxia differs among species (19). Our main objective in this study was to examine gene expression profiles during the late stage of rat fetal lung development. We focused on the late stage of fetal lung development because our research interests involve alveolar epithelial cell proliferation and differentiation. We used a DNA microarray representing 10,000 known rat genes and expressed sequence tags (ESTs) to profile gene expression of fetal lungs on gestational *days 18, 19, 20*, and *21* and newborn and adult rat lungs. Clustering analysis identified an important gene cluster involving lung development. Real-time PCR and Western blot

confirmed the changes in gene expression of selected genes. Several pathways were also identified using GenMAPP and literature review.

2.3 Materials and Methods

2.3.1 Microarray slide preparation.

The DNA microarray slides were prepared in-house using the Pan-Rat 50-mer 10,000K oligonucleotide set (MWG Biotech, High Point, NC), which includes 6,221 known rat genes, 3,594 rat ESTs, and 169 Arabidopsis-negative controls. The oligonucleotides were diluted to 25 µM with 3x saline-sodium citrate (SSC) and printed on epoxy-coated slides (CEL Associates, Pearland, TX) by a microarrayer (OmniGrid 100, GeneMachine, San Carlos, CA). The samples were spotted on each slide in triplicate using 16 ChipMaker Micro Spotting Pins (Telechem International, Sunnyvale, CA). This resulted in three identical 18 x 18 mm blocks on each slide, which allowed us to hybridize six samples on a single slide (Fig.II.1A). The diameter of each spot was 120 µm, and the distance between two spots was 180 µm. The printed slides were incubated in 65% humidity for 48 h, dried, and kept at room temperature. Slide quality was assessed using SYBR Green II staining. No autofluorescence was found when the blank slides were scanned.

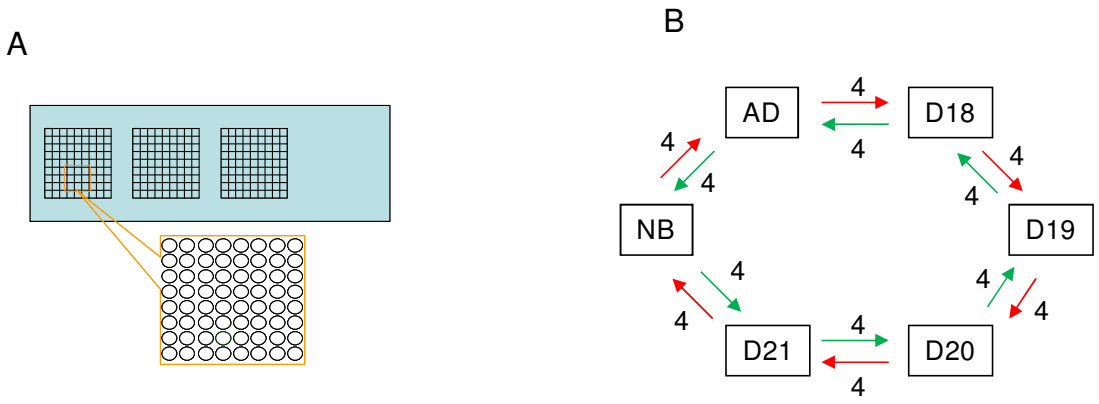

Fig.II.1. DNA microarray slides and experiment design. *A*: slides printed in-house with 3 identical blocks, each containing 10,000 rat genes, which allowed us to hybridize 6 samples on a single slide. *B*: loop design for microarray hybridization study. Each RNA sample was divided into 2 parts: one was labeled with Alexa 546 and the other with Alexa 647. Two cDNAs with different dyes were paired and hybridized to 1 block. Arrows correspond to hybridizations between 2 RNA samples: blunt end labeled green, and arrow end labeled red. Number 4 on the arrow indicates 4 biological replicate hybridizations. Opposite directions of the 2 arrows represent dye flipping. *D18, D19, D20*, and *D21*, fetal lungs at gestational *days 18, 19, 20*, and *21*; NB, newborn lung; AD, adult lung.

2.3.2 Isolation of rat fetal lungs.

We chose six lung tissues, with a focus on the late stage of fetal lung development, for our DNA microarray experiments: four fetal lungs on gestational *days 18, 19, 20*, and *21* (D18, D19, D20, and D21) and newborn (NB) and adult (AD) lungs. The Oklahoma State University Animal Care and Use Committee approved all the animal protocols used in the study. For *day 18–day 21* fetal lungs, timed-pregnant Sprague-Dawley rats were killed by CO_2 anesthesia. After the whole uterine horns were exposed and excised, the fetuses were removed and the fetal lungs were harvested. The isolated lungs were placed in ice-cold DMEM (Invitrogen, Carlsbad, CA). Newborn and adult rat lungs were collected from *day 0* (neonatal) and 2-mo-old rats. Lung epithelial type II cells were isolated from fetal or newborn lungs according to the method of Fraslon-Vanhulle et al. (15). The purity and viability of the cells exceeded 90%, as assessed by alkaline phosphatase staining and trypan blue exclusion. Adult lungs and alveolar type I and type II cells were isolated as previously described (9). Total RNAs were extracted from the lung tissues or cells with Tri-Reagent (Molecular Research Center, Cincinnati, OH).

2.3.3 DNA microarray hybridization.

A loop design was used for our microarray hybridization to compare changes in gene expression between two adjacent time points (Fig.II.1*B*). Because fetal lung development is a sequential event, a loop design has some advantages over a reference design. In a reference design, indirect comparison of adjacent time points through a common reference results in accumulated errors. In a loop design, direct comparison between two adjacent time points significantly increases the efficiency and accuracy of the experiments. Sixteen hybridizations were performed for each sample (4 biological replications, dye flip and hybridizations with 2 adjacent time points). Total RNAs were divided into two aliquots; each (10 μg) was reverse transcribed to cDNA using the modified oligo(dT) dye-specific primers from the 3DNA Array 50 kit (Genisphere, Hatfield, PA). The cDNA was purified with Microcom YM-30 columns (Millipore, Billerica, MA) and mixed with 2x hybridization buffer (50% formamide, 6x SSC, and 0.2% SDS). The cDNA concentrations were adjusted to 300 ng/μl. Five microliters of cDNAs from two adjacent time points were mixed and hybridized to one of three blocks on a microarray slide for ≥24 h at 42°C. After the unbound cDNAs were washed away with 2x SSC buffer (Sigma-Aldrich, St. Louis, MO), the slides were further incubated with 3 DNA capture reagents labeled with green (Alexa 546) or red (Alexa 647) dye for 2–3 h. Then the slides were washed again and scanned (ScanArray Express, Perkin Elmer, Boston, MA). The laser power and photomultiplier tube were adjusted so that ~5% of the spots were saturated.

2.3.4 Microarray data analysis.

The scanned images were first inspected visually to uncover systematic biases or macroartifacts. Because of weak or bad hybridizations, 8 of 48 hybridizations (6 time points X 4 biological replications X 2 dye swap) were discarded. The signal intensity for each spot was obtained from the scanned slides using GenePix 5.0. The ratios between adjacent time points were normalized by LOWESS normalization using RealSpot software, which was developed in our laboratory (10). A quality index (QI) for each spot, based on signal intensity and signal-to-background ratio, was exported from RealSpot. The mean QI values were calculated by Excel. Any spots with mean QI < 1 were filtered. One-class significance analysis of microarray (SAM) statistical test was applied to the remaining genes using a cutoff *q* value of <0.01 (http://www.stat.stanford.edu/~tibs/SAM/). The genes that passed the SAM test were further filtered using a fold change cutoff value of <2 by comparing each of adjacent two time points and a coefficient of variation cutoff value of >0.5. The final genes were clustered by *K*-means clustering using Cluster and TreeView (http://rana.lbl.gov/index.htm?stanford/). For each cluster, the expression patterns were analyzed and the major functional categories were assigned using Gene Ontology (http://www.geneontology.org/). Biological pathways were identified using GenMAPP (http://www.genmapp.org/), a recently developed tool for visualizing expression data in the context of biological pathways. The $\log_2$(ratios) of *day 18* to adult (D18/AD) and newborn to adult (NB/AD) were used for comparison of prenatal, postnatal, and adult lungs.

2.3.5 Real-time PCR.

The gene verification was carried out by real-time PCR on the same RNA samples used for the DNA microarray hybridization. Total RNAs were treated with RNase-free DNase (Ambion, Austin, TX) to remove DNA contamination and reverse-transcribed into cDNA using random hexamers and Maloney's murine leukemia virus reverse transcriptase (Invitrogen). Real-time PCR primers were designed using Primer Express software (Applied Biosystems, Foster City, CA). The length of each primer was 20–25 bp, with a melting temperature of 58–60°C (Table.II.1). Real-time PCR was performed on an ABI 7500 system using SYBR Green I detection (Qiagen, Valencia, CA), as previously described (79). To eliminate the effects of primer dimers, we included a data acquisition step at 2–5°C lower than the annealing temperature of the products. After the amplification, a melt curve was generated to check the specificity of the amplification. A standard curve was constructed on the basis of serial dilutions of a standard (10^7 to 10 copies) and corresponding threshold cycles. Standards were obtained by normal PCR and purified from agarose gel. The copy number was calculated from the standard curve and normalized to 18S rRNA.

Table.II.1. Real-time PCR primers

GenBank ID	Gene Name	Up	Down
AF370446	Lhx3	AACCACTGGATTAGTGACTACCA	GTCCAAGATGTGCTGGTCACAT
AY045577	Epha3	CCCATCAAGTTCTCCGAGAAGTT	GACACTTCCAATGCAGGTTGTG
NM_013414	Bgp	GACAAGTCCCACACAGCAACTC	TGGACATGAAGGCTTTGTCAGA
NM_017066	Ptn	ATACCAGCAGCAACGTCGAAA	GCACACACTCCATTGCCATT
NM_019161	Cdh22	GTGCTGGCTTTGCTGATTCTC	AGCTCGTCGATCAGGAAGATG
NM_019286	Adh3	CGGTTAGTGGATCCCTGTTCA	TATCACCTGGTTTCACACAAGTCA
NM_024141	Thox2	CCAGGGATGACCAAGAATGTG	TGGTCTCAAGTGACGGTAACAGA
NM_031043	Gyg	ACCAAGCCATGGAATTACACGTA	CCACCACAGGTTCAGAAACTCTG
NM_053744	Dlk1	GTGAAGAACCATGGCAGTGTGT	GACAGTCCTTTCCAGAGAATCCA
NM_057190	Nelf	TTTGCCAAAGTGGAGAAGGAA	CCCATGATGTGGATGACATTTG
M11188	18S rRNA	TCCCAGTAAGTGCGGGTCATA	CGAGGGCCTCACTAAACCATC

Primers were designed by Primer Express software. Each primer was 20–25 bp long with a melting temperature of 58–60°C. All genes sequences were from *Rattus norvegicus.* Lhx3, LIM homeodomain protein 3a; EphA3, ephrin A3; Bgp, osteocalcin; Ptn, pleiotrophin; Cdh 22, cadherin 22; Adh3, alcohol dehydrogenase 3; Thox2, NADH/NADH thyroid oxidase; Gyg, glycogenin; Dlk1, delta-like homolog *Drosophila;* Nelf, nasal embryonic luteinizing hormone-releasing hormone factor.

2.3.6 Immunohistochemistry.

The isolated fetal lungs were briefly washed with deionized water and immediately fixed with 4% formaldehyde in PBS. After 24 h of incubation, the lungs were rinsed with PBS, dehydrated in graded alcohol and xylene, and embedded in paraffin (60°C). Paraffin-embedded lungs were sectioned (4 μm) and placed on polylysine-coated glass slides. The lung sections were boiled for 30 min in 20 mM citrate buffer (pH 6.0) for antigen retrieval, which exposed the antigens masked during the sample fixation process. The sections were permeabilized with 0.3% Triton X-100 in PBS for 15 min and blocked with 10% fetal bovine serum in PBS for 30 min and then incubated in goat anti-pleiotrophin (Ptn) or rabbit anti-LIM homeodomain protein 3a (Lhx3) antibodies (1:100 dilution; Abcam, Cambridge, MA) overnight at 4°C. The slides were washed and then incubated with biotinylated anti-goat or anti-rabbit antibody for 30 min and for an additional 30 min with ABC reagent (Vector Laboratories, Burlingame, CA). The slides were developed with 3,3'-

diaminobenzidine until the desired staining appeared. Finally, the slides were mounted with antifade medium (5% n-propyl gallate and 80% glycerol in PBS) and examined using a Nikon Eclipse E600 microscope.

2.3.7 Western blot.

The lung tissues were homogenized in lysis buffer (10 mM Tris·HCl, pH 7.5, 1% Triton X-100, 1 mM EDTA, 1 mM phenylmethylsulfonyl fluoride, 10 μg/ml aprotinin, and 10 μg/ml leupeptin) on ice. Protein concentration was determined using the D_C protein assay kit (Bio-Rad, Hercules, CA). Total proteins were separated by 10% SDS-PAGE and then transferred onto a nitrocellulose membrane. The blot was stained by Ponceau S to check transfer efficiency. The membrane was blocked with 5% dry milk in Tris-buffered saline for 1 h, washed with Tris-buffered saline containing 0.05% Tween 20, and incubated with goat anti-Ptn antibody (1:1,000 dilution) or mouse anti-β-actin antibody (1:1,000 dilution; Bio-Rad) overnight at 4°C. The membrane was washed again and incubated with horseradish peroxidase-conjugated anti-goat or anti-mouse IgG (1:2,000 dilution) for 1 h. Finally, the membrane was developed with enhanced chemiluminescence reagents (Amersham Biosciences, Piscataway, NJ) and exposed to X-ray film.

2.4 Results

2.4.1 DNA microarray data analysis.

To identify the genes that changed during the late stage of fetal lung development, we performed DNA microarray (10,000 genes) analysis. Six samples (D18, D19, D20, D21, NB, and AD) were arranged for hybridization using a loop design (Fig.II.1B). There were a total of 48 hybridizations (4 biological replications and dye-flip): 8 were excluded because of poor images and 40 were used for further data analysis [D18/AD (n = 6), D19/D18 (n = 7), D20/D19 (n = 6), D21/D20 (n = 8), NB/D21 (n = 5), and AD/NB (n = 8)]. The data were subjected to LOWESS normalization. Bad or weak spots were removed by filtration using a cutoff QI < 1. Of these 10,000 genes, 1,512 (928 known genes and 584 ESTs) passed the one-class statistical SAM test using a false discovery rate (q value) of <0.01. Additional criteria were used to identify 583 genes (402 known genes and 181 ESTs): a fold change of ≥2 and a coefficient of variation of <0.5. The gene names, gene identifications, average $\log_2$[(ratio)s], Gene Ontology (GO) identifications, and GO terms are listed in supplemental Table 1 (see online version of this article). The microarray dataset is available at GEO database (http://www.ncbi.nlm.nih.gov/geo; GSE2160 [NCBI GEO]).

2.4.2 Cluster analysis and major functional categories.

We used K-means cluster analysis to cluster the 583 above-mentioned genes into 5–20 nodes. We found that the best approach was to group the genes into seven clusters on the basis

of their expression patterns (Fig.II.2A). Of the 583 genes, 272 were annotated by GO (http://www.geneontology.org). The percentage of major functions for each cluster was calculated and is shown in Fig.II. 2B.

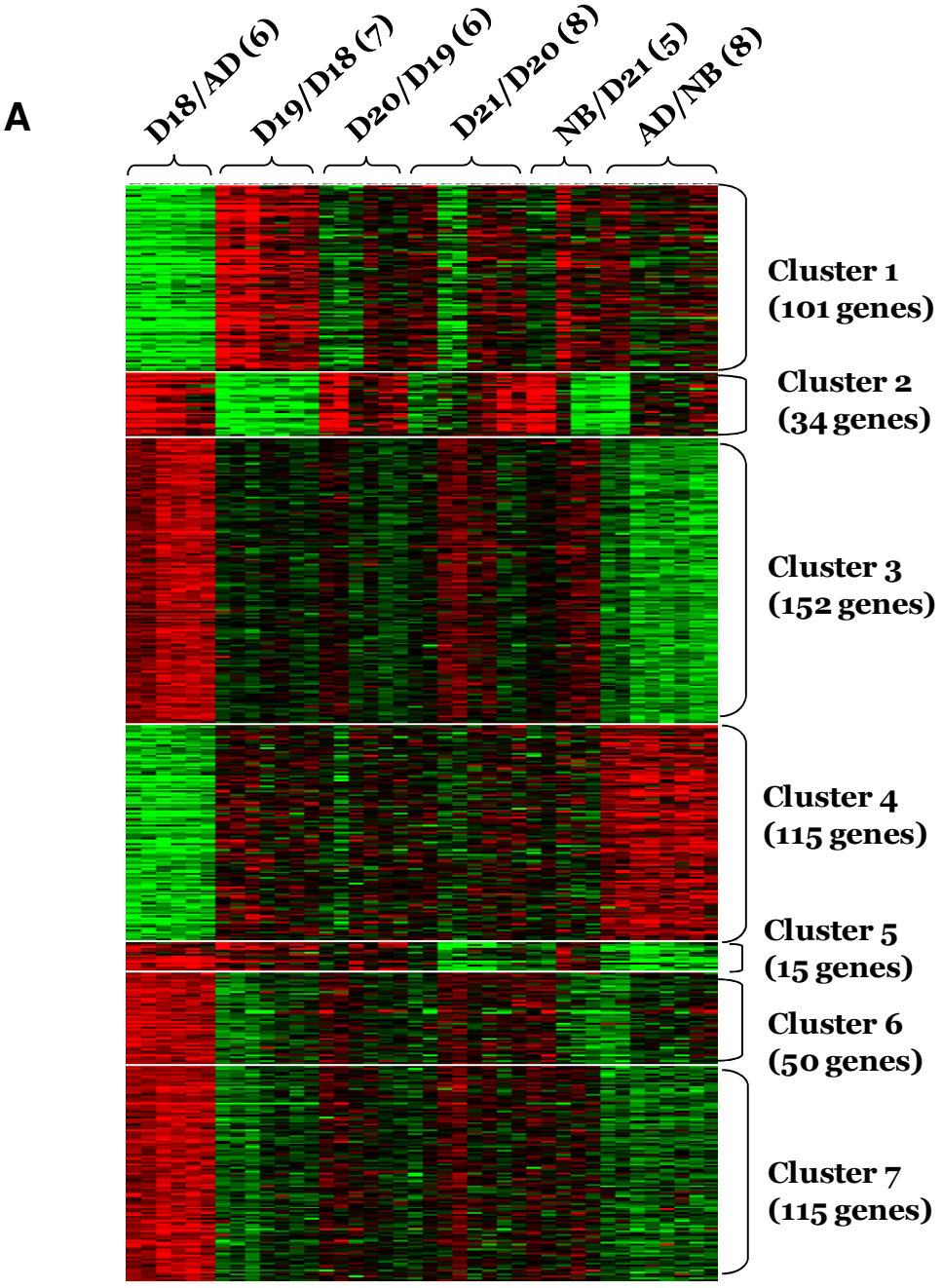

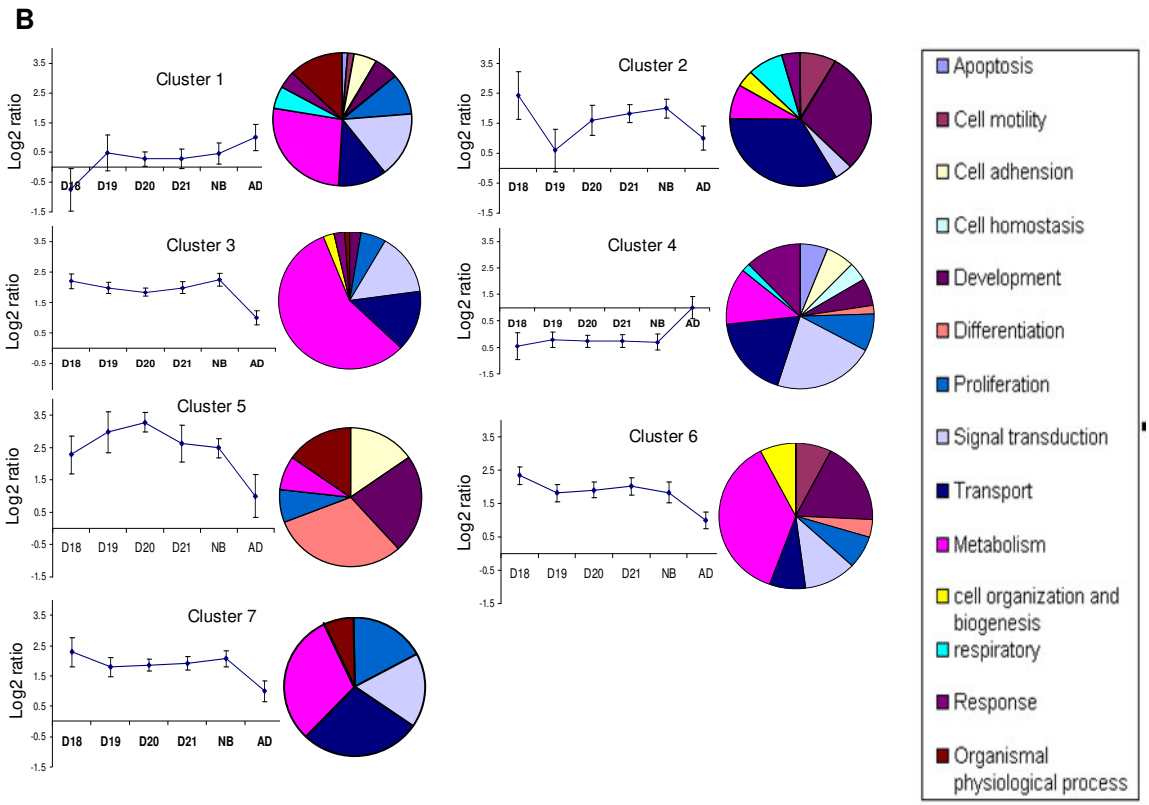

Fig.II.2. Tree view and functional categories for clustered genes. *A*: *K*-means clustering analysis on 583 genes, which significantly changed between ≥ 2 time points ($P < 0.01$, fold change ≥ 2, coefficient of variation ≤ 0.5) using cluster and tree view. Genes were clustered into 7 clusters. Each row corresponds to 1 gene, and each column corresponds to 1 $\log_2$(ratio). Numbers in parentheses adjacent to ratios represent number of hybridizations used for data analysis. Red, upregulation; green, downregulation; black, no change. Brightness of the color represents the value of the ratio. *B*: expression patterns and functional analysis of each cluster. The 7 clusters identified from *K*-means clustering analysis were plotted as $\log_2$ (ratio) vs. time. Distribution of major functional categories for biological process terms are shown in pie charts. The $\log_2$(ratio) is each time point vs. adult. Values are means ± SD.

2.4.3 GenMAPP.

To identify signaling pathways, metabolic pathways, and other functional groups that may be involved in fetal lung development, we used GenMAPP to visualize the changes in gene expression. The log2(D18/AD) and log2(NB/AD) were chosen to represent prenatal, postnatal, and adult lungs. The data sets were imported into GenMAPP. Four major regulatory pathways (TGF-β signaling, inflammatory response, cell cycle, and G protein signaling) and two metabolic

pathways (glycolysis-glycogenesis and proteasome degradation) were identified (data not shown).

2.4.4 Real-time PCR validation.

We next focused on cluster 5, the "differentiation cluster," for further studies. Gene expression in this cluster increased in the canalicular stage (D18–D20) and then decreased (D20 to AD). This group consists of 5 ESTs and 10 known genes. Among the 10 known genes, 8 were directly or indirectly involved in development or cell differentiation. Table.II.2 shows the major functions and the cellular locations of these 10 known genes.

Table.II.2. Cluster 5 genes and their functions

Name	Location	Major Functions	Protein Localization
Lhx3	Neuron, pituitary	Homeobox gene family; homeodomain transcription factor; important in cell migration and development	Nucleus
EphA3	Neuron	Involved in Wnt-Frizzled signaling, which controls various aspects of early development; differentiation; guide for axonal patterning during neuronal development	Membrane
Nelf	Neuron, brain, muscle	Guide for migration of olfactory axon and gonadotropin-releasing hormone neurons; cell development	Cytoplasm
Bgp	Bone	Bone-specific gene	Extracellular matrix
Ptn	Bone	Growth factor activity; heparin binding; regulation of cell cycle; ossification; cell proliferation	Extracellular matrix
Cdh22	Brain, pituitary	Integral to membrane; brain development; Ca^{2+}-dependent cell-cell adhesion	Membrane
Adh3	Mixed tissue	Alcohol oxidation; stimulation of retinoic acid synthesis; stimulation of cell growth	Cytoplasm
Dlk1	Mixed tissue	Membrane-spanning protein containing 6 epidermal growth factor-like repeat motifs, regulating growth and differentiation through cell-cell interaction	Membrane
Thox2	Mixed tissue	NAD(P)H oxidase activity	Membrane
Gyg	Mixed tissue	Glycogenin glucosyltransferase activity; glycogen biosynthesis	Cytoplasm

We attempted to verify the microarray data from the 10 known genes in *cluster 5* using absolute quantitative real-time PCR. The copy number was obtained from the standard curve constructed from the purified PCR products and normalized to 18S rRNA. The expression levels of these genes are shown in Fig.II.3A. Delta-like homolog *Drosophila* 1 (Dlk1) had the highest expression, followed by glycogenin, Ptn, and alcohol dehydrogenase-3 (Adh3). In contrast, expression of Lhx3 was the lowest. The $\log_2$(ratio) between adjacent time points was calculated and compared with the microarray data. As shown in Fig.II.3*B*, 88% of the $\log_2$(ratios) from real-time PCR were consistent with the microarray data, even though absolute changes varied. In general, fold change of real-time PCR was greater than that of the microarray, probably because of the difference between the two methods (solid-state vs. solution hybridization), which makes the real-time PCR more sensitive than microarray.

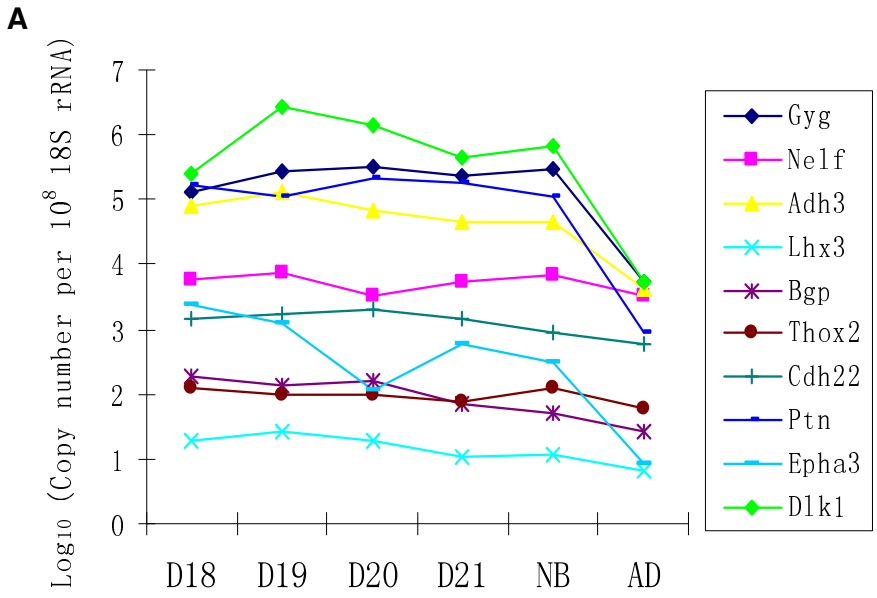

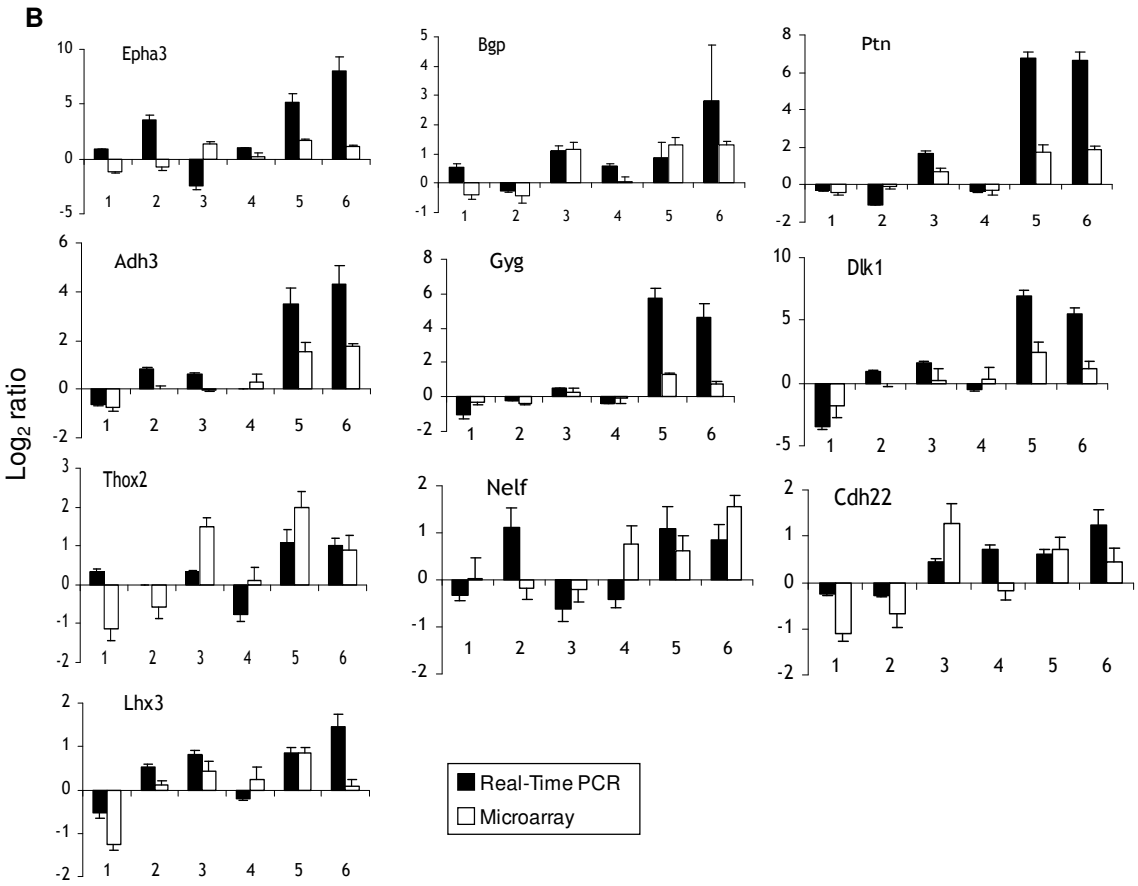

Fig.II.3. mRNA expression of *cluster 5* genes during fetal lung development: comparison of microarray with real-time PCR. Total RNA was extracted from fetal lungs on gestational *days 18–21* and from newborn and adult lungs and reversed transcribed to cDNA. mRNA levels were determined by real-time PCR, and data were normalized to 18S rRNA. A: relative mRNA expression levels of cluster 5 genes. B: comparison of microarray and real-time PCR: D18/D19 (1), D19/D20 (2), D20/D21 (3), D21/NB (4), NB/AD (5), and D18/AD (6). Values are means ± SE; n = 8 (4 animal groups and each assay performed in duplicate) for microarray and real-time PCR.

2.4.5 mRNA expression of Ptn and Lhx3 in fetal lung cells.

The mRNA levels of Ptn and Lhx3 in the isolated lung cells were determined using real-time PCR. Ptn was highly expressed in fetal lung tissues (D18, D19, D20, D21, and NB), but there was essentially no expression in adult lung tissues (AD; Fig.II.4A). Ptn mRNA expression in isolated alveolar epithelial type II cells from fetal lungs on days 18 and 19 and newborn and adult lungs was negligible. Also the mRNA of Ptn was not found in alveolar epithelial type I cells or macrophages isolated from adult lungs. On the other hand, mRNA expression of Lhx3 was high in type II cells isolated from fetal lungs on days 20 and 21 and newborn lungs (Fig.II.4B) but low

in type II cells isolated from fetal lungs on days 18 and 19 and adult lungs and low in type I cells isolated from adult lungs and in macrophages. Relatively low expression of Lhx3 was observed in fetal and adult lung tissues, indicating its specific expression in fetal type II cells.

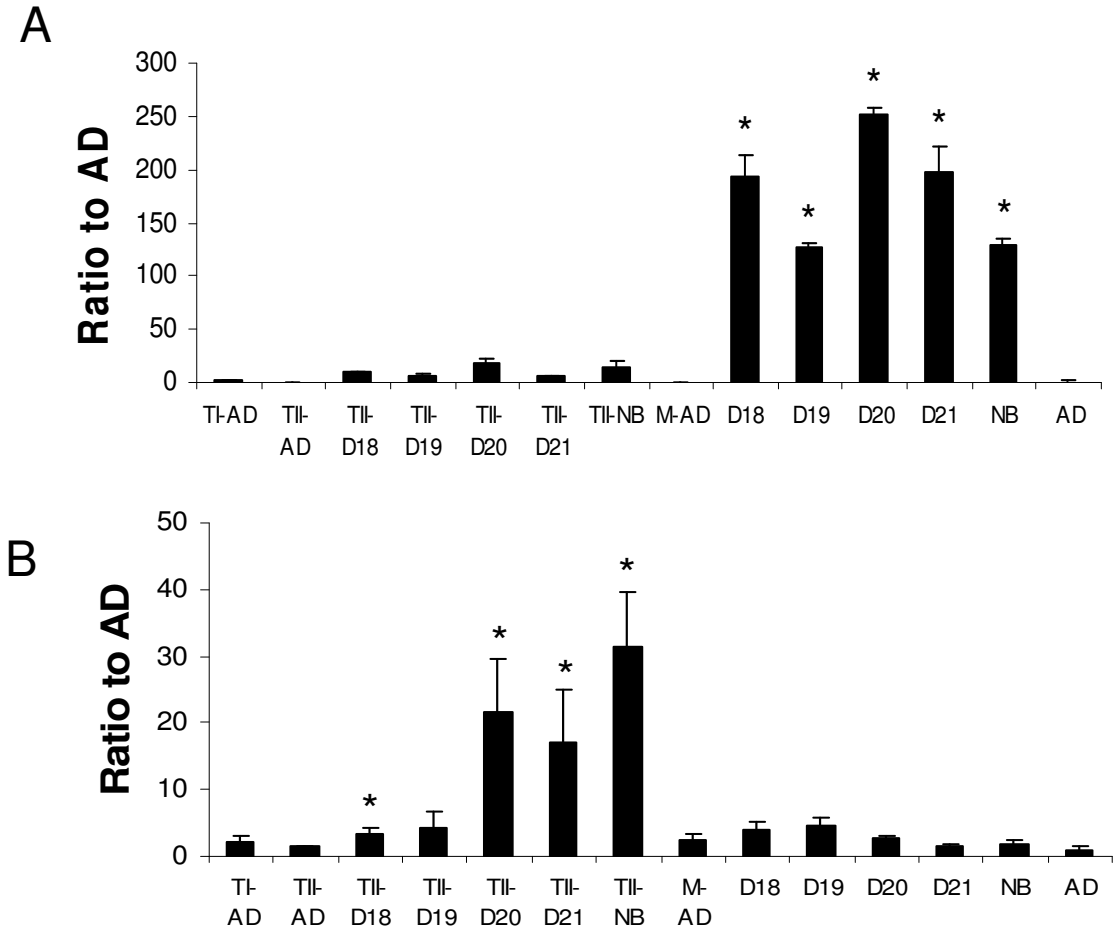

Fig.II.4. Real-time PCR analysis of pleiotrophin (Ptn) and LIM homeodomain protein 3a (Lhx3) in fetal lung cells. Total RNA was extracted from lung tissues and reverse transcribed to cDNA. mRNA abundance of Ptn (*A*) and Lhx3 (*B*) was determined by real-time PCR in adult alveolar type I cells (TI-AD), adult alveolar type II cells (TII-AD), fetal epithelial type II cells on gestational *days 18–21* (TII-D18 to TII-D21), newborn alveolar type II cells (TII-NB), adult microphages (M-AD), fetal lung tissue on gestational *days 18–21*, and newborn and adult lung tissue. Values are means ± SE; $n = 8$ (4 biological preparations, each assay performed in duplicate). *$P < 0.05$ vs. AD or TII-AD.

2.4.6 Ptn and Lhx3 protein expression.

We used Western blot to quantify Ptn protein expression in fetal lung tissues. Ptn protein was significantly upregulated in fetal lungs on *days 20* and *21* and newborn lungs compared with fetal lungs on *days 18* and *19*. However, very little Ptn protein was found in adult lungs (Fig.II.5*A*).

To determine the cellular localization of Ptn and Lhx3 proteins in fetal lungs, we performed immunohistochemistry using the ABC reagent. Lhx3 was primarily expressed in the columnar cells of the developing airways. The positive signal was located in the nucleus and showed a purplelike color on counterstaining with hematoxylin (Fig.II.5*B*). Ptn was located in the mesenchyme adjacent to the developing epithelium and endothelium (Fig.II.5*B*). Some staining was noted on the endothelial cells. No positive staining was found in the negative control without primary antibodies (data not shown).

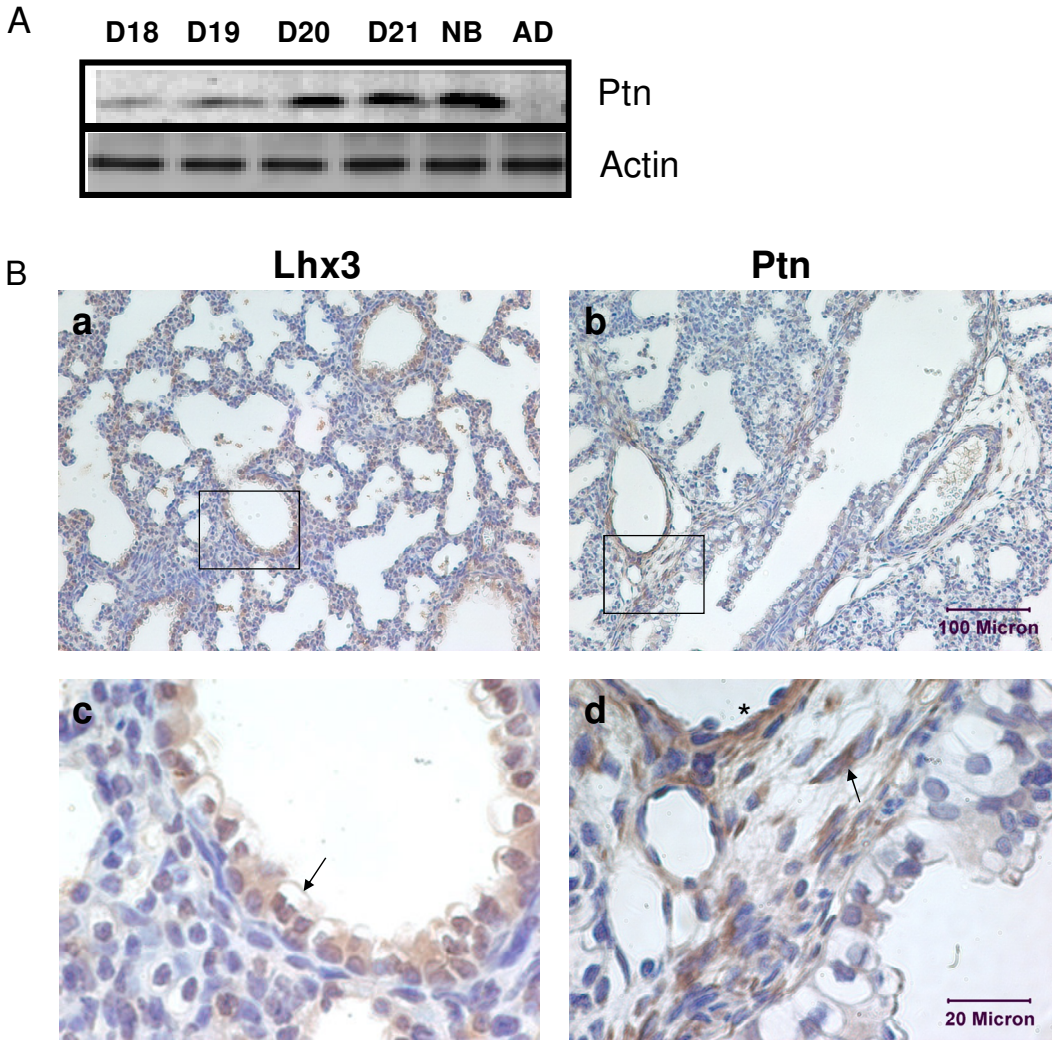

Fig.II.5. Protein expression and cellular location of Lhx3 and Ptn. *A*: Western blot analysis of Ptn in fetal lungs on gestational *days 18–21* and in newborn and adult lungs. β-Actin was used as loading control. *B*: D20 fetal lung tissue sections stained using anti-Lhx3 (*a* and *c*) and anti-Ptn (*b*

and *d*) antibodies. Panels c and d are enlarged fields enclosed in boxes of panels a and b, respectively. Lhx3 was located in the nucleus of columnar epithelial cells (arrow). Endothelial cells (*) and mesenchymal cells (arrow) around the epithelium and blood vessels stained positive for Ptn. Results are representative of lung tissue sections from 4 animals; all show similar staining.

2.5 Discussion

The gene expression profiles of fetal lung development in mice have been reported elsewhere (2, 38). However, the present study is the first to investigate rat fetal lung development using DNA microarray and is different from the previous studies in several ways. *1)* We used a loop design to directly compare two adjacent time points. Therefore, the number of accumulated errors was decreased. *2*) We performed 16 hybridizations for each sample and, thus, had a relatively large number of biological and technical replications. As a result, the accuracy of the experiments was increased. Indeed, real-time PCR verified 88% of the selected genes if compare the gene expression changes between two adjacent time points. *3*) We focused on the late stage of fetal lung development (D18 to NB) to identify the genes involved in cell proliferation and differentiation. This also enabled us to perform a detailed study during this stage with a fetal lung sample from each day. *4*) Using cluster analysis combined with GO, we were able to identify a novel differentiation cluster composed of 10 known genes and 5 ESTs involved in cell proliferation, cell differentiation, and development.

Some genes identified in our study have expression patterns similar to those in mice, such as Dlk1, glyceraldehyde-3-phosphate dehydrogenase, and a number of genes in the tyrosine kinase family. However, a significant number of the genes identified in our study are different from those identified in the mouse studies (2, 38), perhaps because of species difference. Comparative studies revealed different gene profiles of the lungs in response to hypoxia between the rat and the mouse (19). Another possible reason is the difference in DNA microarray platforms and data analysis.

During fetal lung development, cell proliferation and cell population undergo dynamic changes. The rate of cell proliferation increases at the pseudoglandular stage and declines at the canalicular and saccular stages. However, the percentage of dividing interstitial cells decreases from gestational *day 17* to *day 20* and then markedly increases on *day 20*. An opposite trend is seen for epithelial cells (1). This raises the possibility that some of the changes in gene expression may reflect the difference in cell population in the developing lung. Although we cannot rule out the possibility, the changes in gene expression in *cluster 5* seem not to correspond to cell population, at least in the fetal stages (1). The change in Ptn mRNA between

prenatal and adult stages is tremendous (>100-fold) and is probably not due to fewer mesenchymal cells in the adult lung.

Two genes, Ptn and Lhx3, were further characterized at mRNA and protein levels. Ptn and Lhx3 were located in fetal lung fibroblasts and epithelial cells, respectively. Ptn, an 18-kDa heparin-binding cytokine (13), is highly expressed in the late stage of embryogenesis (17, 33, 77) and postnatally in the nervous system (66). It shares 50% sequence homology with midkine, which may play a role in lung morphogenesis. In contrast to Ptn, midkine is primarily localized in epithelial cells of mouse lung from gestational *day 18* to birth. Its expression is high from gestational *days 13–16* but low from *day 18* to birth and is undetectable in adult lungs (55). Midkine expression is stimulated by retinoic acid but inhibited by glucocorticoid (26).

Ptn acts through two cell surface receptors, anaplastic lymphoma kinase (ALK) and the protein tyrosine phosphatase receptor RPTPβ/ζ. ALK is the receptor tyrosine kinase that is expressed in the developing nervous systems and some tumor cells (25, 44). On binding with Ptn, ALK activates the Ras-MAPK and the phosphatidylinositol 3-kinase-Akt signaling pathways (54, 70), leading to the stimulation of cell proliferation and the inhibition of apoptosis.

Ptn also regulates β-catenin phosphorylation through RPTPβ/ζ. In the absence of Ptn, β-catenin is associated with E-cadherin. The binding of Ptn to RPTPβ/ζ results in the dimerization and inactivation of the receptor and, thus, an increase of the tyrosine phosphorylation of β-catenin (42). Phosphorylated β-catenin rapidly dissociates from E-cadherin. Recently, Fyn, a member of the Src family (51), and β-adducin (52) have been found to be downstream targets of the Ptn/RPTPβ/ζ signaling pathway. Because it is the central component of the Wnt signaling pathway (82), β-catenin may be a link between Ptn and Wnt signaling pathways. However, the association between these two pathways and the possible role of the Ptn/ RPTPβ/ζ pathway in fetal lung development remain to be determined.

Lhx3, one of the LIM homeodomain transcription factors, is essential for pituitary development and function (11). Mutations in the human Lhx3 gene result in severe endocrine disease and cause a deficiency in all anterior pituitary hormones except adrenocorticotropin (47, 68). Lhx3 is thought to be one of the genes that play an important role in the development of Rathke's pouch, beginning at around embryonic *day 8.5* in the mouse (64). In situ hybridization reveals the highest expression of Lhx3 in the developing lung and pituitary (61). However, its function in lung development has not been studied.

Ephrin (Eph) A3 is a GPI-anchored membrane glycoprotein and a ligand for Eph receptors. The binding of clustered Eph to Eph receptors activates the downstream cascade of the Eph signaling pathway and regulates vascular aggregation and homeostasis. Recently, EphA3 has been identified as a downstream protein of the Wnt-Frizzled signaling pathway (32). Wnt modulates lung morphogenesis through the canonical β-catenin/lymphocyte enhanger factor-T

cell factor pathway (45). In the presence of Wnt, β-catenin is stabilized and accumulates in the nucleus to activate transcription of its downstream genes, such as N-*myc*, bone morphogenetic protein 4 (Bmp4), and fibroblast growth factor (FGF) (65).

Dlk1 belongs to the family of epithelial growth factor-like homeotic proteins that are involved in regulating growth and differentiation through cell-cell interaction. Dlk1 inhibits the differentiation of preadipocytes to mature adipocytes (67). Dlk1 acts through the Notch pathway (24). The binding of their ligands, Delta-like or Jagged, with Notch receptors results in a proteolytic cleavage of the Notch intracellular domain. The latter translocates into the nucleus and associates with a transcription factor, RBP-Jk. As a result, it activates expression of the downstream target genes, including hairy and enhancer of split (Hes) and Hes-related repressor protein transcriptional repressors. In situ hybridization of fetal lung mouse tissue shows that Dlk1 expression is high on gestational *day 12.5* but downregulated on *day 16.5* (85), similar to our microarray results.

Adh3 catalyzes the synthesis of retinoic acid, a biologically active derivative of vitamin A. Retinoic acid is important for lung branching morphogenesis (36). It regulates expression of the genes encoding for surfactant proteins and the enzymes that produce surfactant lipids (78). Adh3 expression is turned on at the late stages of liver development (76), but its temporal expression during fetal lung development is unknown.

Cadherin-22 is responsible for Ca^{2+}-dependent cell-cell adhesion and is one of the important membrane proteins for mesenchymal-epithelial interaction in brain development (4, 22). Cadherin-22 is temporally and spatially expressed in the developing brain; its mRNA expression reached the highest level during the early postnatal stage and then declined at *day 10* (71). Whether NADH/NADH thyroid oxidase-2 and glycogenin regulate fetal lung development has not been studied, but the similarity between their expression patterns and those of the other development-associated genes in this cluster suggests that they might have roles in this process.

The power of DNA microarray data is to generate hypotheses for further functional studies. From our gene expression data and the gene functions in *cluster 5*, we proposed a working model for regulation of fetal lung development and alveolar epithelial type II cell differentiation. However, we should emphasize that these pathways in fetal lung cells are highly speculative at this stage, because we have not determined the expression of each component in respective cells (except Ptn and Lhx3) as well as their interactions. In fetal lung fibroblasts or other mesenchymal cells, Adh3 catalyzes the synthesis of retinoic acid, which translocates into the nucleus and stimulates expression of Ptn. After its secretion, Ptn binds to the RPTPβ/ζ on the surface of epithelial type II cells. This inhibits the phosphatase activity of RPTPβ/ζ and rapidly increases the tyrosine phosphorylation of β-catenin, which decreases its affinity to cadherin. Next, β-catenin is released, enters the nucleus, and increases the expression of Lhx3 and other target genes. The increased Lhx3 expression may exert a positive-feedback regulation on its expression. Other genes in this

cluster, Dlk1 via the Notch pathway and EphA3 via the Wnt pathway, may coregulate fetal lung development and fetal epithelial type II cell proliferation and differentiation.

The 583 identified genes were grouped into seven clusters. *Cluster 1* is composed of 101 genes (21 ESTs and 80 known genes). The expression level of these genes was low in the fetal lung at *day 18* and high the adult lung. The major functional categories of this cluster are metabolism and signal transduction. Seven genes are associated with cell proliferation. Phospholipase A_2 group 1b (Pla2g1b) promotes cell proliferation and migration via receptor-mediated effects (29). Zinc finger protein hf-1b is a ubiquitous transcription factor. However, when it combines with a muscle factor (hf-1b/mef-2), hf-1b confers cardiac muscle-specific gene expression (46). Hes3, a member of the basic helix-loop-helix transcription factor family, regulates mammalian neural development (34). FGF receptor 2 (FGFR2) is the most common receptor for FGF-1, FGF-7, and FGF-10. $FGFR2^{-/-}$ mice are viable until birth and show severe lung defects (12). Prostaglandin-endoperoxide synthase 2 (ptgs2) is a nuclear membrane protein that may negatively regulate cell proliferation (59). Merlin (Nf2) inhibits cell cycle progression by decreasing cyclin D1 expression (84). 11-β Hydroxysteroid dehydrogenase type 1 (Hsd11b1) regulates lung maturation by synthesizing glucocorticoid locally (20). RTI40 (also called T1α), a lung type I cell-specific protein, can be used as a biochemical marker for acute lung injury (40). The developmental expression of hsd11b and RTI40 in the lung is consistent with our microarray data (21, 81).

The 34 genes (9 ESTs and 25 known genes) in *cluster 2* were decreased in the canalicular stage and then gradually increased in the saccular stage and declined after birth. Eight genes in this cluster are related to ion transport and five to development. Interestingly, four of the five development-related genes are involved in muscle development, including skeletal troponin I (Tnni2), cardiac troponin I (Tnni3), γ-enteric muscle actin (actg2), and cysteine-rich protein 3 (csrp3). Tnni2 and Tnni3 are different isoforms in the thin filament-linked Ca^{2+} regulatory system in vertebrate striated muscle (49). Actg2 is a major component of the organized contractile apparatus of smooth muscle cells (60). Csrp3 is a LIM domain protein that promotes myogenic differentiation and is a novel regulator of myogenesis (5, 48). α-Crystallin B (Cryab), a small heat shock protein involved in sensory organ development, has cytoprotective and oncogenic functions (50).

Cluster 3 is the largest cluster, consisting of 152 genes (112 known genes and 40 ESTs) that exhibit downregulation of expression levels after birth. More than half of these genes are involved in metabolism; most of the metabolic proteins are ribosome proteins for protein biosynthesis. Additionally, five genes have roles in development or cell proliferation. High-mobility group 1 (hmg1) may contribute to the pathogenesis of acute lung injury. Antibodies against hmg1 reduce lipopolysaccharide-induced acute lung injury (74). The synaptonemal complex protein 1 (Sycp1) is

a component of the synaptonemal complexes involved in chromosome pairing during meiosis (14). Intestine and stomach expression 1 (Mist1) is a basic helix-loop-helix transcription factor that regulates developmental patterns through the G protein-coupled signaling pathway (31). Myosin Ib (Myo1b) is a widely expressed protein involved in cell motility (51).

Expression of the 115 genes in *cluster 4* (86 known genes and 29 ESTs) was higher in adult than in fetal and newborn lungs. These genes may be important for normal lung function during adulthood. There are two major functional categories in this cluster: signal transduction and transport. Four genes are involved in cell growth. Latent TGF-β-binding protein-1- or -2-like proteins (Ltbp1 or Ltbp2) are extracellular matrix proteins that regulate TGF-β activity (57). Activin A receptor type II-like-1 (Acvrl1), a member of the TGF-β type I receptor family, is highly expressed in endothelial cells and functions in the normal development of the arterial and venous vascular beds (62, 75). Bmp6 regulates embryonic tissue development, cell proliferation, differentiation, morphogenesis, and apoptosis in multiple systems via the TGF-β-signaling pathway (18).

The gene expression patterns in *cluster 6* (40 known genes and 10 ESTs) and *cluster 7* (50 known genes and 65 ESTs) are similar. About 40% of the genes in *cluster 6* and 30% of the genes in *cluster 7* are related to metabolism. A significant percentage (10%) of the genes in *cluster 6* are involved in development. EphB1 is a developmentally regulated membrane protein involved in neurogenesis (43). Its expression is induced by retinoic acid (58). In rat brain, EphB1 mRNA level is high in the fetal stages but low in the adult (8). α-Tropomyosin (56), α_1-actin (39), and myogenin (83) are involved in muscle development. Protein arginine *n*-methyltransferase, a nuclear enzyme, catalyzes *S*-adenosyl-L-methionine-dependent methylation of arginine residues during organogenesis (37).

A relatively large number of genes in *cluster 7* participate in transport, signal transduction, and proliferation. The proliferation-related genes include TGF-α, high-mobility group protein 2 (hmg2), Ran, pituitary tumor-transforming 1 (Pttg1), and topoisomerase (DNA)-2α (Top2a). Except for TGF-α, all the genes are nuclear proteins and involved in regulation of the cell cycle, protein transcription, or cell maintenance (27, 69, 72, 73). TGF-α is a growth factor that regulates the cell cycle. Overexpression of TGF-α disrupts lung morphogenesis (30) and surfactant homeostasis (23). Expression of TGF-α is decreased during the late stage of fetal lung development (28).

Gene expression profiles of fetal lungs at the late developmental stages were examined in this study. The 583 identified genes were clustered according to their expression patterns. *Cluster 5* contained 10 known genes and 5 ESTs that are involved in cell proliferation, cell differentiation, and development. In general, expression of the genes in this cluster was high in the late stage of fetal lung development but low in adult lungs. Most of these genes have not been studied in the

lung. These genes might be incorporated into several pathways, including retinoic acid signaling, Ptn-β-catenin signaling, and the Notch and Wnt pathways. Our findings may provide important clues for further understanding of molecular mechanisms in fetal lung development.

2.6 References

1. Adamson IY. Development of lung structure. In: *The Lung: Scientific Foundations*, edited by Crystal RG and West JB. Philadelphia, PA: Lippincott-Raven, 1997, p. 993–1001.
2. Bonner AE, Lemon WJ, and You M. Gene expression signatures identify novel regulatory pathways during murine lung development: implications for lung tumorigenesis. *J Med Genet* 40: 408–417, 2003.
3. Borczuk AC, Gorenstein L, Walter KL, Assaad AA, Wang L, and Powell CA. Non-small-cell lung cancer molecular signatures recapitulate lung developmental pathways. *Am J Pathol* 163: 1949–1960, 2003.
4. Boyer B and Thiery JP. Epithelial cell adhesion mechanisms. *J Membr Biol* 112: 97–108, 1989.
5. Braz JC, Gregory K, Pathak A, Zhao W, Sahin B, Klevitsky R, Kimball TF, Lorenz JN, Nairn AC, Liggett SB, Bodi I, Wang S, Schwartz A, Lakatta EG, DePaoli-Roach AA, Robbins J, Hewett TE, Bibb JA, Westfall MV, Kranias EG, and Molkentin JD. PKCregulates cardiac contractility and propensity toward heart failure. *Nat Med* 10: 248–254, 2004.
6. Burri PH. Fetal and postnatal development of the lung. *Annu Rev Physiol* 46: 617–628, 1984.
7. Cardoso WV. Molecular regulation of lung development. *Annu Rev Physiol* 63: 471–494, 2001.
8. Carpenter MK, Shilling H, VandenBos T, Beckmann MP, Cerretti DP, Kott JN, Westrum LE, Davison BL, and Fletcher FA. Ligands for EPH-related tyrosine kinase receptors are developmentally regulated in the CNS. *J Neurosci Res* 42: 199–206, 1995.
9. Chen J, Chen Z, Narasaraju T, Jin N, and Liu L. Isolation of highly pure alveolar epithelial type I and type II cells from rat lungs. *Lab Invest* 84: 727–735, 2004.
10. Chen Z and Liu L. RealSpot: software validating results from DNA microarray data analysis with spot images. *Physiol Genomics* 21: 284– 291, 2005.
11. Dawid IB, Breen JJ, and Toyama R. LIM domains: multiple roles as adapters and functional modifiers in protein interactions. *Trends Genet* 14: 156–162, 1998.
12. De Moerlooze L, Spencer-Dene B, Revest J, Hajihosseini M, Rosewell I, and Dickson C. An important role for the IIIb isoform of fibroblast growth factor receptor 2 (FGFR2) in mesenchymal-epithelial signaling during mouse organogenesis. *Development* 127: 483–492, 2000.
13. Deuel TF, Zhang N, Yeh HJ, Silos-Santiago I, and Wang ZY. Pleiotrophin: a cytokine with diverse functions and a novel signaling pathway. *Arch Biochem Biophys* 397: 162–171, 2002.
14. De Vries FA, de Boer E, van den BM, Baarends WM, Ooms M, Yuan L, Liu JG, van Zeeland AA, Heyting C, and Pastink A. Mouse Sycp1 functions in synaptonemal complex assembly, meiotic recombination, and XY body formation. *Genes Dev* 19: 1376–1389, 2005.
15. Fraslon-Vanhulle C, Bourbon JR, and Batenburg JJ. Culture of fetal alveolar epithelial type II cells. *Cell Tissue Culture Lab Procedures* 2: 2.1–2.12, 1991.

16. Golpon HA, Coldren CD, Zamora MR, Cosgrove GP, Moore MD, Tuder RM, Geraci MW, and Voelkel NF. Emphysema lung tissue gene expression profiling. *Am J Respir Cell Mol Biol* 31: 595–600, 2004.

17. Herradon G, Ezquerra L, Nguyen T, Vogt TF, Bronson R, Silos- Santiago I, and Deuel TF. Pleiotrophin is an important regulator of the renin-angiotensin system in mouse aorta. *Biochem Biophys Res Commun* 324: 1041–1047, 2004.

18. Hogan BL. Bone morphogenetic proteins: multifunctional regulators of vertebrate development. *Genes Dev* 10: 1580–1594, 1996.

19. Hoshikawa Y, Nana-Sinkam P, Moore MD, Sotto-Santiago S, Phang T, Keith RL, Morris KG, Kondo T, Tuder RM, Voelkel NF, and Geraci MW. Hypoxia induces different genes in the lungs of rats compared with mice. *Physiol Genomics* 12: 209–219, 2003.

20. Hundertmark S, Dill A, Buhler H, Stevens P, Looman K, Ragosch V, Seckl JR, and Lipka C. 11_-Hydroxysteroid dehydrogenase type 1: a new regulator of fetal lung maturation. *Horm Metab Res* 34: 537–544, 2002.

21. Hundertmark S, Ragosch V, Schein B, Buhler H, Lorenz U, Fromm M, and Weitzel HK. Gestational age dependence of 11β-hydroxysteroid dehydrogenase and its relationship to the enzymes of phosphatidylcholine synthesis in lung and liver of fetal rat. *Biochim Biophys Acta* 1210: 348–354, 1994.

22. Hynes RO. Integrins: bidirectional, allosteric signaling machines. *Cell* 110: 673–687, 2002.

23. Ikegami M, Le Cras TD, Hardie WD, Stahlman MT, Whitsett JA, and Korfhagen TR. TGF-β perturbs surfactant homeostasis in vivo. *Am J Physiol Lung Cell Mol Physiol* 289: L34–L43, 2005.

24. Iso T, Hamamori Y, and Kedes L. Notch signaling in vascular development. *Arterioscler Thromb Vasc Biol* 23: 543–553, 2003.

25. Iwahara T, Fujimoto J, Wen D, Cupples R, Bucay N, Arakawa T, Mori S, Ratzkin B, and Yamamoto T. Molecular characterization of ALK, a receptor tyrosine kinase expressed specifically in the nervous system. *Oncogene* 14: 439–449, 1997.

26. Kaplan F, Comber J, Sladek R, Hudson TJ, Muglia LJ, Macrae T, Gagnon S, Asada M, Brewer JA, and Sweezey NB. The growth factor midkine is modulated by both glucocorticoid and retinoid in fetal lung development. *Am J Respir Cell Mol Biol* 28: 33–41, 2003.

27. Kierszenbaum AL, Gil M, Rivkin E, and Tres LL. Ran, a GTP-binding protein involved in nucleocytoplasmic transport and microtubule nucleation, relocates from the manchette to the centrosome region during rat spermiogenesis. *Mol Reprod Dev* 63: 131–140, 2002.

28. Kubiak J, Mitra MM, Steve AR, Hunt JD, Davies P, and Pitt BR. Transforming growth factor- gene expression in late-gestation fetal rat lung. *Pediatr Res* 31: 286–290, 1992.

29. Kundu GC and Mukherjee AB. Evidence that porcine pancreatic phospholipase A2 via its high-affinity receptor stimulates extracellular matrix invasion by normal and cancer cells. *J Biol Chem* 272: 2346–2353, 1997.

30. Le Cras TD, Hardie WD, Deutsch GH, Albertine KH, Ikegami M, Whitsett JA, and Korfhagen TR. Transient induction of TGF-β disrupts lung morphogenesis, causing pulmonary disease in adulthood. *Am J Physiol Lung Cell Mol Physiol* 287: L718–L729, 2004.

31. Lemercier C, To RQ, Swanson BJ, Lyons GE, and Konieczny SF. Mist1: a novel basic helix-loop-helix transcription factor exhibits a developmentally regulated expression pattern. *Dev Biol* 182: 101–113, 1997.

32. Li H, Malbon CC, and Wang HY. Gene profiling of Frizzled-1 and Frizzled-2 signaling:

expression of G-protein-coupled receptor chimeras in mouse F9 teratocarcinoma embryonal cells. *Mol Pharmacol* 65: 45–55, 2004.

33. Li YS, Milner PG, Chauhan AK, Watson MA, Hoffman RM, Kodner CM, Milbrandt J, and Deuel TF. Cloning and expression of a developmentally regulated protein that induces mitogenic and neurite outgrowth activity. *Science* 250: 1690–1694, 1990.

34. Lobe CG. Expression of the helix-loop-helix factor, Hes3, during embryo development suggests a role in early midbrain-hindbrain patterning. *Mech Dev* 62: 227–237, 1997.

35. Ma SF, Grigoryev DN, Taylor AD, Nonas S, Sammani S, Ye SQ, and Garcia JG. Bioinformatic identification of novel early stress response genes in rodent models of lung injury. *Am J Physiol Lung Cell Mol Physiol* 289: L468–L477, 2005.

36. Malpel S, Mendelsohn C, and Cardoso WV. Regulation of retinoic acid signaling during lung morphogenesis. *Development* 127: 3057–3067, 2000.

37. Mansure JJ, Furtado DR, Bastos de Oliveira FM, Rumjanek FD, Franco GR, and Fantappie MR. Cloning of a protein arginine methyltransferase PRMT1 homologue from *Schistosoma mansoni*: evidence for roles in nuclear receptor signaling and RNA metabolism. *Biochem Biophys Res Commun* 335: 1163–1172, 2005.

38. Mariani TJ, Reed JJ, and Shapiro SD. Expression profiling of the developing mouse lung: insights into the establishment of the extracellular matrix. *Am J Respir Cell Mol Biol* 26: 541–548, 2002.

39. Mayer Y, Czosnek H, Zeelon PE, Yaffe D, and Nudel U. Expression of the genes coding for the skeletal muscle and cardiac actions in the heart. *Nucleic Acids Res* 12: 1087–1100, 1984.

40. McElroy MC, Pittet JF, Hashimoto S, Allen L, Wiener-Kronish JP, and Dobbs LG. A type I cell-specific protein is a biochemical marker of epithelial injury in a rat model of pneumonia. *Am J Physiol Lung Cell Mol Physiol* 268: L181–L186, 1995.

41. Mendelson CR. Role of transcription factors in fetal lung development and surfactant protein gene expression. *Annu Rev Physiol* 62: 875–915, 2000.

42. Meng K, Rodriguez-Pena A, Dimitrov T, Chen W, Yamin M, Noda M, and Deuel TF. Pleiotrophin signals increased tyrosine phosphorylation of β-catenin through inactivation of the intrinsic catalytic activity of the receptor-type protein tyrosine phosphatase β/ς. *Proc Natl Acad Sci USA* 97: 2603–2608, 2000.

43. Moreno-Flores MT, Martin-Aparicio E, Avila J, Diaz-Nido J, and Wandosell F. Ephrin-B1 promotes dendrite outgrowth on cerebellar granule neurons. *Mol Cell Neurosci* 20: 429–446, 2002.

44. Morris SW, Naeve C, Mathew P, James PL, Kirstein MN, Cui X, and Witte DP. ALK, the chromosome 2 gene locus altered by the t (2;5) in non-Hodgkin's lymphoma, encodes a novel neural receptor tyrosine kinase that is highly related to leukocyte tyrosine kinase (LTK). *Oncogene* 14: 2175–2188, 1997.

45. Mucenski ML, Nation JM, Thitoff AR, Besnard V, Xu Y, Wert SE, Harada N, Taketo MM, Stahlman MT, and Whitsett JA. β-Catenin regulates differentiation of respiratory epithelial cells in vivo. *Am J Physiol Lung Cell Mol Physiol* 289: L971–L979, 2005.

46. Navankasattusas S, Zhu H, Garcia AV, Evans SM, and Chien KR. A ubiquitous factor (HF-1a) and a distinct muscle factor (HF-1b/MEF-2) form an E-box-independent pathway for cardiac muscle gene expression. *Mol Cell Biol* 12: 1469–1479, 1992.

47. Netchine I, Sobrier ML, Krude H, Schnabel D, Maghnie M, Marcos E, Duriez B, Cacheux V, Moers A, Goossens M, Gruters A, and Amselem S. Mutations in LHX3 result in a new syndrome revealed by combined pituitary hormone deficiency. *Nat Genet* 25: 182–186, 2000.

48. Newman B, Cescon D, Woo A, Rakowski H, Erikkson MJ, Sole M, Wigle ED, and Siminovitch KA. W4R variant in CSRP3 encoding muscle LIM protein in a patient with hypertrophic cardiomyopathy. *Mol Genet Metab* 84: 374–375, 2005.

49. Ogut O, Granzier H, and Jin JP. Acidic and basic troponin T isoforms in mature fast-twitch skeletal muscle and effect on contractility. *Am J Physiol Cell Physiol* 276: C1162–C1170, 1999.

50. Parcellier A, Schmitt E, Brunet M, Hammann A, Solary E, and Garrido C. Small heat shock proteins HSP27 and α_B-crystallin: cytoprotective and oncogenic functions. *Antioxid Redox Signal* 7: 404–413, 2005.

51. Pariser H, Ezquerra L, Herradon G, Perez-Pinera P, and Deuel TF. Fyn is a downstream target of the pleiotrophin/receptor protein tyrosine phosphatase β/ς-signaling pathway: regulation of tyrosine phosphorylation of Fyn by pleiotrophin. *Biochem Biophys Res Commun* 332: 664–669, 2005.

52. Pariser H, Herradon G, Ezquerra L, Perez-Pinera P, and Deuel TF. Pleiotrophin regulates serine phosphorylation and the cellular distribution of β-adducin through activation of protein kinase C. *Proc Natl Acad Sci USA* 102: 12407–12412, 2005.

53. Perkowski S, Sun J, Singhal S, Santiago J, Leikauf GD, and Albelda SM. Gene expression profiling of the early pulmonary response to hyperoxia in mice. *Am J Respir Cell Mol Biol* 28: 682–696, 2003.

54. Powers C, Aigner A, Stoica GE, McDonnell K, and Wellstein A. Pleiotrophin signaling through anaplastic lymphoma kinase is rate-limiting for glioblastoma growth. *J Biol Chem* 277: 14153–14158, 2002.

55. Reynolds PR, Mucenski ML, and Whitsett JA. Thyroid transcription factor (TTF)-1 regulates the expression of midkine (MK) during lung morphogenesis. *Dev Dyn* 227: 227–237, 2003.

56. Ruiz-Opazo N and Nadal-Ginard B. α-Tropomyosin gene organization. Alternative splicing of duplicated isotype-specific exons accounts for the production of smooth and striated muscle isoforms. *J Biol Chem* 262: 4755–4765, 1987.

57. Saharinen J, Hyytiainen M, Taipale J, and Keski-Oja J. Latent transforming growth factor-β binding proteins (LTBPs)—structural extracellular matrix proteins for targeting TGF-β action. *Cytokine Growth Factor Rev* 10: 99–117, 1999.

58. Sapin V, Bouillet P, Oulad-Abdelghani M, Dastugue B, Chambon P, and Dolle P. Differential expression of retinoic acid-inducible (Stra) genes during mouse placentation. *Mech Dev* 92: 295–299, 2000.

59. Sato Y, Arai N, Negishi A, and Ohya K. Expression of cyclooxygenase genes and involvement of endogenous prostaglandin during osteogenesis in the rat tibial bone marrow cavity. *J Med Dent Sci* 44: 81–92, 1997.

60. Sawtell NM and Lessard JL. Cellular distribution of smooth muscle actins during mammalian embryogenesis: expression of the α-vascular but not the γ-enteric isoform in differentiating striated myocytes. *J Cell Biol* 109: 2929–2937, 1989.

61. Schmitt S, Biason-Lauber A, Betts D, and Schoenle EJ. Genomic structure, chromosomal localization, and expression pattern of the human LIM-homeobox3 (LHX 3) gene. *Biochem Biophys Res Commun* 274: 49–56, 2000.

62. Seki T, Hong KH, and Oh SP. Nonoverlapping expression patterns of ALK1 and ALK5 reveal distinct roles of each receptor in vascular development. *Lab Invest* 86: 116–129, 2006.

63. Shannon JM and Hyatt BA. Epithelial-mesenchymal interactions in the developing lung. *Annu Rev Physiol* 66: 625–645, 2004.

64. Sheng HZ, Zhadanov AB, Mosinger B Jr, Fujii T, Bertuzzi S, Grinberg A, Lee EJ, Huang SP, Mahon KA, and Westphal H. Specification of pituitary cell lineages by the LIM homeobox gene Lhx3. *Science* 272: 1004–1007, 1996.

65. Shu W, Guttentag S, Wang Z, Andl T, Ballard P, Lu MM, Piccolo S, Birchmeier W, Whitsett JA, Millar SE, and Morrisey EE. Wnt/β-catenin signaling acts upstream of N-*myc*, BMP4, and FGF signaling to regulate proximal-distal patterning in the lung. *Dev Biol* 283: 226–239, 2005.

66. Silos-Santiago I, Yeh HJ, Gurrieri MA, Guillerman RP, Li YS, Wolf J, Snider W, and Deuel TF. Localization of pleiotrophin and its mRNA in subpopulations of neurons and their corresponding axonal tracts suggests important roles in neural-glial interactions during development and in maturity. *J Neurobiol* 31: 283–296, 1996.

67. Smas CM and Sul HS. Pref-1, a protein containing EGF-like repeats, inhibits adipocyte differentiation. *Cell* 73: 725–734, 1993.

68. Sobrier ML, Attie-Bitach T, Netchine I, Encha-Razavi F, Vekemans M, and Amselem S. Pathophysiology of syndromic combined pituitary hormone deficiency due to a LHX3 defect in light of LHX3 and LHX4 expression during early human development. *Gene Expr Patterns* 5: 279–284, 2004

69. Squire JA, McPherson JP, Beatty BG, and Goldenberg GJ. Allelic fusion of DNA topoisomerase II α and retinoic acid receptor-α genes in adriamycin-resistant p388 murine leukemia revealed by fluorescence in situ hybridization. *Cytogenet Cell Genet* 75: 164–166, 1996.

70. Stoica GE, Kuo A, Aigner A, Sunitha I, Souttou B, Malerczyk C, Caughey DJ, Wen D, Karavanov A, Riegel AT, and Wellstein A. Identification of anaplastic lymphoma kinase as a receptor for the growth factor pleiotrophin. *J Biol Chem* 276: 16772–16779, 2001.

71. Sugimoto K, Honda S, Yamamoto T, Ueki T, Monden M, Kaji A, Matsumoto K, and Nakamura T. Molecular cloning and characterization of a newly identified member of the cadherin family, PB-cadherin. *J Biol Chem* 271: 11548–11556, 1996

72. Tfelt-Hansen J, Yano S, Bandyopadhyay S, Carroll R, Brown EM, and Chattopadhyay N. Expression of pituitary tumor transforming gene (PTTG) and its binding protein in human astrocytes and astrocytoma cells: function and regulation of PTTG in U87 astrocytoma cells. *Endocrinology* 145: 4222–4231, 2004.

73. Thomas JO. HMG1 and 2: architectural DNA-binding proteins. *Biochem Soc Trans* 29: 395–401, 2001.

74. Ueno H, Matsuda T, Hashimoto S, Amaya F, Kitamura Y, Tanaka M, Kobayashi A, Maruyama I, Yamada S, Hasegawa N, Soejima J, Koh H, and Ishizaka A. Contributions of high mobility group box protein in experimental and clinical acute lung injury. *Am J Respir Crit Care Med* 170: 1310–1316, 2004.

75. Urness LD, Sorensen LK, and Li DY. Arteriovenous malformations in mice lacking activin receptor-like kinase-1. *Nat Genet* 26: 328–331, 2000.

76. Van OC, Snyder RC, Paeper BW, and Duester G. Temporal expression of the human alcohol dehydrogenase gene family during liver development correlates with differential promoter activation by hepatocyte nuclear factor 1, CCAAT/enhancer-binding protein-α, liver activator protein, and D-element-binding protein. *Mol Cell Biol* 12: 3023–3031, 1992.

77. Vanderwinden JM, Mailleux P, Schiffmann SN, and Vanderhaeghen JJ. Cellular distribution of the new growth factor pleiotrophin (HB-GAM) mRNA in developing and adult rat tissues. *Anat Embryol (Berl)* 186: 387–406, 1992.

78. Warburton D, Schwarz M, Tefft D, Flores-Delgado G, Anderson KD, and Cardoso WV. The molecular basis of lung morphogenesis. *Mech Dev* 92: 55–81, 2000.

79. Weng T, Jin N, and Liu L. Differentiation between amplicon polymerization and nonspecific products in SYBR green I real-time polymerase chain reaction. *Anal Biochem* 342: 167–169, 2005.

80. Whitsett JA and Tichelaar JW. Forkhead transcription factor HFH-4 and respiratory epithelial cell differentiation. *Am J Respir Cell Mol Biol* 21: 153–154, 1999.

81. Williams MC, Cao Y, Hinds A, Rishi AK, and Wetterwald A. T1 α protein is developmentally regulated and expressed by alveolar type I cells, choroid plexus, and ciliary epithelia of adult rats. *Am J Respir Cell Mol Biol* 14: 577–585, 1996.

82. Wodarz A and Nusse R. Mechanisms of Wnt signaling in development. *Annu Rev Cell Dev Biol* 14: 59–88, 1998.

83. Wright WE, Sassoon DA, and Lin VK. Myogenin, a factor regulating myogenesis, has a domain homologous to MyoD. *Cell* 56: 607–617, 1989.

84. Xiao GH, Gallagher R, Shetler J, Skele K, Altomare DA, Pestell RG, Jhanwar S, and Testa JR. The NF2 tumor suppressor gene product, merlin, inhibits cell proliferation and cell cycle progression by repressing cyclin D1 expression. *Mol Cell Biol* 25: 2384–2394, 2005

85. Yevtodiyenko A and Schmidt JV. Dlk1 expression marks developing endothelium and sites of branching morphogenesis in the mouse embryo and placenta. *Dev Dyn* 235: 1115–1123, 2006.

2.7 Acknowledgements

We thank Dr. Zhongming Chen for writting the Realspot software and helping with the slide printing, DNA microarray hybridization and data analysis. We are grateful to Dr. Nili Jin for her assistance with the Real-time PCR and Dr. Li Gao for the immunostaining of Lhx3. We thank Candice Marsh and Tisha Posey for editorial assistance. This work was supported by National Heart, Lung, and Blood Institute Grants R01 HL-052146 and R01 HL-071628 (L. Liu).

CHAPTER III

PLEIOTROPHIN REGULATES LUNG EPITHELIAL CELL PROLIFERATION AND DIFFERENTIATION DURING FETAL LUNG DEVELOPMENT VIA B-CATENIN AND DLK1

3.1 Abstract

The role of pleiotrophin in fetal lung development was investigated. We found that pleiotrophin and its receptor, protein tyrosine phosphatase receptor β/ζ, were highly expressed in mesenchymal and epithelial cells of the fetal lungs, respectively. Using isolated fetal alveolar epithelial type II cells, we demonstrated that pleiotrophin promoted fetal type II cell proliferation and arrested type II cell trans-differentiation into alveolar epithelial type I cells. Pleiotrophin also increased wound healing of injured type II cell monolayer. Knock-down of pleiotrophin influenced lung branching morphogenesis in a fetal lung organ culture model. Pleiotrophin increased the tyrosine phosphorylation of β-catenin, promoted β-catenin translocation into the nucleus and activated TCF/LEF transcription factors. Dlk1, a membrane ligand that initiates the Notch signaling pathway, was identified as a down-stream target of the pleiotrophin/β-catenin pathway by endogenous dlk1 expression, promoter assay and chromatin immunoprecipitation. These results provide evidence that pleiotrophin regulates fetal type II cell proliferation and differentiation via integration of multiple signaling pathways including pleiotrophin, β-catenin and Notch pathways.

Key Words: fetal lung development, pleiotrophin, cell differentiation, proliferation, β-catenin

.

3.2 Introduction

Fetal lung development is a complex biological process. Rat lung originates from the foregut endoderm as a bifurcation at embryonic day 10 (E10) and undergoes several generations of dichotomous branching morphogenesis to form a respiratory tree thereafter (17). The columnar epithelial cells differentiate into Clara cells and epithelial cells. Although surfactant protein C (SP-C) is detected as early as E13, fetal alveolar epithelial type II cells (fAEC II) are not fully differentiated until E18 when glycogen-pool-enriched AEC II precurcers become cuboidal and differentiate into cells containing lamellar bodies. fAEC II can further differentiate and give rise to the alveolar epithelial type I cells (AEC I).

The regulation of fetal lung development includes coordinated regulation of molecular pathways as well as reciprocal interactions among mesenchymal cells, epithelial cells and the extracelluar matrix (40). Precise signals from mesenchymal cells regulate lung branching morphogenesis and lead to cell fate determination and the subsequent generation of cell type diversity in the lung epithelium. For example, mesenchymal cells secrete fibroblast growth factor 10 (FGF10) (5; 38). FGF10 in turn binds to its receptor which is located on the surface of epithelial cells. The binding transduces a message to downstream signaling in order to regulate cell proliferation, differentiation, migration and branching morphorgenesis. Similarly, the epithelial cells also secrete signal molecules to interact with the mesenchyme. Sonic hedgehog (Shh) is a growth factor expressed in the developing epithelium. Its receptor, Patched-1 (Ptc), is located on mesenchymal cells. The interaction between Shh and Ptc has been shown to be required for lung bud formation (22). Other growth factors such as platelet derived growth factor (PDGF), transforming growth factor (TGF-β), epidermal growth factor (EGF) and vascular endothelial growth factor (VEGF) also play active roles in mesenchyme-epithelium interactions (40).

Pleiotrophin (PTN), a heparin binding cytokine, is involved in cell transformation, growth, survival, migration and angiogenesis (9). PTN is localized in the extracellar matrix and mesenchymal cells. It shares 50% sequence homology with midkine. PTN was first identified as a growth factor from the bovine uterus (25) and as a neurite outgrowth promoting factor in the neonatal rat brain (34). PTN expression peaks in the late stage of embryogenesis (16; 44) and postnatally in the nervous system (20; 42). PTN is also up-regulated in injured cells and is important for new tissue formation during recovery from injury (49). PTN levels are much lower in adult tissue than that in fetal tissue; however, PTN is overexpressed in a number of cancers including human breast cancers (46) and melanocytic tumors (39).

PTN signals through the cell surface receptor, protein tyrosine phosphatase receptor (RPTP β/ζ). In U373-MG glioblastoma cells, the binding of PTN with RPTP β/ζ results in the dimerization and inactivation of the receptor, leading to an increase in tyrosine phosphorylation of β-catenin (24) . β-catenin is a transcriptional co-factor and an adaptor protein linking cadherins to

the cytoskeleton. Since β-catenin is the central component of the Wnt signaling pathway, there may be a cross-talk between PTN and Wnt signaling pathways. PTN may also act via the receptor tyrosine kinase, anaplastic lymphoma kinase receptor (ALK) (43).

There is little information available regarding PTN in the lung. PTN is expressed in fetal lungs (44) and lung cancer cell lines (19). Our DNA microarray analysis of fetal lungs reveals that *ptn* is highly expressed during the late stage of fetal lung development (47). This is confirmed by real-time PCR and Western blot. However, whether PTN has a role in fetal lung development is unknown.

In this study, we first examined the expression pattern of PTN and its receptor, RPTP β/ζ during fetal lung development. Using primary fAEC II, we evaluated the role of PTN in cell proliferation, differentiation and wound healing. We also determined the effects of PTN on fetal lung branching morphogenesis by knocking down the PTN expression with adenovirus-mediated small interfering RNA (siRNA). Finally, we dissected the signaling pathways initiated by PTN. Our results show that PTN regulates fetal lung epithelial cell proliferation and differentiation via β-catenin signaling pathway.

3.3 MATERIALS AND METHODS

3.3.1 Chemicals and reagents

TRI reagents were purchased from Molecular Research Center, Inc. (Cincinnati, OH). Oligo dT, random hexamers and pGL3 firefly luciferase reporter vector were from Promega (Madison, WI). RNase-free™ DNase was from Ambion (Austin, TX). M-MLV reverse transcriptase, pENTR plasmid, LipfectamineTM 2000 and LTX, Minimal essential medium (MEM) and BGJb medium were from Invitrogen (Carlsbad, CA). SYBR Green I detection reagents were from Qiagen (Valencia, CA). NE-PER Nuclear and Cytoplasmic Extraction Reagents and M-PER mammalian protein extraction reagents were from Pierce (Rockford, IL). Protein A or G agarose beads were from Santa Cruz Biotechnology (Santa Cruz, CA). Matrigel, anti-RPTP β/ζ and anti-β-catenin monoclonal antibodies were from BD Bioscience (Franklin Lakes, NJ). Advantage 2 Polymerase Mix and Advantage GC Genomic Polymerase Mix were from Clontech (Mountain View, CA). EZ ChIP kit and anti-phosphotyrosine antibodies were from Upstate Biotechnology (Lake Placid, NY). Human recombinant pleiotrophin, collagenase, trypsin and DNase I were from Sigma-Aldrich (St. Louis, MO). Goat anti-pleiotrophin, rabbit anti-Dlk1 and mouse anti-BrdU antibodies were from Abcam (Cambridge, MA). Mouse anti-LB180 antibody was from Covance (Berkeley, CA). Alexa 568-conjugated anti-goat and Alexa 488-conjugated anti-mouse antibodies were from Molecular Probes (Eugene, OR). ABC reagents were from Vector Laboratories (Burlingame, CA). TSATM-plus HRP system was from PerkinElmer (Waltham, MA). L2 cell line was from ATCC (Manassas, VA).

3.3.2 Real-time PCR

Total RNAs were isolated using TRI reagents and treated with RNase-free™ DNase to remove DNA contamination. 1 µg of total RNAs were reverse-transcribed into cDNA using oligo dT and random hexamers and M-MLV reverse transcriptase. The primers were designed using Primer Express® software (Applied Biosystems, Foster City, CA): PTN, 5' ATACCAGCAGCAACGTCGAAA (forward) and 5' GCACACACTCCATTGCCATT (reward), Dlk1, 5' GTGAAGAACCATGGCAGTGTGT (forward) and 5'_GACAGTCCTTTCCAGAGAATCCA (reward), and 18S rRNA 5' TCCCAGTAAGTGCGGGTCATA (forward) and 5' CGAGGGCCTCACTAAACCATC (reward). Real-time PCR was performed on an ABI 7500 system using SYBR Green I detection as previously described (47). To eliminate the effects of primer dimers, we included a data acquisition step at a temperature of 2 ~ 5 °C lower than the annealing temperature of the products. After the amplification, a dissociation curve was generated to check the specificity of the amplification. The data were normalized to 18S rRNA.

3.3.3 Immunohistochemistry

Fetal lung tissues were fixed in 4% formaldehyde for 24 hrs, embedded in paraffin and sectioned at a 4 µm thickness. The slides were dewaxed, rehydrated, boiled in citric buffer (pH 6.0) for 20 min for antigen retrieval and permeabilized by a 10-min incubation in 0.3% Triton X-100. The slides were blocked in 10% normal horse serum and then incubated with goat anti-PTN (1:100) or mouse anti-RPTP β/ζ (1:200) at 4ºC overnight. After being rinsed with phosphate-buffered saline (PBS, pH 7.4), the slides were further incubated in corresponding secondary antibodies (1:100) for 1 hr. The slides were rinsed again and incubated in ABC reagents for 30 min. The signal was amplified using the TSATM-plus HRP system. Signal was detected using DAB substrate. The slides were counter-stained by hemeotoxylin and viewed under a Nikon Eclipse E600 microscope with a Plan Flour, ELWD 40 x/0.6 or 20x/0.5 objective lenses. The images were captured with an Insight 2 color mosaic camera and the basic spot software (Diagnostic Instruments Inc.).

3.3.4 Immunocytochemistry

fAEC II were fixed in 4% formaldehyde for 15 min, followed by a 10-min incubation in 0.3% Triton X-100 for permeabilization. After being blocked in 10% fetal bovine serum (FBS) for 30 min, the cells were incubated with anti-LB180 (1:200) or anti-T1-α (1:250) antibodies at 4℃ overnight. The cells were rinsed with PBS, and then incubated with Alexa 488-conjugated anti-mouse antibodies (1:250) for 1 hr. Finally, cells were washed and viewed by a Nikon Eclipse TE2000-U inverted fluorescence microscope with a Plan Flour, ELWD 40 x/0.6 or 20 x /0.5 objective lens. The images were captured with a Photometrics CoolSnap CCD camera (Roper Scientific) and the Metavue software (Universal Imaging Co.).

3.3.5 fAEC II isolation and culture

fAEC II were isolated as described (4). The Oklahoma State University Animal use and Care Committee approved all the procedures used in this study. Timed-Pregnant Sprague Dawley rats with a gestational day of 20 were sacrificed by carbon dioxide asphyxia. Fetuses were carefully separated from the uterus. Fetal lungs were excised from the fetuses and washed with cold Hanks' balanced salt solution (HBSS). After removing the surrounding trachea, thymus and heart, the lungs were chopped into 1 mm^3 cubes and digested with MEM containing 1 mg/ml collagenase, 1 mg/ml trypsin and 0.4 mg/ml DNase I for 10 min for 4 times. Released cells were filtered through 160 and 37 μm nylon gauze filters. The cells were then collected by centrifugation at 160 x *g* for 10 min and resuspended in MEM containing 20% FBS, 100 U/ml penicillin and 10 μg/ml streptomycin at a final concentration of 1.7 $X10^6$ cells/ml. To remove the fibroblasts, 40 ml of the cells were seeded in a 20 cm plastic dish for differential adhesion. After 4 rounds of a 45-min adherence, the cells were filtered through a 15 μm nylon gauze filter, centrifuged and seeded on the plate for further culture. The resulting fAEC II had a purity of ~90% and a viability of > 95%.

For the trans-differentiation experiment, primary fAEC II were cultured in full MEM medium (FMEM, MEM supplemented with 10% FBS, 1% nonessential amino acids, and 1% penicillin and streptomycin) for 24 hrs. Media were changed to chemical defined serum-free medium (12). (DSFM, DMEM/F12 1:1 supplemented with 1.25 mg/ml bovine serum albumin, 1% nonessential amino acids and 1% penicillin and streptomycin) without or with 50 ng/ml human recombinant PTN. The cells were cultured for 4 more days and media were changed every two days. Finally, the cells were fixed and used for immunofluorescence.

3.3.6 Wound healing assay

Primary fAEC II were cultured overnight in plastic dishes in FMEM. Culture media were changed to DSFM in the presence of different doses of PTN. Culture continued until a monolayer was formed (normally on day 2). The cell monolayer were then scratched with a yellow tip to mimic injury and the gaps were photographed every 6 hrs. The wound width was measured, and the wound closure was defined as the wound width at a specific time minus the distance of the original wound width.

For the co-culture experiment, primary fibroblasts were collected during the differential adhesion stage when isolating fAEC II. 0.5 x 10^6 of fAEC II were seeded outside of a collagen-coated insert with 0.2 μm pore size and fibroblasts (0.5 x 10^6) were seeded inside the insert. Both cells were cultured in FMEM. The insert was placed in each well of a 24-well plate. After 24 hrs,

the media were changed to DSFM and the fAEC II monolayer was scratched for the wound healing assay.

3.3.7 Cell proliferation assay

Primary fAEC II were cultured in FMEM for 24 hrs. Then the media were changed to DSFM without or with 50 ng/ml PTN. The cells were cultured for additional 36 hrs. Bromodeoxy-uridine (BrdU, 10 μM) was added to the medium 12 hrs before collecting the cells. Finally, the cells were fixed in 4% paraformadehyde and stained with anti-BrdU antibodies (1:100).

3.3.8 Western blot

Cells were lysed in the M-PER mammalian protein extraction reagent with protease inhibitor cocktail on ice for 10 min. The lysate was centrifuged at 12,000 xg for 10 min to clear the cell debris. Protein concentrations in the supernatant were determined the using the D_C Protein Assay Kit. The same amount of total protein was separated by 10% SDS-PAGE and then transferred onto a nitrocellulose membrane. The membrane was blocked with 5% dry milk in Tris-Buffered Saline (TBS) for 1 hr. Then, the membrane was incubated with primary antibodies (anti-RPTP β/ζ: 1:500, anti-β-catenin: 1:1000, anti-γ-tubulin: 1:1000, and anti-phosphotyrosine: 1:1000) overnight at 4°C. After being washed with TBS containing 0.05% Tween 20, the membrane was incubated with corresponding secondary antibodies (1:2000) for 1 hr. Finally, the membrane was developed with ECL reagents and exposed to X-ray film.

3.3.9 Construction of siRNA adenoviral vector

A highly efficient siRNA vector expressing 4 shRNAs under the control of mU6, hU6, H1 and 7SK promoters was previously developed in our laboratory (14). Four siRNA sequences specific to the coding region of PTN (549-569, 570-590, 607-627 and 909-929) were selected based on the computer program (http://i.cs.hku.hk/~sirna/software/sirna.php). A vector containing 4 unrelated siRNA sequences was used as a control. These siRNA sequences were cloned into a modified pENTR plasmid containing a CMV-driven EGFP protein for tracking the virus transduction. The siRNA and EGFP sequences were transferred from the pENTR recombinant vector to the adenoviral vector, pAd/PL-DEST vector by a LR recombinant reaction using the Gateway technology. The plasmid from the positive clone was digested with *Pac* I and transfected into a 293A producer cell line with the Lipfectamine™ 2000 reagent. The adenovirus-containing cells were harvested, and the generated virus was used to infect 293A cells to amplify the viral stock. The titer was determined by counting the GFP positive cells.

3.3.10 Fetal lung organ culture

Timed-pregnant rats with a gestational day 14 (E14) were killed by CO_2 asphyxia. Embryos were carefully removed from the uterus and placed in cold HBSS. Fetal lungs were isolated from the fetus by microdissection needles. Two or three lungs were kept on a 3 cm insert, which were placed in a 6-well plate with 1.5 ml BGJb supplemented with 100 U/ml penicillin, 100 µg/ml streptomycin, and 0.2 mg/ml ascorbic acid. The fetal lungs were cultured for 1 to 3 days. The viruses were added to the lungs inside of the insert at day 0, moved outside of the insert after a 3-hr treatment and removed after 24 hrs. Medium was changed every day. The fetal lungs were photographed every 24 hrs to record the morphological changes. To determine the changes in lung branching morphogenesis, the terminal buds of each lung were counted and normalized to those at day 0 of the same lung. The sizes of terminal and inside buds were determined with Metaview™ (Universal Imaging Corporation). About 30 buds were evaluated for each lung.

3.3.11 Tyrosine phosphorylation of β-catenin

Primary fAEC II were cultured in FMEM for one day, and then in DSFM for an additional day. The cells were treated with 50 ng/ml PTN for 0, 5, 10, 20, 60 or 120 min and lyzed in the M-PER mammalian protein extraction reagent (supplemented with 1% Halt phosphatase inhibitor cocktail and 1% protease inhibitor cocktail, and 1 mM sodium orthovanadate). The cell lysate (250 µg protein) were incubated with anti-β-catenin antibodies (2 µg) at 4℃ for 2 hrs. 10 µl protein A and 20 µl protein G agarose beads were added to the mixtures and incubated overnight at 4℃ by gentle end-to-end mixing. The agarose beads were washed 6 times with PBS. The proteins were eluted by boiling in 1X SDS sample buffer for detection of phosphorylation and β-catenin by Western blotting.

3.3.12 Translocation of β-catenin

Primary fAEC II were cultured in FMEM for 24 hrs and in DSFM for another 24 hrs. The cells were treated with 50 or 100 ng/ml PTN for 12 hrs. The nuclear and cytoplasmic fractions were separated using the NE-PER Nuclear and Cytoplasmic Extraction Reagents. The amounts of β-catenin in the cytoplasmic and nuclear fractions were determined using Western blot.

3.3.13 fAEC II culture on Matrigel

Matrigel was thawed fully at 4℃ overnight, and kept on ice until use. 200 µl of Matrigel was added to each well of 12-well plate and incubated for 1 hr at room temperature to solidification. Primary fAEC II was seeded at a density of 5×10^5 cells/well in FMEM. After 24 hrs, media were changed to DSFM and the cells were treated with various concentrations of Wnt3a or LiCl for 48 hrs. The cells were collected in 1 ml Tri-reagent for isolation of total RNA.

3.3.14 TOPflash assay

Freshly isolated fAEC II (5 x 10^6) were transfected with phRL-TK (1.14 µg) and TOPflash or FOPflash (1.3 µg) by electroporation using the Amaxa NHBE Nucleofector kit for normal human bronchial epithelial cells and the Program T-13. The cells (2.5 x 10^6/well) were seeded in a 48-well plate and cultured in 10% FBS-DMEM for 24 hrs. The fAEC II were then treated with 100 ng/ml PTN for 24 hrs and harvested for a dual-luciferase assay.

3.3.15 *Dlk 1* promoter assay

The *Dlk1* promoter (-1471 to 190) was amplified from mouse genomic DNA by overlap PCR. Three sets of primers were designed to amply *Dlk1* promoter from mouse genomic DNA. The first fragment A (631 bp) ranging from -1471 to -848 was amplified by Advantage 2 Polymerase Mix with the primers (5'-CGTGCTAGCCAAAGGAGCTATGTCAATGAC-3' and 5'-AGCACTGATTCTTTCCAACATG-3'). The second fragment B (624 bp) ranging from -894 to -271 and the third fragment C (503 bp) ranging from -305 to 190 were amplified by Advantage GC Genomic Polymerase Mix with the primer sets of (5'-CATACGTGTTGCTGCGAGGTGTGTACATGTT-3', 5'-GGCCCGCTTAGCGCAAGTCTCAGGAACCAA-3') and (5'-CTGGCTTGGTTCCTGAGACTTGCGCTAA-3', 5'-GCCAAGCTTGGAGGGCTCCGGTCGCGATCATCTC-3'). Using the gel-purified three Dlk1 fragments mixture as template, the full-length *Dlk1* promoter was obtained by over-lap PCR with two outside primers (5'-CGTGCTAGCCAAAGGAGCTATGTCAATGAC-3' and 5'-GCCAAGCTTGGAGGGCTCCGGTCGCGATCATCTC-3'). The purified PCR products were digested by *Nhe1* and *Hind3* and cloned into the pGL3 firefly luciferase reporter vector to replace the SV40 promoter through *Nhe*1-*Hind3* sites. The amplified *Dlk1* promoter was verified by DNA sequencing. The *Dlk1* promoter-driven firefly luciferase vector was named as pDlk1-Fluc.

Freshly isolated fAEC II (4 x 10^6) were transfected with 1 µg pDlk1-Fluc, 1.14 µg *Renilla* luciferase vector phRL-TK, 100 or 500 ng wild type β-catenin or constructively activated mutant ΔGSK β-catenin using the Amexa Nucleofector kit for normal human bronchial epithelial cells and the Program T-13. The cells (2 x 10^6/well) were seeded into a 48-well plate and cultured in 10% FBS-DMEM for 24 hrs. The medium was changed with fresh 10% FBS-DMEM medium with or without PTN (100 ng/ml) and the cells were harvested for dual luciferase assay after a 24-hr treatment.

3.3.16 Chromatin Immunoprecipitation (ChIP)

The EZ ChIP kit was used for the CHIP assay. fAEC II were fixed in 1% formaldehyde in PBS for 10 min at room temperature. Then, glycine was added at a final concentration of 0.125 M to stop the cross-linking. 6 x 10^6 cells were washed by cold PBS for 2 times and then sonicated in 300 µl SDS lysis buffer (Branson Sonifier 450, Output power 7, 20 seconds for 20 times). For each sample, chromatin from 1.5 x 10^6 cells was immunoprecipitated with 2 µg normal mouse

IgG, or mouse monoclonal antibody for β-catenin as described in the kit manual. After reversal of the cross-linking by adding 200 mM NaCl and incubating at 65℃ overnight, 2 µl of purified immuno-selected DNAs were used for PCR (32 cycles, 94 ℃, 30 s; 56℃, 30 s; 72℃, 30 s). 5 µl of the reaction products were run on 1.5% agarose gel. Two pairs of primers were used to amplify two putative TCF/LEF binding sites and flanking sequences: Dlk1-BS1, forward, 5'TGGAGATTAAATTCAAGCTGTCAG3' and reverse, 5'GCAGCCAAACTTGAGTTTGATC3'; Dlk1-BS2, forward, 5'CATTTGAC<R>GTGAACATATTGG3' (R=A/G) and reverse, 5' GCCCAG<W>CCCCAAATCTGTC3' (W=A/T). The degenerated primers were designed to amplify both rat and mouse Dlk1 promoter sequences. CCDN1 promoter fragment (-173-+117) was amplified as a positive control for TCF/LEF binding using a primer pair: forward, 5'TTCTCTGCCCGGCTTTGAT3' and reverse, 5'CACAGGAGCTGGTGTTCCATG3'. GAPDH promoter, which has no TCF/LEF binding site, served as a negative control and was amplified using a primer pair: forward, 5'GTGCAAAAGACCCTGAACAATG3' and reverse, 5'GAAGCTATTCTAGTCTGATAACCTCC3'.

3.4 RESULTS

3.4.1 PTN and its receptor, RPTP β/ζ expression in the developing lung

We have previously shown that PTN mRNA and protein are highly expressed in the late stage of fetal lung development by analyzing fetal lungs at different gestational days as well as lungs of newborn and adult rats using DNA microarray analysis, real-time PCR and Western blot (47). We further investigated temporal and spatial expression of PTN during rat lung development by ABC immunostaining. PTN was barely detectable in the embryonic day (E16) lungs (Fig.III.1A). A strong staining in the mesenchyme adjacent to the developing epithelium and endothelium of the E18 and E20 lungs was seen. Little PTN signals were observed in adult lungs. No positive signals were found in the negative controls without primary antibodies (data not shown). Real-time PCR revealed that PTN was enriched in fetal lung fibroblasts in comparison with fetal lung tissues (Fig.III.1B).

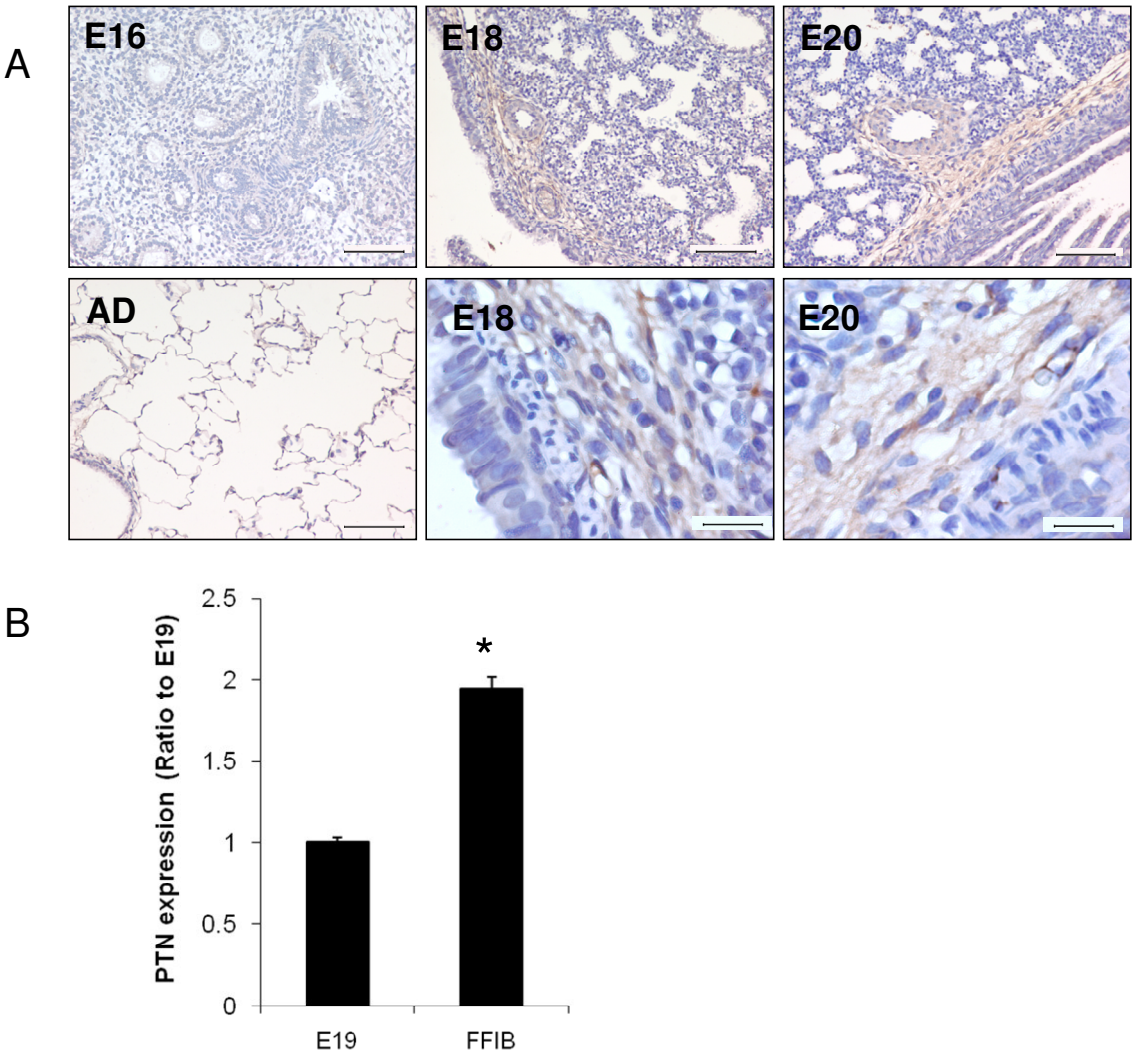

Fig.III.1. PTN expression during fetal lung development. (A) Immunostaining of PTN in the developing lungs. Embryonic day 16, 18, and 20 (E16, E18, E20) and adult (AD) lung tissue sections were stained using anti-PTN antibodies and the Vectastain ABC kit. Scale: 100 µm. The lower right two panels are high magnifications (Scale bar: 20 µm). (B) Real-time PCR analysis of PTN mRNA expression in E19 fetal lung tissue (E19) and isolated E19 fetal fibroblasts (FFIB). The results were normalized to 18S rRNA and expressed as a ratio of lung tissue. Data shown are means ± S. E., *P<0.05 v.s. lung tissue (n=3 cell preparations, assayed in duplicate).

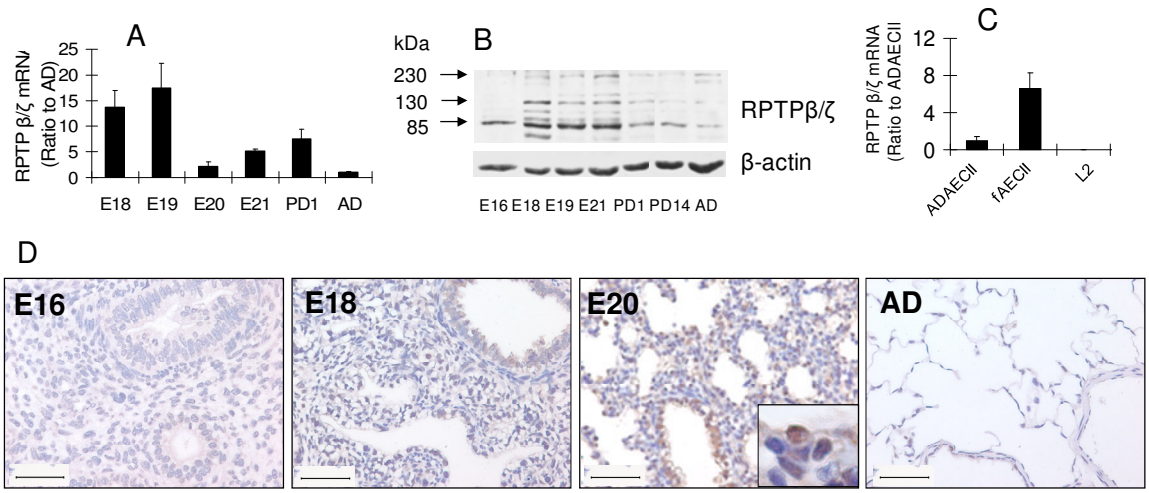

Fig.III.2. RPTP β/ζ expression during fetal lung development. (A) mRNA levels of *RPTP β/ζ* in lung tissues; (B) Protein levels of RPTP β/ζ in lung tissues; (C) mRNA levels of *RPTP β/ζ* in various cells. mRNA and protein levels were determined by real-time PCR and Western blot. E18-E21: fetal lungs; PD1 and PD14: postnatal day 1 and 14 lungs. AD: adult lungs. AdAECII: adult type II cells; fAEC II: E20 primary fetal type II cells; L2: a cell line derived from adult rat lungs. The mRNA levels were normalized to 18S rRNA and expressed as a percentage of AD or AdAECII. Data shown are means ± S.E. (n=6) *(D)* Immunostaining of E16, 18, 20 and AD lungs with anti-RPTP β/ζ antibodies. Scale Bar: 50 µm

We also examined the expression of RPTP β/ζ, one of the PTN receptors, during fetal lung development. As shown by real-time PCR, *RPTP β/ζ* mRNA was highly expressed in E18 and E19 fetal lungs (Fig.III.2A). Western blot revealed 3 bands with molecular masses of 230, 130 and 85 kDa (Fig.III.2B), which correspond to 3 alternatively spliced species of RPTP β/ζ (24). The RPTP β/ζ protein was highly expressed in E18-21 fetal lungs, but relatively low in postnatal day 1, day 14 and adult lung tissues. A high expression of RPTP β/ζ protein in the E21 lungs in comparison with mRNA may be due to its stability. The time-restricted RPTP β/ζ expression corresponds with the PTN expression, indicating that the PTN pathway may be active during the late stage of fetal lung development. To further identify which types of cells express RPTP β/ζ, real-time PCR was used to examine the RPTP β/ζ mRNA expression level in fAEC II, adult type II cells (ADAEC II) and L2 cells (a rat lung epithelial cell line derived from the adult rat lung). RPTP β/ζ expressed highly in fAEC II but lowly in ADAEC II (Fig.III.2C). L2 had no expression of the receptor. RPTP β/ζ cellular localization was further viewed using ABC staining in E16, E18, E20 and adult lung tissues. As shown in Fig.III.2D, RPTP β/ζ staining was strong in E18 and E20 lungs but was not detectable in E16 or adult lungs. Consistent with the real-time PCR results, RPTP β/ζ was localized in airway epithelial cells.

3.4.2 PTN arrests fAEC II trans-differentiation into AEC I

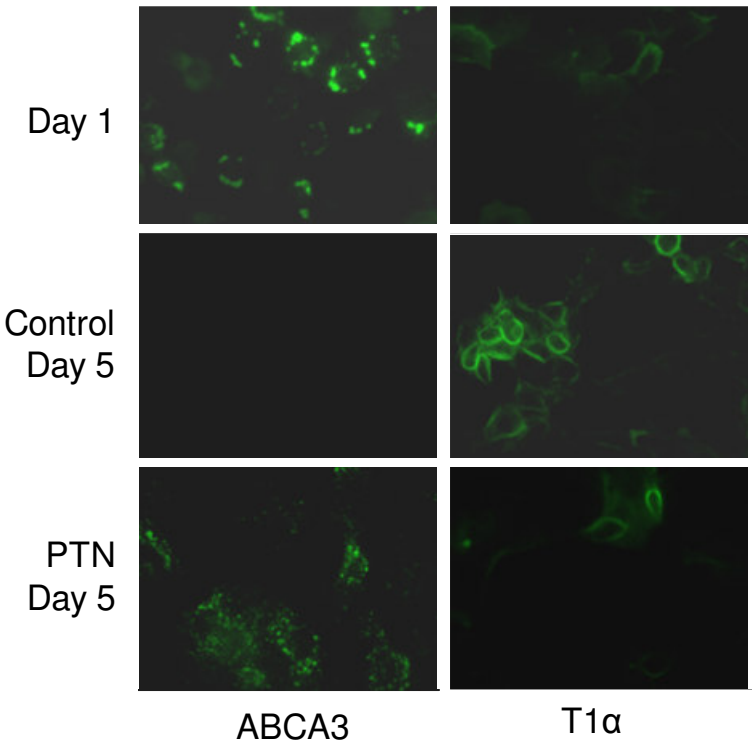

Fig.III.3. Effect of PTN on fAEC II trans-differentiation. Primary fAEC II were cultured for 1 or 5 days on plastics. PTN (50 ng/ml) was added at day 1. ABCA3 (type II cell marker) and T1α (Type I cell marker) were stained by immunofluorescence.

When AEC II were cultured on plastic dishes, the cells gradually lost the AEC II phenotype and trans-differentiated into AEC I. Using this *in vitro* system, we examined the effect of PTN on fAEC II trans-differentiation. Primary fAEC II were cultured on plastic dishes overnight and then treated with 50 ng/ml of PTN. After being cultured for 4 more days, AEC II cells were stained with antibodies against ABCA3 (AEC II specific marker) and T1α (AEC I specific marker). At day 1, the cells had strong ABCA3 staining, but weak T1α staining (Fig.III.3). After day 5 of culture, the control cells had no ABCA3 staining and a clear T1α staining, indicating that fAEC II trans-differentiated into AEC I. However, in the PTN-treated fAEC II, strong ABCA3 staining still remained. The results suggest that PTN can arrest the fAEC II trans-differentiation into AEC I.

3.4.3 PTN increases fAEC II proliferation

To determine whether PTN can promote fAEC II proliferation, primary fAEC II were treated with PTN and labeled with BrdU. The cells were then fixed and stained with anti-BrdU

antibodies to view the proliferating cells. As shown in Fig.III.4, the PTN-treated cells contained about twice as much proliferating cells as the control cells without any treatment.

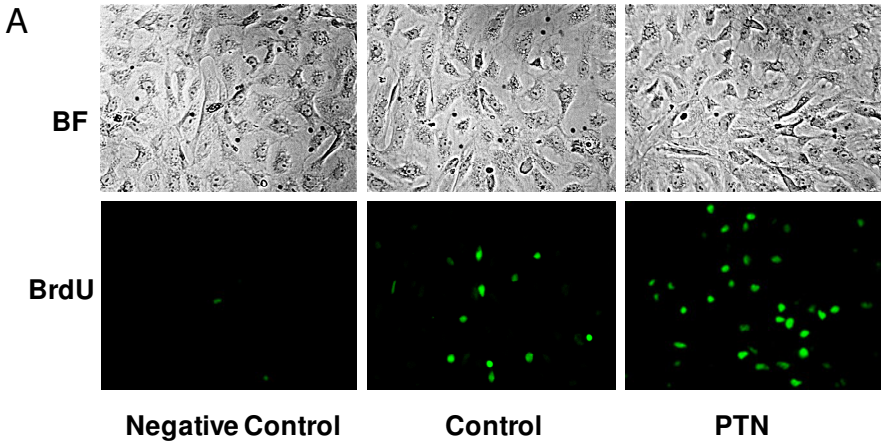

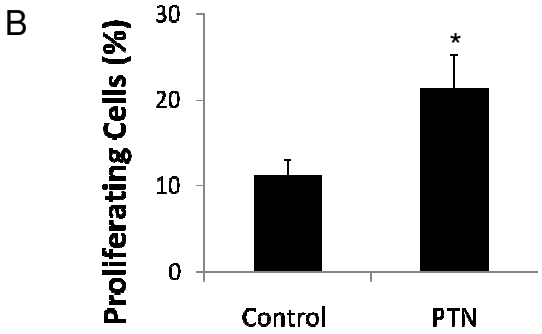

Fig.III.4. PTN stimulates fAEC II proliferation. Primary fAEC II were cultured in serum-free medium on plastic dishes. The cells were treated with 50 ng/ml PTN at day 1. After 36 hours, the cells were collected and stained with anti-BrdU antibodies to view the proliferating cells. (A) Representative images. BF: brightfield. (B) Quantitation. The proliferating cells (BrdU-positive cells) were expressed as a percentage of total cells (means ± S.E.). *P<0.05 v.s. Control, n=5.

3.4.4 PTN promotes wound healing

We determined whether PTN enhances alveolar epithelial cell repair. fAEC II were cultured in serum-free medium with PTN. After washing, a linear wound was created using a pipette tip and the bright field images were taken at various time points. PTN significantly increased the wound closure of fAEC II in a dose-dependent manner (Fig.III.5A). The wound closure was further quantified as the gap width at 0 h minus the gap width at late time points (Fig.III.5B). When anti-PTN antibody was added together with PTN, the wound closure induced by PTN was blocked (Fig.III.5C). The control IgG had no effects. Since PTN was enriched in fetal lung fibroblasts, we

further examined whether it was the PTN secreted from the fibroblasts that are responsible for fAEC II repair. fAEC II were co-cultured in a 6-well plate with fetal lung fibroblasts in a transwell insert placed in the plate and thus fibroblasts may secrete growth factors into the AEC II culture medium. Fibroblasts significantly promoted the fAEC II wound closure. This effect was again blocked by PTN antibodies, but not the control IgG. These results indicate that PTN is secreted from fibroblasts and acts on fAEC II to promote wound healing.

Previously, PTN was reported to be able to stimulate the epithelial-mesenchymal-like transition by altering actin cytoskeleton organization (29). We examined whether PTN influences F-actin distribution. fAEC II treated with PTN were stained with Alexa Fluor 568 tagged phalloidin. The cells that were away from the scratched gap did not show much difference in stimulated and nonstimulated cells (data not shown). However, the PTN-treated cells on the edge of the wound gap had sharper and longer F-actin staining compared to untreated control cells (Fig.III.5E). The re-distribution of the actin cytoskeleton would allow the cells to migrate.

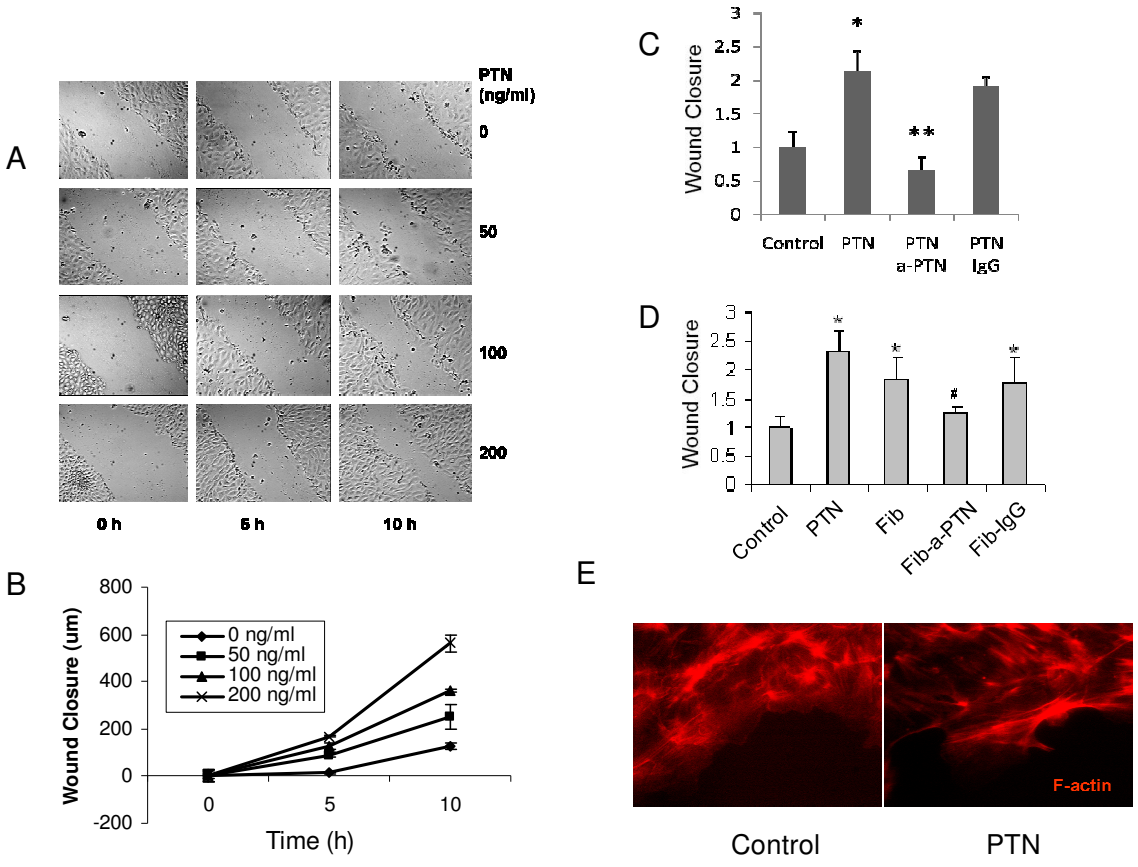

Fig.III.5. PTN promotes wound healing of fAEC II monolayer. (A) fAEC II were isolated from E20 lungs and cultured for 2 days. Different doses of PTN were added at day 1. On day 2, fAEC II monolayers were scratched and the generated gaps were photographed every 5 hrs. (B) Wound closure was measured as the difference between the original wound width and the final wound

width. (C) Effect of anti-PTN antibodies. PTN (100 ng/ml) was added at day 1 with or without anti-PTN antibodies or IgG (2 μg/ml). Wound closure was measured 16 hrs after the scratching and expressed as a percentage of control. (D) fAEC II were co-cultured with fibroblasts on transwell inserts. Anti-PTN antibodies or IgG (2 μg/ml) were added at day 1. fAEC II cultured in the insert alone in the absence (control) or presence of PTN (100 ng/ml) were used as negative and positive controls. Wound closure was measured 16 hrs after the scratching. Fib: fibroblasts; Fib-a-PTN (fibroblasts plus anti-PTN antibodies; Fib-IgG: fibroblasts plus IgG. All data shown are means ± S.E. *P<0.05 v.s. control; **P<0.05 v.s. PTN; # P<0.05 v.s. fibroblasts, n=3 independent cell preparations. (E) F-actin Staining. The control and PTN-treated fAEC II at the end of wound healing assay were fixed in 4% Formaldehyde for 30 min, permeabilized in 1% Triton X-100 for 10 min, and blocked in 10% FBS and 1% BSA for 15 min. The cells were then incubated with 1 μM Alexa Fluor 568 Phalloidin for 1.5 hrs at 4 ℃. After wash, the fluorescence images were viewed under a Nikon Inverted Fluorescence Microscope.

3.4.5 PTN promotes fetal lung branching morphogenesis

Since PTN has been shown to play an important role in renal branching morphogenesis (37), we sought to determine if PTN plays a role in fetal lung branching morphogenesis. We silenced PTN in a fetal lung organ culture by using the pK4-shRNA vector (14) and examined the effects of the treatment on lung branching morphogenesis. An adenoviral vector carrying 4 siRNAs targeted to the different regions of rat *PTN* was constructed to knockdown *PTN* and another vector with 4 non-relevant siRNAs as a control. The vectors contain CMV promoter-driven GFP for monitoring transduction efficiency. The silencing efficiency of the PTN adenovirus was over 90% as tested in fetal lung fibroblasts (data not shown). E14 fetal lungs were cultured 3 days on 30 mm Millicell inserts (Millipore) placed in six-well plates with 1.5 ml of BGJb medium in each well in the presence of various doses of viruses. The transduction efficiency gradually increased as a function of virus dose as seen by GFP fluorescence (Fig.III.6A). Western blot analysis also revealed an increase in GFP expression with increasing amounts of viruses (Fig.III.6B). The quantitation of transduction efficiency as GFP expression level was shown in Fig.III.6C. The silencing efficiency increased as measured by PTN mRNA levels when dose increased and reached a maximum level at 30 x 10^7 pfu (Fig.III.6C and 6D). The PTN protein level was also decreased by the PTN siRNA (Fig.III.6E). The control virus had no effect on PTN mRNA and protein levels expression (Fig.III.6D and 6E). Cell viability was not significantly changed as determined by measuring LDH release (Fig.III.6C). In lungs infected with siRNA adenovirus, the counts of terminal buds decreased (Fig.III.6F and 6G). The control virus had no significant effects on terminal bud numbers. There were no significant differences on the sizes of terminal buds on surface and inside of the lungs between siRNA-treated and control virus-treated or nonvirus-treated groups (Fig.III.6H).

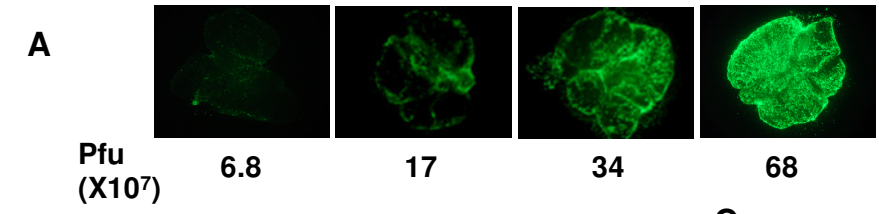
A
Pfu (X10⁷)
6.8
17
34
68

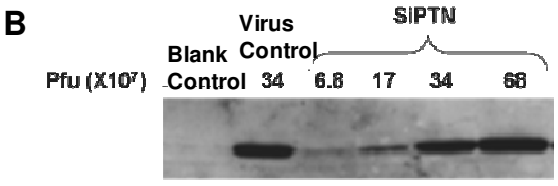
B
Virus Control
SiPTN
Blank Control
Pfu (X10⁷)
34
6.8
17
34
68

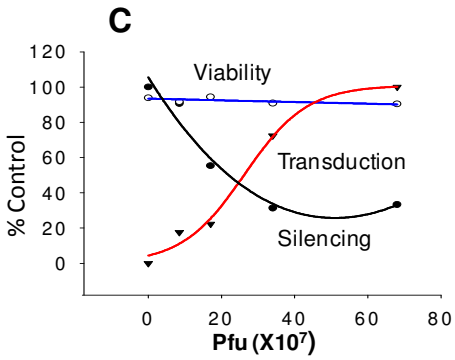
C
Viability
Transduction
Silencing
% Control
Pfu (X10⁷)

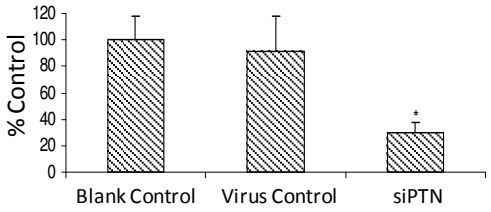
D
% Control
Blank Control
Virus Control
siPTN

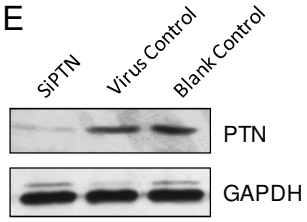
E
SiPTN
Virus Control
Blank Control
PTN
GAPDH

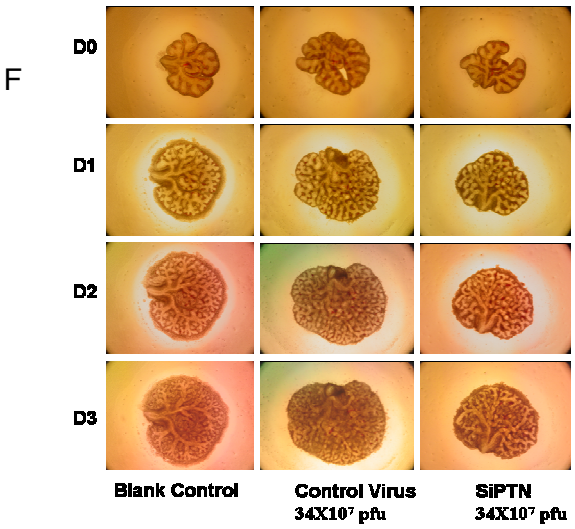
F
D0
D1
D2
D3
Blank Control
Control Virus
34X10⁷ pfu
SiPTN
34X10⁷ pfu

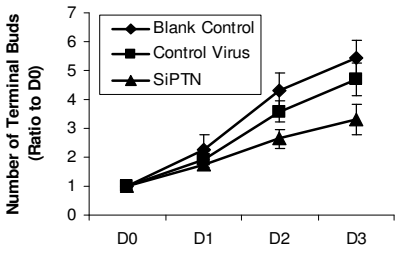
G
Number of Terminal Buds
(Ratio to D0)
Blank Control
Control Virus
SiPTN
D0
D1
D2
D3

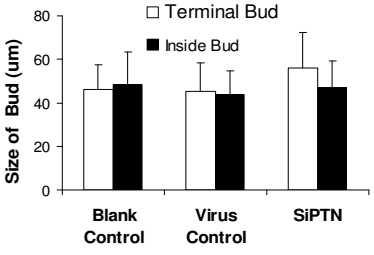
H
Terminal Bud
Inside Bud
Size of Bud (um)
Blank Control
Virus Control
SiPTN

Fig.III.6. Effect of PTN on fetal lung branching morphogenesis. (A-C) E14 fetal lungs were isolated and treated with various doses of a PTN siRNA adenovirus or a virus control. GFP fluorescence was taken at day 3 (A) and fetal lung tissues were analyzed by Western blot using anti-GFP antibodies (B). The transduction efficiency, silencing efficiency and cell viability were monitored and expressed as a percentage of untreated lungs or a maximal value (C). Transduction efficiency was measured by determining GFP expression levels. Silencing efficiency was measured by determining *ptn* mRNA levels using real-time PCR. mRNA levels were normalized to 18S rRNA. Viability was measured by determining LDH release. (D-H) E14 fetal lungs were treated with a PTN siRNA adenovirus or a virus control (34 x 10^7 pfu) for 3 days. PTN mRNA (D) and protein (E) levels were determined by real-time PCR and Western blot. Photographs were taken at day 0 to day 3 (D0-D3) (F). Terminal bud numbers (G) were counted and normalized to D0. The sizes of terminal buds on surface and inside of the lungs were also measured at D3 (H). Data shown are means ± S.E. n=6 from 3 different pregnant rats.

3.4.6 PTN signals through the RPTP β/ζ and β-catenin pathway

We hypothesized that the binding of PTN to the RPTP β/ζ receptor would lead to its inactivation and an increase in β-catenin tyrosine phosphorylation, causing the translocation of β-catenin into nuclei. To examine whether PTN stimulates tyrosine phosphorylation of β-catenin, fAEC II were serum-starved for 24 hrs and incubated with PTN (50 ng/ml) for 0-120 min. At the end of incubation, the cells were lysed and immunoprecipitated with anti-β-catenin antibodies, followed by Western blot using anti-phosphotyrosine antibodies. As shown in Fig.III.7A, PTN increased tyrosine phosphorylation of β-catenin in a time-dependent manner with a peak at 10-60 min. The tyrosine phosphorylation of β-catenin decreased after a 2-hr treatment.

We next examined whether PTN can cause β-catenin translocation into the nuclei. fAEC II were treated with PTN for 6 hrs. The cells were then collected and the nuclei were isolated. As shown in Fig.III.7B, PTN increased the nuclear β-catenin content.

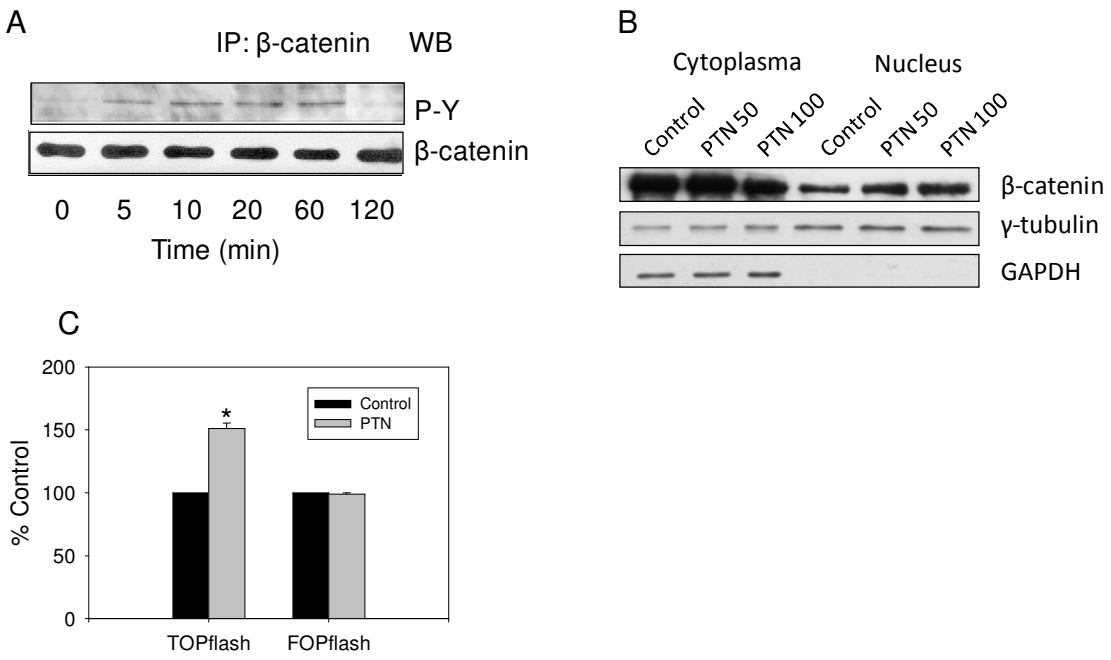

Fig.III.7. PTN initiates signaling pathway through RPTP β/ζ and β-catenin. (A) Tyrosine phosphorylation. fAEC II were serum-starved overnight and stimulated with 50 ng/ml PTN for 0-120 min. β-catenin was immunoprecipitated (IP) with anti-β-catenin antibodies and probed by Western blot (WB) with anti-phosphotyrosine (P-Y). (B) β-catenin translocation. fAECII were cultured on plastic dishes for 2 days and then treated with 50 or 100 ng/ml PTN for 6 hrs in serum-free medium. β-catenin amounts in the cytoplasma and nucleus were examined using Western blot. GAPDH and γ-tubulin were used as cytoplasmic and nuclear markers as well as loading controls. (C) TOPflash assay for TCF/LEF activation. fAEC II were transfected with TOPflash or FOPflash and phRL-TK *Renilla* luciferase and then treated with PTN (100 ng/ml) for an additional 24 hrs. The Firefly and *Renilla* luciferase activities were determined. The results were expressed as a percentage of control (untreated cells). Data shown are means ± S.E. *P<0.05 v.s. control, n=9, 3 cell preparations assayed in triplicate.

To further examine whether the cellular translocation of β-catenin subsequently activates TCF/LEF transcription factors, we used a reporter gene TOPflash assay to determine the activity of TCF/LEF transcription factors. The TOPflash plasmid contains multiple copies of the TCF/LEF binding site and a thymidine kinase minimal promoter-driven firefly luciferase. We transfected primary fAEC II with the Amaxa Nucleofector due to its high transfection efficiency on primary cells. We achieved >60% transfection efficiency using the NHBE Nucleofector kit for normal human bronchial epithelial cells and the Program T-13 as tested by a CMV-GFP vector. As shown in Fig.III.7C, PTN increased the luciferase activity. However, PTN had little effect on

FOPflash, a negative control that has a mutated TCF site in the TOPflash. The results suggest that PTN activates TCF/LEF transcription factors.

3.4.7 Dlk1 is a down-stream target of PTN signaling

β-catenin/TCF can be activated by LiCl or Wnt ligand. We determined whether LiCl or Wnt3a affects *Dlk1* expression in primary fAEC II. E20 fAEC II were cultured on matrigel for 24 hrs and treated with Wnt3a (0-20 ng/ml) or LiCl (0-20 mM) for 2 days. As shown in Fig.III.8A and B, both LiCl and Wnt3a decreased *Dlk1* mRNA expression. The maximal inhibition was 44% and 73% for Wnt3a and LiCl, respectively.

We further examined whether *β*-catenin affected *Dlk1* promoter activity. We co-transfected freshly isolated E20 fAEC II with pDlk1-FLluc, phRL-TK *Renilla* luciferase and wild type β-catenin. After overnight culture, the cells were stimulated with PTN (100 ng/ml). As shown in Fig.III.8C, co-transfection of *β*-catenin decreased *Dlk1* promoter activity in a dose-dependent manner. The addition of PTN further reduced the Dlk1 promoter activity. ΔGSK-*β*-catenin is a constitutively active form of *β*-catenin, which has 4 point mutations in the GSK-3*β* phosphorylation sites of *β*-catenin (S/T >A) and thus cannot be phosphorylated by GSK-3*β* (3). ΔGSK-*β*-catenin had more profound effects on Dlk1 promoter activity. The results suggest that PTN and *β*-catenin regulate *Dlk1* gene expression at the transcriptional level. It is worthy to note that PTN did not influence the *Dlk1* promoter activity in the absence of co-transfection of β-catenin, indicating that the co-activation of Wnt/β-catenin pathway is required for the PTN signaling.

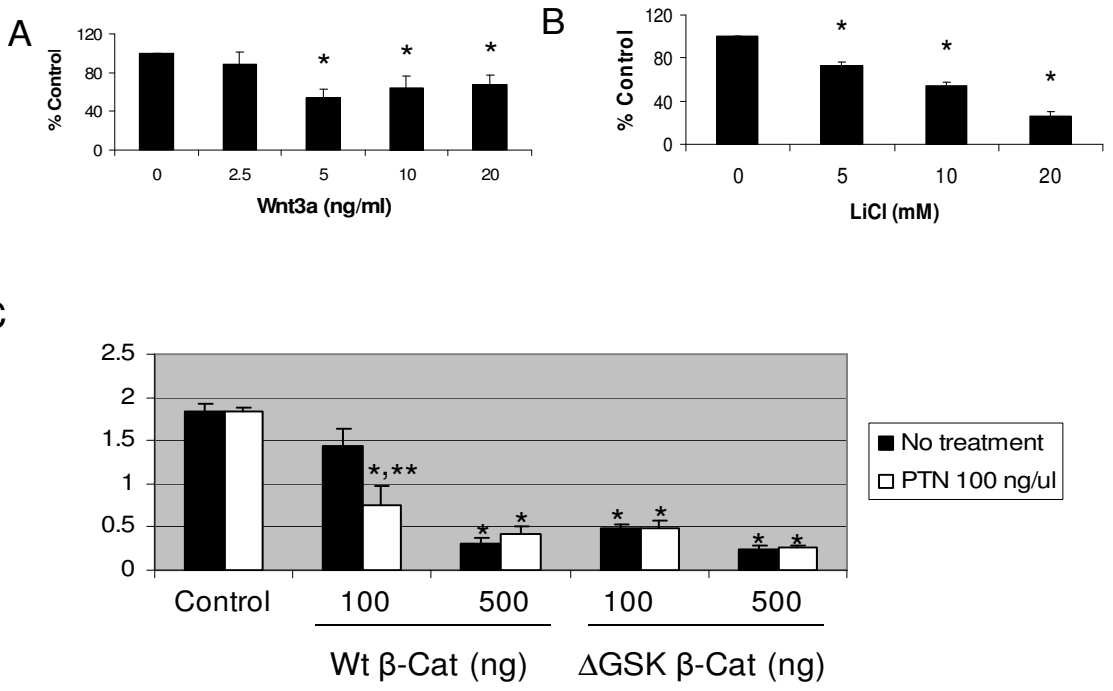

Fig.III.8. Effects of the activation of β-catenin pathway on Dlk1 expression. fAEC II were cultured on Matrigel with various concentrations of Wnt3a (A) or LiCl (B). *dlk1* mRNA level was determined by real-time PCR and normalized to 18S rRNA. Data shown are means ± S.E., *P< 0.05 v.s. untreated control cells (0), n=6, assayed in duplicate from 3 independent cell preparations. (C) Effect of β-catenin on *Dlk1* promoter activity. fAEC II (3 x 10^6) were co-transfected with pDlk1-FLluc, phRL-TK and wt β-catenin or ΔGSK β-catenin mutant by the Amaxa Nucleofector. After a 24-hr culture, the cells were incubated with PTN for 24 hrs. The *Dlk1* promoter activity was expressed as a ratio of Firefly over *Renilla* luciferase activities. Data shown are means ± S.E. *P<0.05 v.s. control (without wt β-catenin and PTN treatment); **P<0.05 v.s minus PTN and 100 ng β-catenin. n=3 independent cell preparations.

To determine whether *Dlk1* is a direct target of TCF/LEF, we performed a Chromatin Immunoprecipitation (ChIP) assay using the EZ ChIP kit. E20 fAEC II (1.5 x10^6) were treated with 20 ng/ml Wnt3a for 8 hrs. The chromatin was immunoprecipitated with 2 μg normal mouse IgG, or mouse monoclonal antibodies against β-catenin. The immuno-selected DNAs were amplified using the primers for two putative TCF/LEF binding sites (Dlk1-BS1 and Dlk1-BS2) and the flanking sequences of the Dlk1 promoter (Fig.III.9A). Wnt3a increased the binding of β-catenin to the promoter of cyclin D1 (CNND1), a known target of TCF/LEF/β-catenin (Fig.III.9B). β-catenin did not bind to the promoter of GAPDH that does not contain the TCF/LEF binding site. β-catenin bound to both TCF/LEF binding sites on the Dlk1 promoter and this binding was enhanced by Wnt3a (Fig.III.9B). The negative control using normal mouse IgG did not have any bands. These results suggest that Dlk1 is a direct target of TCF/LEF.

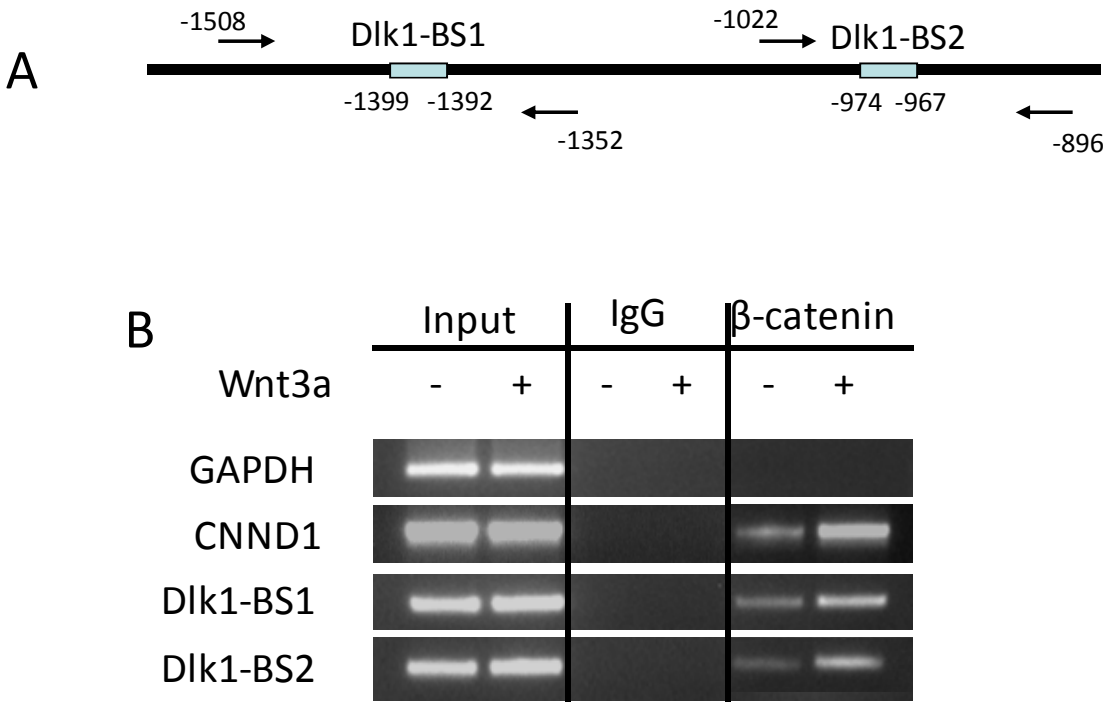

Fig.III.9. ChIP assay showing that Dlk1 is a direct target of TCF/LEF in fAEC II. (A) Two putative TCF/LEF binding sites (Dlk1-BS1, -1399 to -1392 and Dlk1-BS2, -974 to -967) of the Dlk1 promoter. The arrows indicate primers used for PCR amplification. (B) The immunoprecipitated DNAs using anti-β-catenin antibodies were PCR-amplified using the primer pairs for Dlk1-BS1 and Dlk1-BS2. GAPDH and cyclin D1 (CNND1) served as negative and positive controls, respectively. Normal IgG was used as an IP control.

3.5 DISCUSSION

In this study, we investigated the role of PTN in fetal epithelial cell proliferation and differentiation and underlying mechanisms. PTN and its receptor, RPTP β/ζ were found in mesenchymal and epithelial cells of the fetal lungs at the late stages of development. PTN promoted fAEC II proliferation and epithelial repair, but inhibited fAEC II trans-differentiation into AEC I. The knockdown of PTN in E14 fetal lung organ culture decreased lung branching morphogenesis. Furthermore, PTN increased the tyrosine phosphorylation of β-catenin and translocation of β-catenin into the nucleus, and activated the TCF/LEF transcription factors, leading to transcriptional depression of *Dlk1*.

Fetal lung development are divided into 5 stages: embroyonic (E0-13); pseudoglandular (E13-18); canalicular (E18-20); sacular (E20 – term) and alveolar stages (term – adult). Branching morphogenesis occurs at the pseudoglandular stage and accomplished by inducing

the formation of buds from the outmost periphery of the epithelial tubes. Alveolar epithelial cell differentiation is a two-step process. At the canalicular stage, the columnar epithelial cells or pre-type II cells differentiate into mature type II cells, which in turn trans-differentiate into type I cells in the secular stage. PTN has multiple roles in fetal lung development at various stages. PTN is necessary for lung branching morphogenesis at the early stage of development; PTN also promotes epithelial type II cell proliferation and migration but suppresses the trans-differentiation of type II cells into type I cells at the late stage of development.

At 50 ng/ml, PTN has a marked effect on cell proliferation and differentiation. However, this dose appears to have a modest effect on wound healing and a higher dose is required for this assay. It is therefore likely that there are different effective doses for different functional consequences caused by PTN.

PTN has been reported to be highly expressed during the late stages of embryogenesis (16; 20; 44). Our previous real-time PCR and Western blot results have shown that PTN mRNA and protein expression levels were high at the late stage of fetal lung development (47). The current detailed immunohistochemical studies of fetal lungs at different stages confirmed that PTN was mainly expressed in mesenchymal cells surrounding the epithelium at E18 to E20. Similar analyses of the PTN receptor, RPTP β/ζ revealed its localization in columnar and alveolar epithelial cells and its high expression at E20. Therefore, both PTN and its receptor RPTP β/ζ had the highest expression during the stage when alveolar epithelial cells proliferation and differentiation occur. The restricted temporal and spatial expression of these two genes suggests that PTN is a mediator of mesenchymal-epithelial interactions during fetal lung development, possibly reflecting their roles in fAEC II proliferation and differentiation.

It is well known that epithelial-mesenchymal interaction is essential for normal growth, morphogenesis and cell differentiation in the developing lung (40). Signals from the mesenchymal cells determine the patterning of the epithelium as well as the differentiated phenotype of the epithelium. Removal of the mesenchyme from the developing lung impairs lung branching morphogenesis and stops the epithelium from proliferating and differentiating (41). During the late stage of fetal lung development, fAEC II differentiate from progenitor cells and further trans-differentiate into AEC I. Many factors secreted from the mesenchyme have been identified to regulate fAEC II differentiation including FGF10 (23). Our current study identified PTN as an additional such factor.

PTN increased fAEC II proliferation and inhibited fAEC II trans-differentiation. The regulation of cell proliferation is coupled with that of cell differentiation. The cells that enter differentiation pathway normally go into G0 phase and stop proliferating (15; 36; 45). The cell proliferation and differentiation are independent but well coupled processes that can be precisely regulated by many factors. In normal development, the progenitor cells generate enough cells for

differentiation, and then exit from cell cycle and start to differentiate into mature cells (36). In myogenic precursor cells, this process is achieved by upregulating P21 which inhibits the cdk activities (45). Reversely, it has been demonstrated that the overexpression of the cell cycle protein, cyclin D1 blocks the terminal differentiation (33). Collectively, PTN may act as a link between fAEC II proliferation and differentiation. It may achieve this by keeping the fAEC II in a proliferating state and maintains its phenotype. Since coordinated cell proliferation and differentiation are essential for normal organogenesis. PTN may play an essential role in fetal lung development.

Recently, PTN was found to play a role in epithelial-mesenchymal transition (EMT) (29). PTN-treated U373 epithelial cells exhibited fibroblast-like cells with elongated shape, increased cell migration and disappeared cell polarity. We found that PTN increased wound healing, possibly due to an increased cell migration. This is supported by the observation that PTN-treated fAEC II had fibroblast-like F-actin distribution on the edge of the wound area. Furthermore, canonical Wnt signaling pathway is important for the cancer cell invasion and migration (27). Our results showed that PTN activated the Wnt/β-catenin signaling. The effect of PTN on fAEC II wound healing may also be partly due to the cell proliferation or migration.

PTN has been identified as an important factor on renal branching morphogenesis (37). Glial-derived neurotrophic factor (GDNF), a peptide growth factor which is required for ureteric bud outgrowth, induces the branching in isolated ureteric bud explants at the presence of PTN. However, purified PTN alone also induces ureteric bud outgrowth. This result suggests that PTN is necessary for GDNF signaling. Additionally, using whole embryonic kidney organ culture, PTN induces the ureteric bud outgrowth. Similar to renal branching, the lung undergoes branching morphogenesis during the development. Knockdown of PTN expression decreased the number of terminal buds, indicating its role in lung branching morphogenesis. However, how PTN regulates lung branching morphogenesis remains to be determined.

We found that PTN increased the tyrosine phosphorylation of β-catenin in fAECII, resulting in β-catenin accumulation in the nucleus and thus increase LEF/TCF transcriptional activity. Tyrosine phosphorylation of β-catenin at Y654 and Y142 reduces the binding affinity of β-catenin to E-cadherin and α-catenin, respectively (21; 31; 35). Several lines of evidence have demonstrated that tyrosine phosphorylation of β-catenin abolishes adhesion and increase the transcription activity (30). Thus, PTN may act as a key regulator in switching the role of β-catenin from cell adhesion to transcription. Since PTN enhanced TCF/LEF activity as assessed by the TOPflash assay, we, for the first time, integrated the PTN/RPTP β/ζ pathway with the canonical β-catenin/LEF-TCF pathway.

Wnt regulates lung morphogenesis through the canonical β-catenin/LEF-TCF pathway (32). β-catenin signaling is essential for cell fate determination in epithelium and mesenchyme in

the developing lung (8; 26). In the absence of Wnt signal, β-catenin is phosphorylated at several serine-threonine sites by glycogen synthase kinase 3beta and casein kinase and is subsequently marked for proteasomal degradation (10; 30; 48). In the presence of Wnts, β-catenin is stabilized and accumulates in the nucleus to activate the transcription of its downstream genes such as N-myc, bone morphogenetic protein 4 and FGF. In U373 cells, PTN increases tyrosine phorphorylation of β-catenin and releases β-catenin from the membrane (29). However, subsequent β-catenin nuclear accumulation is not reported. In the present studies, we observed that PTN not only increased tyrosine phosphorylation of β-catenin, but also resulted in the β-catenin nuclear translocation and the activation of TCF/LEF in fAEC II. Our results suggest that PTN may enhance the Wnt/β-catenin signaling and thus regulate lung development.

Both canonical Wnt and Notch signaling pathway is indispensable for stem and progenitor cell fate determination and subsequent differentiation during embryonic development and adult life (1; 6; 7; 11; 28). These two pathways are reciprocally regulated. Abolishment of Wnt signaling leads to instable notch activities during somitogenesis (2). These results suggested that Wnt pathway may act as an upstream regulator of Notch pathway. Dlk-1 is a ligand of Notch receptor. Another member of this family, Dll1 was identified as a direct target of TCF/LEF transcription factors (13; 18). The following evidence support that PTN/Wnt-β-catenin signaling pathways negatively regulate Dlk1 in fAEC II: (i) *β*-catenin decreased *Dlk1* promoter activity in a dose-dependent manner and the addition of PTN further reduced the *Dlk1* promoter activity. ΔGSK-*β*-catenin, a constitutively activated *β*-catenin mutant, had more profound effects on the *Dlk1* promoter activity. (ii) ChIP assay showed that β-catenin bound to both TCF/LEF binding sites on the *Dlk1* promoter and this binding was enhanced by Wnt3a. and (iii) Dlk1 was down-regulated in Wnt3a- or LiCl-treated fAEC II. Together with the fact that PTN activated the Wnt signaling pathway, these results suggest a novel molecular link between Notch and Wnt signaling pathways during fetal lung development.

3.6 REFERENCES

1. Aoyama K, Delaney C, Varnum-Finney B, Kohn AD, Moon RT and Bernstein ID. The interaction of the Wnt and Notch pathways modulates natural killer versus T cell differentiation. *Stem Cells* 25: 2488-2497, 2007.
2. Aulehla A, Wehrle C, Brand-Saberi B, Kemler R, Gossler A, Kanzler B and Herrmann BG. Wnt3a plays a major role in the segmentation clock controlling somitogenesis. *Dev Cell* 4: 395-406, 2003.
3. Barth AI, Stewart DB and Nelson WJ. T cell factor-activated transcription is not sufficient to induce anchorage-independent growth of epithelial cells expressing mutant beta-catenin. *Proc Natl Acad Sci U S A* 96: 4947-4952, 1999.
4. Batenburg JJ, Otto-Verberne CJ, Ten Have-Opbroek AA and Klazinga W. Isolation of alveolar type II cells from fetal rat lung by differential adherence in monolayer culture. *Biochim Biophys Acta* 960: 441-453, 1988.

5. Bellusci S, Grindley J, Emoto H, Itoh N and Hogan BL. Fibroblast growth factor 10 (FGF10) and branching morphogenesis in the embryonic mouse lung. *Development* 124: 4867-4878, 1997.

6. Cheng P and Gabrilovich D. Notch signaling in differentiation and function of dendritic cells. *Immunol Res* 41: 1-14, 2008.

7. Cohen ED, Tian Y and Morrisey EE. Wnt signaling: an essential regulator of cardiovascular differentiation, morphogenesis and progenitor self-renewal. *Development* 135: 789-798, 2008.

8. De Langhe SP, Carraro G, Tefft D, Li C, Xu X, Chai Y, Minoo P, Hajihosseini MK, Drouin J, Kaartinen V and Bellusci S. Formation and differentiation of multiple mesenchymal lineages during lung development is regulated by beta-catenin signaling. *PLoS ONE* 3: e1516, 2008.

9. Deuel TF, Zhang N, Yeh HJ, Silos-Santiago I and Wang ZY. Pleiotrophin: a cytokine with diverse functions and a novel signaling pathway. *Arch Biochem Biophys* 397: 162-171, 2002.

10. Eberhart CG and Argani P. Wnt signaling in human development: beta-catenin nuclear translocation in fetal lung, kidney, placenta, capillaries, adrenal, and cartilage. *Pediatr Dev Pathol* 4: 351-357, 2001.

11. Eijken M, Meijer IM, Westbroek I, Koedam M, Chiba H, Uitterlinden AG, Pols HA and van Leeuwen JP. Wnt signaling acts and is regulated in a human osteoblast differentiation dependent manner. *J Cell Biochem* 104: 568-579, 2008.

12. Fraslon C, Rolland G, Bourbon JR, Rieutort M and Valenza C. Culture of fetal alveolar epithelial type II cells in serum-free medium. *In Vitro Cell Dev Biol* 27A: 843-852, 1991.

13. Galceran J, Sustmann C, Hsu SC, Folberth S and Grosschedl R. LEF1-mediated regulation of Delta-like1 links Wnt and Notch signaling in somitogenesis. *Genes Dev* 18: 2718-2723, 2004.

14. Gou D, Weng T, Wang Y, Wang Z, Zhang H, Gao L, Chen Z, Wang P and Liu L. A novel approach for the construction of multiple shRNA expression vectors. *J Gene Med* 9: 751-763, 2007.

15. Heller H, Gredinger E and Bengal E. Rac1 inhibits myogenic differentiation by preventing the complete withdrawal of myoblasts from the cell cycle. *J Biol Chem* 276: 37307-37316, 2001.

16. Herradon G, Ezquerra L, Nguyen T, Vogt TF, Bronson R, Silos-Santiago I and Deuel TF. Pleiotrophin is an important regulator of the renin-angiotensin system in mouse aorta. *Biochem Biophys Res Commun* 324: 1041-1047, 2004.

17. Hilfer SR. Morphogenesis of the lung: control of embryonic and fetal branching. *Annu Rev Physiol* 58: 93-113, 1996.

18. Hofmann M, Schuster-Gossler K, Watabe-Rudolph M, Aulehla A, Herrmann BG and Gossler A. WNT signaling, in synergy with T/TBX6, controls Notch signaling by regulating Dll1 expression in the presomitic mesoderm of mouse embryos. *Genes Dev* 18: 2712-2717, 2004.

19. Jager R, Noll K, Havemann K, Pfluger KH, Knabbe C, Rauvala H and Zugmaier G. Differential expression and biological activity of the heparin-binding growth-associated molecule (HB-GAM) in lung cancer cell lines. *Int J Cancer* 73: 537-543, 1997.

20. Li YS, Milner PG, Chauhan AK, Watson MA, Hoffman RM, Kodner CM, Milbrandt J and Deuel TF. Cloning and expression of a developmentally regulated protein that induces mitogenic and neurite outgrowth activity. *Science* 250: 1690-1694, 1990.

21. Lilien J and Balsamo J. The regulation of cadherin-mediated adhesion by tyrosine phosphorylation/dephosphorylation of beta-catenin. *Curr Opin Cell Biol* 17: 459-465, 2005.

22. Litingtung Y, Lei L, Westphal H and Chiang C. Sonic hedgehog is essential to foregut development. *Nat Genet* 20: 58-61, 1998.

23. Maeda Y, Dave V and Whitsett JA. Transcriptional control of lung morphogenesis. *Physiol Rev* 87: 219-244, 2007.

24. Meng K, Rodriguez-Pena A, Dimitrov T, Chen W, Yamin M, Noda M and Deuel TF. Pleiotrophin signals increased tyrosine phosphorylation of beta-catenin through inactivation of the intrinsic catalytic activity of the receptor-type protein tyrosine phosphatase beta/zeta. *Proc Natl Acad Sci U S A* 97: 2603-2608, 2000.

25. Milner PG, Li YS, Hoffman RM, Kodner CM, Siegel NR and Deuel TF. A novel 17 kD heparin-binding growth factor (HBGF-8) in bovine uterus: purification and N-terminal amino acid sequence. *Biochem Biophys Res Commun* 165: 1096-1103, 1989.

26. Mucenski ML, Nation JM, Thitoff AR, Besnard V, Xu Y, Wert SE, Harada N, Taketo MM, Stahlman MT and Whitsett JA. beta-catenin regulates differentiation of respiratory epithelial cells in vivo. *Am J Physiol Lung Cell Mol Physiol* 289: L971-L979, 2005.

27. Neth P, Ries C, Karow M, Egea V, Ilmer M and Jochum M. The Wnt signal transduction pathway in stem cells and cancer cells: influence on cellular invasion. *Stem Cell Rev* 3: 18-29, 2007.

28. Osborne BA and Minter LM. Notch signalling during peripheral T-cell activation and differentiation. *Nat Rev Immunol* 7: 64-75, 2007.

29. Perez-Pinera P, Alcantara S, Dimitrov T, Vega JA and Deuel TF. Pleiotrophin disrupts calcium-dependent homophilic cell-cell adhesion and initiates an epithelial-mesenchymal transition. *Proc Natl Acad Sci U S A* 103: 17795-17800, 2006.

30. Piedra J, Martinez D, Castano J, Miravet S, Dunach M and de Herreros AG. Regulation of beta-catenin structure and activity by tyrosine phosphorylation. *J Biol Chem* 276: 20436-20443, 2001.

31. Piedra J, Miravet S, Castano J, Palmer HG, Heisterkamp N, Garcia de HA and Dunach M. p120 Catenin-associated Fer and Fyn tyrosine kinases regulate beta-catenin Tyr-142 phosphorylation and beta-catenin-alpha-catenin Interaction. *Mol Cell Biol* 23: 2287-2297, 2003.

32. Pongracz JE and Stockley RA. Wnt signalling in lung development and diseases. *Respir Res* 7: 15, 2006.

33. Rao SS, Chu C and Kohtz DS. Ectopic expression of cyclin D1 prevents activation of gene transcription by myogenic basic helix-loop-helix regulators. *Mol Cell Biol* 14: 5259-5267, 1994.

34. Rauvala H. An 18-kd heparin-binding protein of developing brain that is distinct from fibroblast growth factors. *EMBO J* 8: 2933-2941, 1989.

35. Roura S, Miravet S, Piedra J, Garcia dH and Dunach M. Regulation of E-cadherin/Catenin association by tyrosine phosphorylation. *J Biol Chem* 274: 36734-36740, 1999.

36. Sachs L. Constitutive uncoupling of pathways of gene expression that control growth and differentiation in myeloid leukemia: a model for the origin and progression of malignancy. *Proc Natl Acad Sci U S A* 77: 6152-6156, 1980.

37. Sakurai H, Bush KT and Nigam SK. Identification of pleiotrophin as a mesenchymal factor involved in ureteric bud branching morphogenesis. *Development* 128: 3283-3293, 2001.

38. Sekine K, Ohuchi H, Fujiwara M, Yamasaki M, Yoshizawa T, Sato T, Yagishita N, Matsui D, Koga Y, Itoh N and Kato S. Fgf10 is essential for limb and lung formation. *Nat Genet* 21: 138-141, 1999.

39. Seykora JT, Jih D, Elenitsas R, Horng WH and Elder DE. Gene expression profiling of melanocytic lesions. *Am J Dermatopathol* 25: 6-11, 2003.

40. Shannon JM and Hyatt BA. Epithelial-mesenchymal interactions in the developing lung. *Annu Rev Physiol* 66: 625-645, 2004.

41. Shannon JM, Nielsen LD, Gebb SA and Randell SH. Mesenchyme specifies epithelial differentiation in reciprocal recombinants of embryonic lung and trachea. *Dev Dyn* 212: 482-494, 1998.

42. Silos-Santiago I, Yeh HJ, Gurrieri MA, Guillerman RP, Li YS, Wolf J, Snider W and Deuel TF. Localization of pleiotrophin and its mRNA in subpopulations of neurons and their corresponding axonal tracts suggests important roles in neural-glial interactions during development and in maturity. *J Neurobiol* 31: 283-296, 1996.

43. Stoica GE, Kuo A, Aigner A, Sunitha I, Souttou B, Malerczyk C, Caughey DJ, Wen D, Karavanov A, Riegel AT and Wellstein A. Identification of anaplastic lymphoma kinase as a receptor for the growth factor pleiotrophin. *J Biol Chem* 276: 16772-16779, 2001.

44. Vanderwinden JM, Mailleux P, Schiffmann SN and Vanderhaeghen JJ. Cellular distribution of the new growth factor pleiotrophin (HB-GAM) mRNA in developing and adult rat tissues. *Anat Embryol (Berl)* 186: 387-406, 1992.

45. Walsh K and Perlman H. Cell cycle exit upon myogenic differentiation. *Curr Opin Genet Dev* 7: 597-602, 1997.

46. Wellstein A, Fang WJ, Khatri A, Lu Y, Swain SS, Dickson RB, Sasse J, Riegel AT and Lippman ME. A heparin-binding growth factor secreted from breast cancer cells homologous to a developmentally regulated cytokine. *J Biol Chem* 267: 2582-2587, 1992.

47. Weng T, Chen Z, Jin N, Gao L and Liu L. Gene Expression Profiling Identifies Regulatory Pathways Involved in the Late Stage of Rat Fetal Lung Development. *Am J Physiol Lung Cell Mol Physiol* 291: L1027-L1037, 2006.

48. Wodarz A and Nusse R. Mechanisms of Wnt signaling in development. *Annu Rev Cell Dev Biol* 14: 59-88, 1998.

49. Yeh HJ, He YY, Xu J, Hsu CY and Deuel TF. Upregulation of pleiotrophin gene expression in developing microvasculature, macrophages, and astrocytes after acute ischemic brain injury. *J Neurosci* 18: 3699-3707, 1998.

3.7 Acknowledgements

We thank Dr. Li Gao for measuring the Dlk1 promoter activity and doing the Topflash and Chip assay, Dr. Manoj Bhaskaran for doing the immunostaining, Yujie Guo for assistance with some of the Real-time PCR, Dr. Deming Gou for constructing the Dlk1 promoter, Dr. Narayanaperumal J. Sarathy for doing the Western blots for some of the proteins, Dr. Narendranth Reddy Chintagari for helping with the isolation of fetal AEC II cells, and Dr. Kexiong Zhang for assistance with the fetal lung isolation. We are grateful to Dr. Angela Barth (Stanford U) for β-catenin and ΔGSK β-catenin constructs and Dr. Mary Williams (Boston U) for T1α antibodies. This work was supported by NIH grants R01 HL-052146, R01 HL-071628 and R01 HL-083188 (LL). TTW was supported by a predoctoral fellowship from the American Heart Association (0610143Z).

CHAPTER IV

DEFICIENCY OF PTN RESULTS IN ABNORMAL LUNG DEVELOPMENT IN ADULT MICE

4.1 Abstract

Pleiotrophin (PTN) is a heprin-binding cytokine which has multiple roles on cell proliferation, differentiation, and apoptosis. No *in vivo* studies have been carried out to investigate the role of PTN in fetal lung development. In this study, using PTN knockout ($PTN^{-/-}$) and wild-type ($PTN^{+/+}$) mice, we examined the lung morphology and cell marker gene expression during lung development. The lung morphology had no significant difference between $PTN^{-/-}$ and $PTN^{+/+}$ mice during the fetal and early postnatal stages. However, on postnatal day 15 and 35, the lungs of $PTN^{-/-}$ mice were less mature and developed than those of $PTN^{+/+}$ mice of the same age. These lungs exhibited hyperplasia, which was accompanied with significantly smaller alveoli and thicker septa. In the adult stage, the mRNA expression of SP-A, B, and C, and CCSP all increased significantly, while P2X7R and T1-α expression decreased, and α-SMA expression was significantly higher in $PTN^{-/-}$ mouse lungs. Our data indicated that deprivation of PTN expression may slow lung maturation by arresting lung development at juvenile and adult, where alveolar epithelial type II cells were accumulated but failed to further differentiate into alveolar epithelial type I cells. Our data demonstrate for the first time that PTN may play an important role in alveolarization during lung development.

4.2 Introduction

Pulmonary development is an important biological process. The lung originates from the foregut endoderm and develops by repeated bifurcal branching morphogenesis. The mammalian pulmonary system is among the latest organs to be mature functionally. During normal lung development, the mesenchymal-epithelial interactions play crucial roles in inducing the origination of the lung bud, promoting the lung branching morphogenesis, and stimulating epithelial differentiation. Signals from the mesenchyme are critical to induce the formation of the epithelium. Removing the mesenchyme from the embryonic lung rudiment impairs branching morphogenesis. The lung mesenchyme alone is sufficient to induce branching morphogenesis in non-lung epitheliums such as salivary gland (17) and embryonic trachea, whose mesenchyme has been removed (1; 34). On the other hand, epithelial cells also express and secrete growth factors to regulate the differentiation and proliferation of mesenchymal cells. The mesenchymal-epithelial interactions are mediated by many signaling molecules, such as transcription factors, growth factors, and extracellular matrix proteins. These factors include those secreted from mesenchymal cells, such as fibroblast growth factors (FGFs), and their receptors, retinoid acid (RA), and Wnt proteins, and those expressed by epithelial cells, including vascular endothelial growth factors (VEGF), Platelet-derived growth factor (PDGF), and Sonic Hedgehog (Shh) (26).

Previously, using cDNA microarray, we identified Pleitrophin (PTN) as a growth factor, that was differentially expressed during fetal lung development (31). PTN is a highly conserved extracellular growth factor and shares 50% homology with Midkine (MK), the only other heparin binding cytokine in the family. The expression of PTN is precisely regulated during development. PTN is mainly located in the basement membrane of the developing epithelium and in mesenchymal tissues undergoing remodeling, suggesting that it may regulate cell differentiation and mesenchymal-epithelial interactions (19). In the adult stage, PTN expression is only restricted to central nervous system (18; 23). PTN has multiple functions. It regulates neurite outgrowth, plays an important role in neural and cancer development, enhances the cell proliferation and migration, and inhibits the apoptosis of various cells. Additionally, PTN has been implicated in epithelial-mesenchymal interactions during the organogenesis (15; 22). However, the role of PTN on fetal lung development is barely studied.

We have previously shown that PTN is mainly located in the mesenchymal area surrounding the developing epithelium, and its receptor, protein receptor tyrosine phosphatase β/ζ (RPTPβ/ζ), is in the airway and developing alveolar epithelium, indicating that PTN may play an important role in the mesenchymal-epithelium interaction during fetal lung development (32). Additionally, PTN is able to increase the proliferation and inhibit the differentiation of primary cultured fetal lung epithelial cells. However, no *in vivo* studies have been carried out to investigate the role of PTN in normal lung development.

Several research groups have used PTN knockout ($PTN^{-/-}$) mice to study PTN functions. The $PTN^{-/-}$ mice are fertile and appear to be anatomically normal. However, mice deficient of PTN expression exhibit enhanced hippocampal long-term potentiation (2). Deficiency of PTN results in increased proliferation rate of neuronal stem cells in the adult mouse cerebral cortex (11). Consistently, exogenous PTN reduces the neuronal stem cell proliferation through inhibiting the expression of FGF-2 and promotes cell differentiation (11). However, whether $PTN^{-/-}$ mice have normal lung development is not known.

In this study, we used $PTN^{-/-}$ mice to investigate the role of PTN in fetal lung development. Using Real-time PCR and Western Blot, we examined cell marker gene expression to monitor cell differentiation during development. We also investigated the morphological changes of the developing lung using morphometric analysis. Our study is the first report to demonstrate the role of PTN in fetal lung development *in vivo*.

4.3 Material and Methods

4.3.1 Pleiotrophin Knockout Mice

Mice deficient in PTN gene (a kind gift from Dr. T. Muramatsu) were generated as described (24). To achieve a genetic identity, $PTN^{+/-}$ mice were backcrossed with C57BL/6J mice for several generations (21; 37). The offspring's genotype was determined by PCR using the genomic DNA isolated from a part of the ear. $PTN^{-/-}$ and $PTN^{+/+}$ mice were generated by mating two $PTN^{+/-}$ mice with each other. Timed pregnant $PTN^{-/-}$ and $PTN^{+/+}$ mice were obtained by mating a male and a female $PTN^{-/-}$ or $PTN^{+/+}$ mouse. The day when a vaginal plug was observed was defined as embryonic day 0.5.

4.3.2 Tissue section preparation

The fetal mouse lungs were prepared as described (31). Briefly, timed pregnant mice were killed by carbon-dioxide. The fetuses were removed from the uterus to harvest the fetal lungs. The isolated lungs were immediately fixed in 4% formaldehyde in PBS for 24 hours. Postnatal day 1 and 7 mice were killed by carbon-dioxide, and the lungs were separated and fixed. Postnatal day 15 and adult mice were killed by injection of anesthetic (40 mg Ketamine and 8 mg Xylazine per 1 kg animals). The lungs were perfused with Hank's Balanced Salt Solution (HBSS) (Invitrogen, Carlsbad, CA) and fixed by instilling 4% formaldehyde-PBS into the trachea under a hydrostatic pressure of 20 cm for 10 min. Then, the lungs were separated and placed in 4% formaldehyde-PBS for additional 24 hours. The fixed lungs were washed in PBS, dehydrated in series of different concentrations of ethanol and xylene, and paraffin-embedded (60℃). The lung sections were cut (4 μm thickness) and placed on polysine glass slides. Hematoxyline and eosin staining was performed to study the lung morphology.

4.3.3 Morphometric Analysis

The morphometric analysis was carried out by examining 15 fields selected from 3 sections for each treatment group. To eliminate regional differences, at least one field was taken from each of the following three regions: the upper lobes, the right lower lobe and the left lower lobe. The alveolarization was assessed by measuring mean linear intercept (MLI), the diameter and lumen size of the alveoli. The MLI was obtained by drawing 4 lines across the lung section (two diagonal lines, one horizontal line and one vertical line across the whole field, the areas with alveolar sacs and bronchioles were avoided) and dividing the length of the line by the number of intercepts encountered. For alveolar diameter and lumen size, and septa thickness, the slides were examined at 800X magnification. The diameter of the alveoli was obtained by measuring the longest diameter of 500 randomly selected, non-overlapping alveoli for each treatment group. The septa thickness was obtained by randomly measuring the thickness of 4 septa of each alveoli and at least 15 alveoli per fields using the Image J software. The alveolar lumen size was evaluated

using Image J by measuring the closed area of all the alveoli in each field. All the images were analyzed blindly.

4.3.4 Real-time PCR

Total RNAs from $PTN^{-/-}$ and $PTN^{+/+}$ mouse lungs were isolated using TRI reagent. Genomic DNA contamination was removed with RNase-freeTM DNase (Ambion Inc., Austin, TX). 1 μg total RNAs were reverse-transcribed into cDNA using oligo dT and random hexamers (promega, Madison, WI) and M-MLV reverse transcriptase (Invitrogen, Carlsbad, CA). The primers for real-time PCR were designed using Primer Express® software (Applied Biosystems, Foster City, CA): T1-α forward: 5'-ACCGTGCCAGTGTTGTTCTG-3', reverse: 5'-AGCACCTGTGGTTGTTATTTTGT-3'; SP-A forward: 5'-GAGGAGCTTCAGACTGCACTC-3', reverse: 5'-AGACTTTATCCCCCACTGACAG-3'; SP-B forward: 5'-CTGCTTCCTACCCTCTGCTG-3', reverse: 5'-CTTGGCACAGGTCATTAGCTC-3'; SP-C forward: 5'-ATGGACATGAGTAGCAAAGAGGT-3', reverse: 5'-CACGATGAGAAGGCGTTTGAG-3'; CCSP forward: 5'-ATGAAGATCGCCATCACAATCAC-3', reverse: 5'-GGATGCCACATAACCAGACTCT-3'; Midkine forward: 5'-GAAGAAGGCGCGGTACAATG-3', reverse: 5'-GAGGTGCAGGGCTTAGTCA-3'; 18S forward: 5'-ATTGCTCAATCTCGGGTGGCTG-3' and reverse: 5'-CGTTCTTAGTTGGTGGAGCGATTTG 3'. Real-time PCR was performed on 7900HT Fast Real-Time PCR System using SYBR Green I detection (Eurogentec, San Diego, CA) as previously described (33). After the amplification, a dissociation curve was generated to check the specificity of the amplification. The data were normalized to 18S rRNA.

4.3.5 Western Blot

The lung tissues were homogenized in M-PER lysis buffer (Pierce, Rockford, IL) on ice. Protein concentration was determined using the DC protein assay kit (Bio-Rad, Hercules, CA). Total proteins were separated by 10% SDS-PAGE and then transferred onto a nitrocellulose membrane. The blot was stained by Ponceau S to check transfer efficiency. The membrane was blocked with 5% dry milk in Tris-buffered saline for 1 hour, washed with Tris-buffered saline containing 0.05% Tween 20, and incubated with mouse anti α-SMA (1:2000, Sigma, St. Louis, MO), rabbit anti-vimentin (1:500, Abcam, Cambridge, MA) or rabbit anti-β-actin antibodies (1:1,000 dilution; Bio-Rad, Hercules, CA) overnight at 4℃. The membrane was washed again and incubated with horseradish peroxidase-conjugated anti-rabbit or anti-mouse IgG (1:2,000, Jackson ImmunoResearch Laboratories, West Grove, PA) for 1 hour. Finally, the membrane was developed with enhanced chemiluminescence reagents (Amersham Biosciences, Piscataway, NJ) and exposed to X-ray film.

Immunohistochemistry

The lungs sections were deparaffinized in xylene, and rehydrated in grade ethanol. After being washed in PBS, the sections were incubated in 3% peroxide for 10 min to remove the endogenous preoxidase, permeabilized with 0.3% Triton X-100 in PBS for 20 min, kept in 20 mM citrate buffer (pH 6.0) for 5 min for antigen retrieval and blocked with 10% FBS in PBS for 1 hour. Then the slides were incubated with primary antibodies overnight at 4℃, followed by 1 hour incubation with secondary antibodies. After rinse, the slides were further incubated with fresh ABC reagent (Vector Laboratories, Burlingame, CA) for 30 min and then developed in DAB reagent until desire staining was observed. Finally the slides were counter-stained with Hematoxylin (Vector Laboratories, Burlingame, CA) for 1 min, mounted with permanent anti-fade medium (Vector Laboratories, Burlingame, CA) and examined using a Nikon Eclipse E600 microscope.

4.4 Results

4.4.1 $PTN^{-/-}$ mouse lung was less developed in adult

The $PTN^{-/-}$ mice were fertile and had no obvious physiological abnormalities. The lung to body weight of the $PTN^{-/-}$ mice were slightly lower but not significantly different compared to the $PTN^{+/+}$ mice (Fig.IV.1).

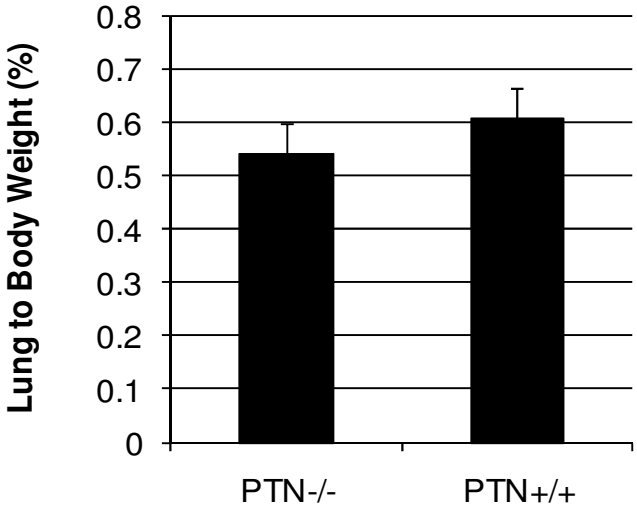

Fig.IV.1. $PTN^{-/-}$ mice have slightly decreased lung to body weight. The lungs were collected from 4 to 6 months old $PTN^{-/-}$ and $PTN^{+/+}$ mice, and the lung weight to body weight were measured (n=7 for $PTN^{-/-}$ mice and n=4 for $PTN^{+/+}$ mice, P=0.055).

To examine the morphological changes during development, we collected the lungs from $PTN^{-/-}$ and $PTN^{+/+}$ mice at embryonic day 14.5, and 17.5 (E14.5 and E17.5), postnatal day 1, 7, 15 and 35 (P1, P7, P15, and P35). The E14.5 and E17.5 lungs of $PTN^{-/-}$ mice had no significantly difference from those of $PTN^{+/+}$ mice (Fig.II.2 panel A and B). At the early postnatal stages (P1 and P7), still no difference was observed between $PTN^{+/+}$ and $PTN^{-/-}$ mice. However, there were consistent and appreciable differences between lung sections of $PTN^{+/+}$ and $PTN^{-/-}$ mice on P15 and P35. In both age groups, alveolar septa from $PTN^{-/-}$ mice were thicker than those from age-matched $PTN^{+/+}$ mice (Fig.IV.2A). On average, in the $PTN^{-/-}$ mice, the septa thickness increased more than 100%. The average alveolar lumen size decreased ~ 50% and alveolar diameter diminished ~30% compared with the $PTN^{+/+}$ mice (Fig.IV.2B). In accordance with these data, the mean linear intercept of the $PTN^{-/-}$ mice decreased ~20% in P35 (Fig.IV.2B). The thickened and hypercellular alveolar septa in $PTN^{-/-}$ mice appeared to be less mature or developed and less inflated than those in $PTN^{+/+}$ mice of the same age. One P35 $PTN^{-/-}$ mouse had moderately increased numbers of monocytes and macrophages in alveolar lumens, but this was not a change seen consistently between $PTN^{+/+}$ and $PTN^{-/-}$ animals. No consistent pathological abnormalities were detected through the whole developing stage.

A

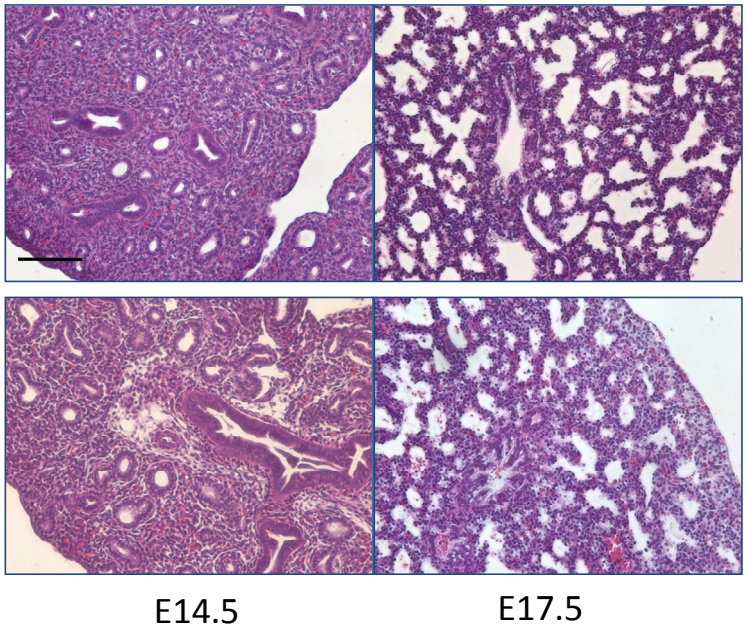

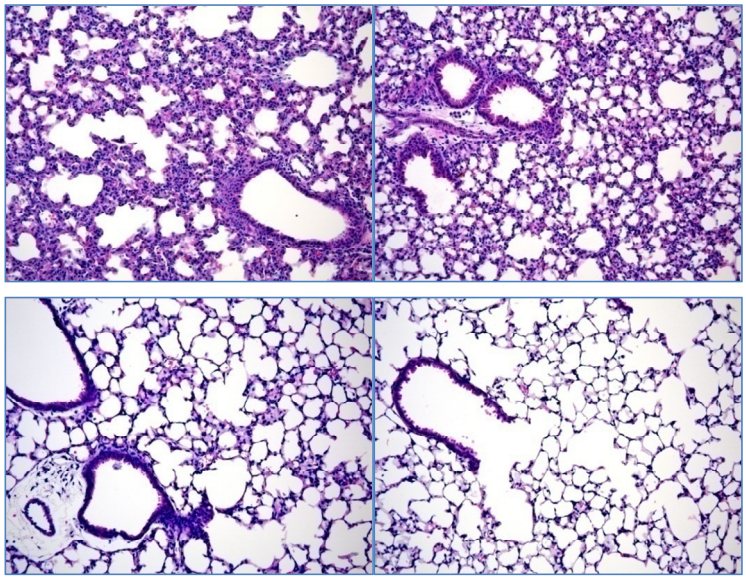

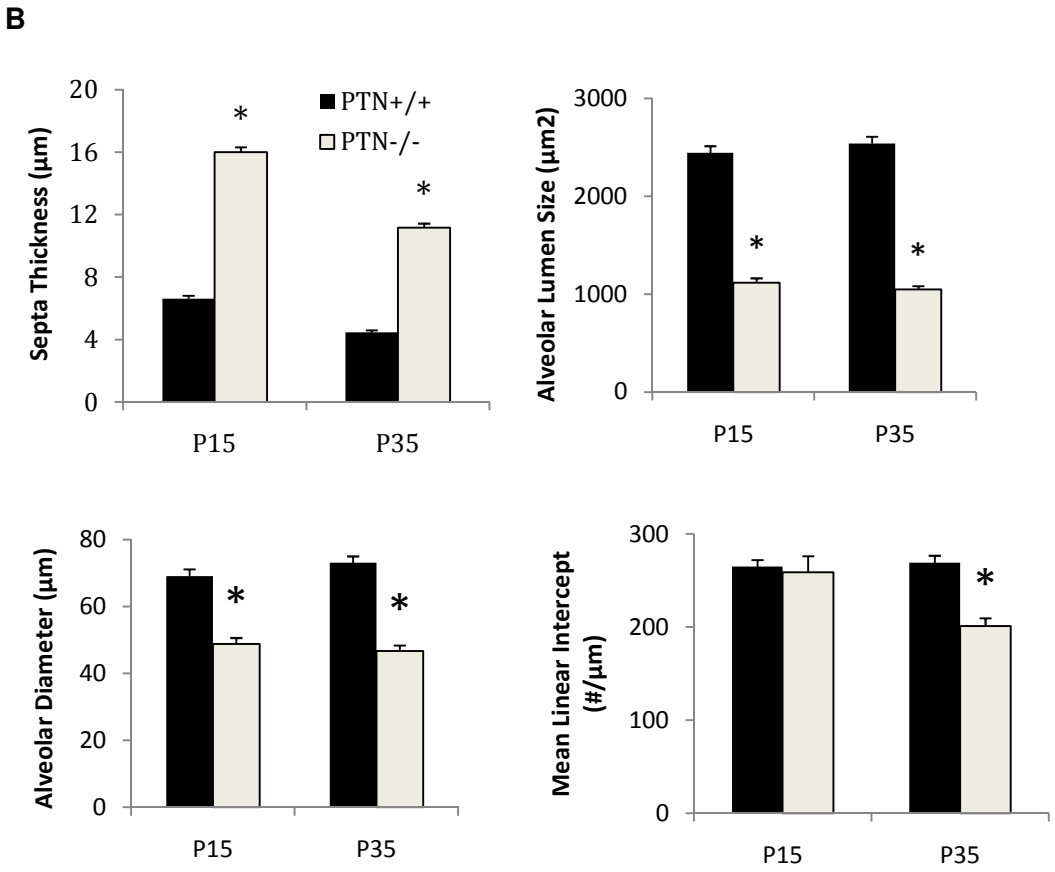

Fig.IV.2. PTN$^{-/-}$ mice have abnormal lung morphology during the alveolar stage. The lungs were collected at embryonic day 14.5, 17.5 (E14.5 and E17.5), postnatal day 15 and 35 (P15 to P35) from PTN$^{-/-}$ and PTN$^{+/+}$ mouse lungs. (A) Representative hemotoxylin-eosin stained lung section from different developing stages (Magnification 200X, scale bar: 100 µm). PTN$^{-/-}$ mice showed less developed saccules marked with hypercellular and thickened septa on P15 and P35. (B) Morphometric assay of the P15 and P35 lungs in PTN$^{-/-}$ and PTN$^{+/+}$ mice. The septa thickness, alveolar lumen size, maximal diameter of the alveoli, and mean linear intercept were assessed. Significant changes were observed in most of these parameters in P35 PTN $^{-/-}$ mice. Data are means ± S.E. (*P<0.001, n=3 mice from different litters).

4.4.2 Cell marker gene expression in PTN $^{-/-}$ mice

To evaluate the differentiation of epithelial and mesenchymal cells in PTN$^{-/-}$ mouse lungs, real-time PCR and western blot were carried out to examine the cell marker gene expression.

AEC II differentiation was evaluated according to the expression of Surfactant proteins. The mRNA expression of SP-A, B and C showed no difference from E15 to P15 between PTN$^{-/-}$ and

PTN$^{+/+}$ mice. However SP-A, B and C all increased around 2-3 fold at P35 in the PTN$^{-/-}$ mice (Fig.IV.3).

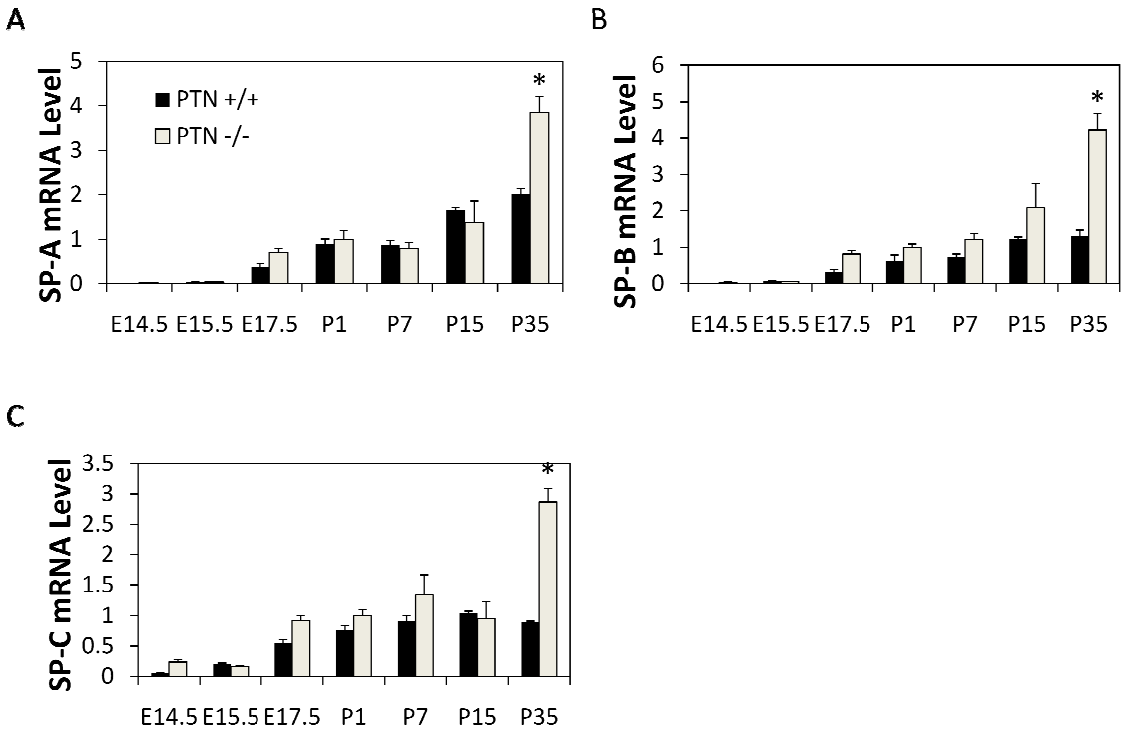

Fig.IV.3. AEC II marker expression in PTN$^{-/-}$ and PTN$^{+/+}$ mice. Total RNA were extracted from PTN$^{-/-}$ and PTN$^{+/+}$ mouse lungs at different developmental stages. Real-time PCR were used to determine the mRNA expression of SP-A (A), SP-B (B) and SP-C (C). The results were normalized to 18S rRNA and were expressed as a ratio to P1 PTN$^{-/-}$ mice. Data are means ± S.E., * $P<0.01$ v.s. PTN$^{+/+}$ at the same age, n=2 biological replications X 2 technical replications for E 14.5 and E17.5, n=2 technical replications for E 15.5, n=3 biological replications X 2 technical replications for the others.

The mRNA expression of AEC I marker, T1-α and P2X7R, both decreased in P15 PTN$^{-/-}$ mice as shown by the real-time PCR (Fig.IV.4). However, the expression of T1-α and P2X7R had no difference between PTN$^{+/+}$ and PTN$^{-/-}$ mice in the fetal and early postnatal stages (Fig.IV.4).

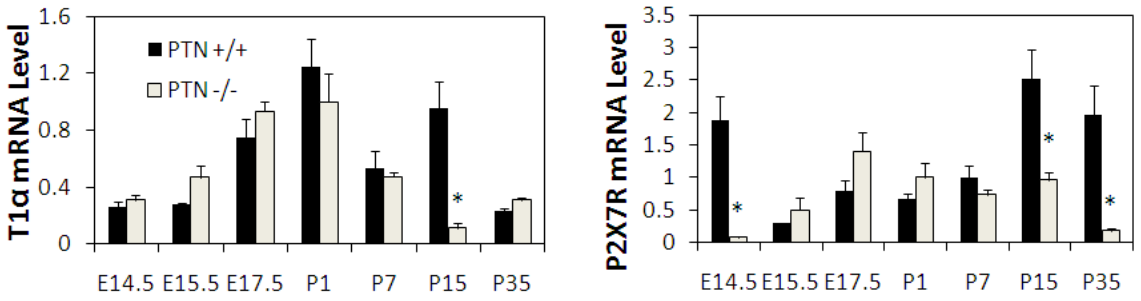

Fig.IV.4. AEC I marker expression in PTN$^{-/-}$ and PTN$^{+/+}$ mice. Total mRNAs were collected from PTN$^{-/-}$ and PTN$^{+/+}$ mouse lungs at different developmental stages, and reverse-transcripted into cDNA. The mRNA expression of T1α and P2X7R were determined using Real-time PCR. The results were normalized to 18S rRNA and were expressed as a ratio to P1 PTN$^{-/-}$ mice. Data are means ± S.E., * P<0.01 v.s. PTN$^{+/+}$ at the same age, n=2 biological replications X 2 technical replications for E 14.5 and E17.5, n=2 technical replications for E 15.5, n=3 biological replications X 2 technical replications for the others.

The expression of Clara cell 10KD protein (CC10), a Clara cell specific marker, was increased ~2.5 fold in P15 and more than 6 fold in P35 PTN$^{-/-}$ mice (Fig.IV.5).

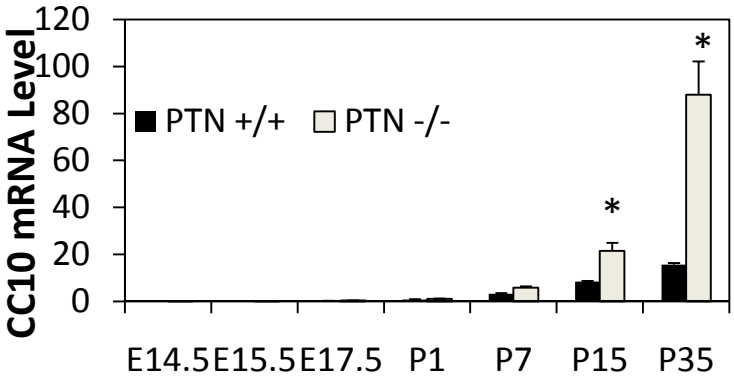

Fig.IV.5. mRNA expression of Clara cell marker in PTN$^{-/-}$ and PTN$^{+/+}$ mice. PTN$^{-/-}$ and PTN$^{+/+}$ mouse lungs were collected at different developmental stages. Total RNA were extracted and reverse-transcripted into cDNA. Real-time PCR was used to quantitate the mRNA expression of CC10. 18S rRNA was used as an internal control. Data were normalized to P1 PTN$^{-/-}$ mice and expressed as means ± S.E., * P<0.01 v.s. PTN$^{+/+}$ at the same age, n=2 biological replications X 2 technical replications for E 14.5 and E17.5, n=2 technical replications for E 15.5, and n=3 biological replications X 2 technical replications for the others.

The protein expression of alpha smooth muscle actin (α-SMA), a myofibroblast marker, significantly increased in P15 and P35 PTN$^{-/-}$ mice (Fig.IV.6). Vimentin, a mesenchymal cell marker, was not different between PTN$^{-/-}$ and PTN$^{+/+}$ mice (Fig.IV.6).

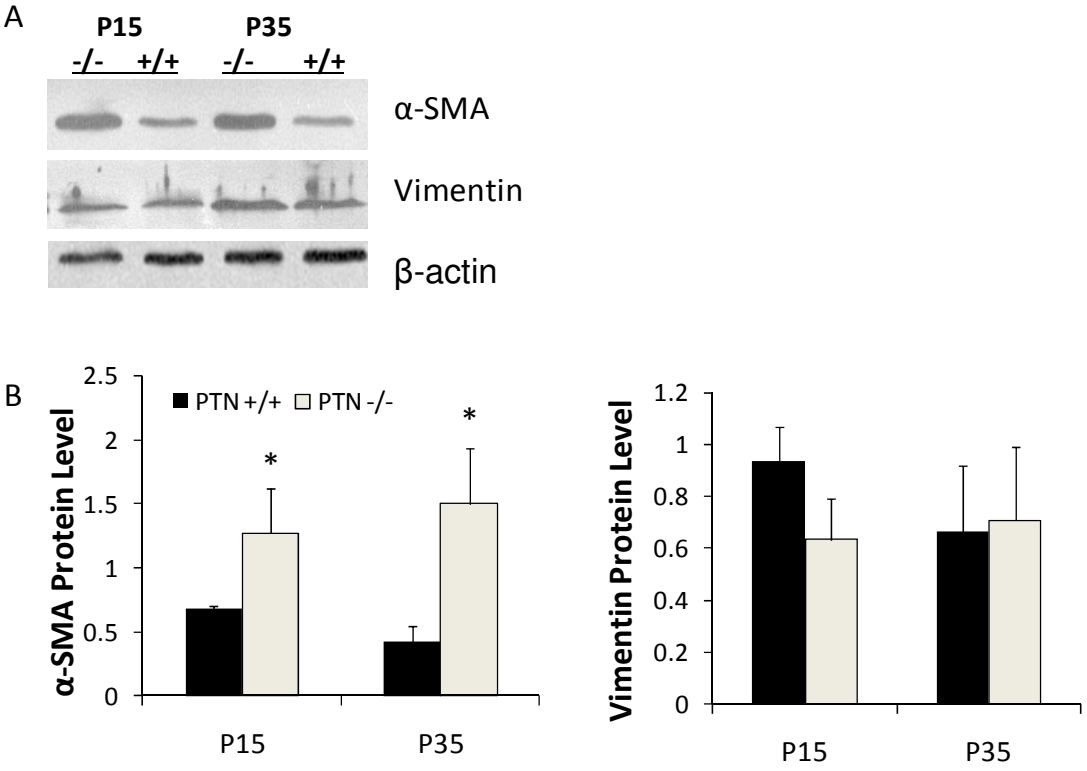

Fig.IV.6. Mesenchymal cell marker expression during the fetal lung development. Total proteins were collected from P15 and P35 PTN$^{-/-}$ and PTN$^{+/+}$ mouse lungs. Western blot were carried out using antibodies against α-SMA and Vimentin. β-actin was used as a loading control. (A) The representative protein bands were shown. (B) The densities of the bands were measured and normalized to β-actin. Data are mean ± S.E. (n=2 for E14.5 and E17.5, n=3 for the others).

The mRNA expression of MK, the only other member of the PTN family, was nearly double in E14.5 and P35 PTN$^{-/-}$ mouse lung, but had no significant difference between PTN$^{-/-}$ and PTN$^{+/+}$ lungs at the other stages (Fig.IV.7), indicating that MK and PTN may at least have some distinct roles during fetal lung development.

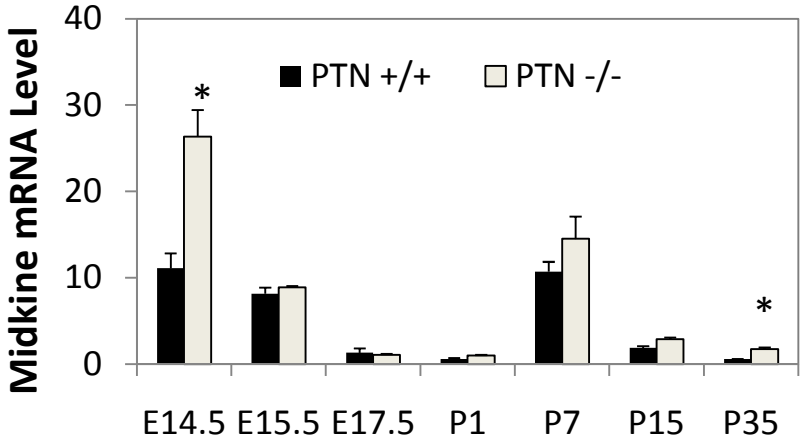

Fig.IV.7. Real-time PCR quantitates the mRNA expression of Midkine in $PTN^{-/-}$ and $PTN^{+/+}$ mouse lung during development. Total mRNA were extracted from $PTN^{-/-}$ and $PTN^{+/+}$ mouse lungs at different development stages, and reverse-transcripted into cDNA. Real-time PCR were carried out to measure the mRNA expression of CC10. The results were normalized to 18S and were expressed as a ratio to P1 $PTN^{-/-}$ mice. Data are mean ± S.E., * $P<0.01$ v.s. $PTN^{+/+}$ at the same age, n=2 biological replications X 2 technical replications for E 14.5 and E17.5, n=2 technical replications for E 15.5, n=3 biological replications X 2 technical replications for the others.

4.5 Discussion

In this study, we compared fetal lung development between $PTN^{-/-}$ and $PTN^{+/+}$ mice. We have previously shown that PTN is highly expressed at the late stage of fetal lung development and reaches a peak level shortly after birth. In adult, PTN expression is very low (18). $PTN^{-/-}$ mice showed no abnormalities in lung morphology and cell marker expression at the early stages of development including the stage when PTN has the highest expression level. However, consistent differences were observed on P15 and P35 when PTN expression was low. At these stages, $PTN^{-/-}$ lungs were less mature and developed; the sacs showed thickened and hypercellular alveolar septa. The differences caused by PTN deficiency at the early stage are probably accumulated and magnified at the late developing stage. This phenomenon was observed previously. For example, the rats that had transient in utero disruption of cystic fibrosis conductance transmembrane regulator (CFTR) on gestational day 16 did not result in abnormal lung function until 30 days of age with symptom progressed as aged (12). Exposing neonatal mice to oxygen impairs lung development, and results in enlarged airway and alveolar size in adult (35).Several adult onset diseases can also result from changes in the fetal environment, such as asthma, hypertension, obesity and diabetes (7; 9; 20; 27).

At the alveolar stage, the lung is characterized by repeated growth and separation of thousands of alveoli, which dramatically increases the surface area for gas exchange. From our study, the thicker septa and smaller alveolar size observed in $PTN^{-/-}$ mice indicated that PTN may have an important role in lung alveolarization. In the $PTN^{-/-}$ mouse lung, the saccules were hypercellular with dramatically increased lung parenchyma density and thickened septa. The normal development of the saccules seemed perturbed. The lung lacked the single capillary layer septa which are typical of the lungs at the adult stage. Thickened septa can be an indicator of underdeveloped lungs and are related to several lung diseases, such as interstitial lung disease with fibrosis, idiopathic pulmonary fibrosis (IPF) and pulmonary hyperplasia (13; 29; 36). Thick septa and pulmonary hyperplasia are also observed in mice treated with growth factors such as Keratinocyte growth factor (KGF) or inflammatory cytokines such as IL-1β (5; 30). Interestingly, inactivating glycogen synthase kinase-3(beta) (GSK-3β), a key inhibitor for Wnt/β-catenin pathway, also induces airway smooth muscle hyperplasia in asthma (4). Since PTN is related to the Wnt/β-catenin pathway, it provides a possible regulatory mechanism of PTN. Our data suggest that PTN is required, at least in part, for the alveolarization of the lung through altering proliferation and differentiation of mutiple cell types.

AEC I and AEC II are essential for normal lung function. A significantly increased expression of SP-A, SP-B, SP-C and CC10 mRNA in adult $PTN^{-/-}$ mouse lung indicates that more AEC II and Clara cells may be accumulated. However, additional evidence is needed to elucidate whether this is due to an increased proliferation of these cells, a simply increased marker gene expression or an increased differentiation from precursor cells. These AEC II appear to fail to further trans-differentiate into squamous cells as seen from the decreased mRNA expression of AEC I marker, T1-α and P2X7R. These results seem to controdict previous *in vitro* findings that PTN promotes fetal AEC II proliferation and arrests the fetal AEC II trans-differentiation into AEC I cells in primary cell culture (32). However, in comparison with cell culture, the lung tissue has a much more complex environment, which includes multiple interactions among different cells and extracellular matrix. Additionally, PTN acts on various lung cells, including epithelial cells, endothelial cells and mesenchymal cells (8; 25).

Beside its effects on epithelial cells, PTN also influences the differention and proliferation of mesenchymal cell through a direct or indirect mechanism. α-SMA is a marker of myofibroblast. It is normally expressed along trachea, proximal airway and large vascular tubes. In the distal lung, α-SMA is expressed by interstitial myofibroblasts in the septa. The function of smooth muscle cells is to control the contraction and proliferation, and to synthesize matrix proteins, including collagen and elastin. Abnormal expression of α-SMA is associated with some lung diseases, such as lymphangioleiomyomatosis (LAM) (16; 28), and asthma (3; 6). In P15 and P35 $PTN^{-/-}$ mouse lung, α-SMA expression was significantly increased. Smooth muscle cell hyperplasia was also

observed in the conducting airways. The enhanced proliferation of myofibroblast in the interstitial tissue may partly contribute to the increased septa thickness.

PTN shares some functional redundancy with MK and they may partly compensate for each other when one of them is deficient. In MK knockout mice, PTN expression was dramatically up-regulated in several organs (10), including spinal cord, dorsal root ganglia, eye, heart, aorta, bladder, and urethra. However, in the brain, bone marrow and lung, PTN expression was not increased in MK knockout mice, suggesting that PTN and MK may play distinct roles in these organs. $PTN^{-/-}$ mice do show significant abnormality in the brain and bone development (11; 14). Increased proliferation and decreased differentiation of neural stem cells were observed in the developing $PTN^{-/-}$ mice brain (11). Similarly, PTN knockout decelerates the growth of the weight-bearing bone and inhibits bone remodeling (14). PTN and MK may also have distinct roles in the lung. First, our results showed that MK expression did not change dramatically in $PTN^{-/-}$ mice during lung development, except E14.5 and P35. Second, MK and PTN have distinct expression pattern in the developing lung: MK is mainly expressed in the developing epithelial cells, while PTN is located to the base membrane (19). Third, MK expression is high in embryonic stage and decreases after embryonic day 16.5; but PTN level is highest at early postnatal stage (19). Taken together, PTN may not be compensated by the increased expression of MK in the lung, indicating that the roles of MK and PTN in the lung are different. This may explain why $PTN^{-/-}$ mice have more abnormalities in the lungs than some of the other organs.

In summary, PTN signaling appears to be essential to the late stage of the fetal lung development, especially for saccular structure formation and alveolarization. This may be due to PTN's effect on epithelial and mesenchymal cells. PTN deficiency increases proliferation of many lung cells, including Clara cells, AEC II and myofibroblasts, and inhibits the further trans-differentiation of AEC II into AEC I.

4.6 References

1. ALESCIO T and CASSINI A. Induction in vitro of tracheal buds by pulmonary mesenchyme grafted on tracheal epithelium. *J Exp Zool* 150: 83-94, 1962.
2. Amet LE, Lauri SE, Hienola A, Croll SD, Lu Y, Levorse JM, Prabhakaran B, Taira T, Rauvala H and Vogt TF. Enhanced hippocampal long-term potentiation in mice lacking heparin-binding growth-associated molecule. *Mol Cell Neurosci* 17: 1014-1024, 2001.
3. Ammit AJ and Panettieri RA, Jr. Airway smooth muscle cell hyperplasia: a therapeutic target in airway remodeling in asthma? *Prog Cell Cycle Res* 5: 49-57, 2003.
4. Bentley JK, Deng H, Linn MJ, Lei J, Dokshin GA, Fingar DC, Bitar KN, Henderson WR, Jr. and Hershenson MB. Airway smooth muscle hyperplasia and hypertrophy correlate with glycogen synthase kinase-3(beta) phosphorylation in a mouse model of asthma. *Am J Physiol Lung Cell Mol Physiol* 296: L176-L184, 2009.
5. Bry K, Whitsett JA and Lappalainen U. IL-1beta disrupts postnatal lung morphogenesis in the mouse. *Am J Respir Cell Mol Biol* 36: 32-42, 2007.

6. Chung KF and Sterk PJ. The airway smooth muscle cell: a major contributor to asthma? *Eur Respir J* 15: 438-439, 2000.

7. David J.P.Barker. *Fetal Origins Of Cardiovascular And Lung Disease*. Marcel Dekker, 2001.

8. Deuel TF, Zhang N, Yeh HJ, Silos-Santiago I and Wang ZY. Pleiotrophin: a cytokine with diverse functions and a novel signaling pathway. *Arch Biochem Biophys* 397: 162-171, 2002.

9. Gillman MW and Rich-Edwards JW. The fetal origin of adult disease: from sceptic to convert. *Paediatr Perinat Epidemiol* 14: 192-193, 2000.

10. Herradon G, Ezquerra L, Nguyen T, Silos-Santiago I and Deuel TF. Midkine regulates pleiotrophin organ-specific gene expression: evidence for transcriptional regulation and functional redundancy within the pleiotrophin/midkine developmental gene family. *Biochem Biophys Res Commun* 333: 714-721, 2005.

11. Hienola A, Pekkanen M, Raulo E, Vanttola P and Rauvala H. HB-GAM inhibits proliferation and enhances differentiation of neural stem cells. *Mol Cell Neurosci* 26: 75-88, 2004.

12. Hudak JJ, Killeen E, Chandran A, Cohen JC and Larson JE. Adult onset lung disease following transient disruption of fetal stretch-induced differentiation. *Respir Res* 10: 34, 2009.

13. Hyde DM, King TE, Jr., McDermott T, Waldron JA, Jr., Colby TV, Thurlbeck WM, Flint WM, Ackerson L and Cherniack RM. Idiopathic pulmonary fibrosis. Quantitative assessment of lung pathology. Comparison of a semiquantitative and a morphometric histopathologic scoring system. *Am Rev Respir Dis* 146: 1042-1047, 1992.

14. Imai S, Heino TJ, Hienola A, Kurata K, Buki K, Matsusue Y, Vaananen HK and Rauvala H. Osteocyte-derived HB-GAM (pleiotrophin) is associated with bone formation and mechanical loading. *Bone* 44: 785-794, 2009.

15. Kadomatsu K and Muramatsu T. Midkine and pleiotrophin in neural development and cancer. *Cancer Lett* 204: 127-143, 2004.

16. Krymskaya VP. Smooth muscle-like cells in pulmonary lymphangioleiomyomatosis. *Proc Am Thorac Soc* 5: 119-126, 2008.

17. Lawson KA. Mesenchyme specificity in rodent salivary gland development: the response of salivary epithelium to lung mesenchyme in vitro. *J Embryol Exp Morphol* 32: 469-493, 1974.

18. Li YS, Milner PG, Chauhan AK, Watson MA, Hoffman RM, Kodner CM, Milbrandt J and Deuel TF. Cloning and expression of a developmentally regulated protein that induces mitogenic and neurite outgrowth activity. *Science* 250: 1690-1694, 1990.

19. Mitsiadis TA, Salmivirta M, Muramatsu T, Muramatsu H, Rauvala H, Lehtonen E, Jalkanen M and Thesleff I. Expression of the heparin-binding cytokines, midkine (MK) and HB-GAM (pleiotrophin) is associated with epithelial-mesenchymal interactions during fetal development and organogenesis. *Development* 121: 37-51, 1995.

20. Morris JA. Fetal origin of maturity-onset diabetes mellitus: genetic or environmental cause? *Med Hypotheses* 51: 285-288, 1998.

21. Muramatsu H, Zou P, Kurosawa N, Ichihara-Tanaka K, Maruyama K, Inoh K, Sakai T, Chen L, Sato M and Muramatsu T. Female infertility in mice deficient in midkine and pleiotrophin, which form a distinct family of growth factors. *Genes Cells* 11: 1405-1417, 2006.

22. Muramatsu T. Midkine and pleiotrophin: two related proteins involved in development, survival, inflammation and tumorigenesis. *J Biochem* 132: 359-371, 2002.

23. Neame PJ, Treep JT and Young CN. An 18-kDa glycoprotein from bovine nasal cartilage. Isolation and primary structure of small, cartilage-derived glycoprotein. *J Biol Chem* 265: 9628-9633, 1990.

24. Ochiai K, Muramatsu H, Yamamoto S, Ando H and Muramatsu T. The role of midkine and pleiotrophin in liver regeneration. *Liver Int* 24: 484-491, 2004.

25. Perez-Pinera P, Berenson JR and Deuel TF. Pleiotrophin, a multifunctional angiogenic factor: mechanisms and pathways in normal and pathological angiogenesis. *Curr Opin Hematol* 15: 210-214, 2008.

26. Shannon JM and Hyatt BA. Epithelial-mesenchymal interactions in the developing lung. *Annu Rev Physiol* 66: 625-645, 2004.

27. Symonds ME, Stephenson T and Budge H. Early determinants of cardiovascular disease: the role of early diet in later blood pressure control. *Am J Clin Nutr* 89: 1518S-1522S, 2009.

28. Taveira-Dasilva AM, Hedin C, Stylianou MP, Travis WD, Matsui K, Ferrans VJ and Moss J. Reversible airflow obstruction, proliferation of abnormal smooth muscle cells, and impairment of gas exchange as predictors of outcome in lymphangioleiomyomatosis. *Am J Respir Crit Care Med* 164: 1072-1076, 2001.

29. Thomas MP, Storer J, Goodsit E and Snearly R. Pulmonary muscular hyperplasia. A report of functional data in three cases with a brief review of the literature. *Dis Chest* 51: 1-10, 1967.

30. Welsh DA, Summer WR, Dobard EP, Nelson S and Mason CM. Keratinocyte growth factor prevents ventilator-induced lung injury in an ex vivo rat model. *Am J Respir Crit Care Med* 162: 1081-1086, 2000.

31. Weng T, Chen Z, Jin N, Gao L and Liu L. Gene expression profiling identifies regulatory pathways involved in the late stage of rat fetal lung development. *Am J Physiol Lung Cell Mol Physiol* 291: L1027-L1037, 2006.

32. Weng T, Gao L, Bhaskaran M, Guo Y, Gou D, Narayanaperumal J, Chintagari NR, Zhang K and Liu L. Pleiotrophin regulates lung epithelial cell proliferation and differentiation during fetal lung development via {beta}-catenin and Dlk1. *J Biol Chem* 2009.

33. Weng T, Jin N and Liu L. Differentiation between amplicon polymerization and nonspecific products in SYBR green I real-time polymerase chain reaction. *Anal Biochem* 342: 167-169, 2005.

34. Wessells NK. Mammalian lung development: interactions in formation and morphogenesis of tracheal buds. *J Exp Zool* 175: 455-466, 1970.

35. Yee M, Chess PR, Grath-Morrow SA, Wang ZD, Gelein R, Zhou R, Dean DA, Notter RH and O'Reilly MA. Neonatal oxygen adversely affects lung function in adult mice without

altering surfactant composition or activity. *American Journal of Physiology-Lung Cellular and Molecular Physiology* 297: L641-L649, 2009.

36. Yousem SA. Respiratory bronchiolitis-associated interstitial lung disease with fibrosis is a lesion distinct from fibrotic nonspecific interstitial pneumonia: a proposal. *Mod Pathol* 19: 1474-1479, 2006.
37. Zou P, Muramatsu H, Sone M, Hayashi H, Nakashima T and Muramatsu T. Mice doubly deficient in the midkine and pleiotrophin genes exhibit deficits in the expression of beta-tectorin gene and in auditory response. *Lab Invest* 86: 645-653, 2006.

4.7 Acknowledgements

Contribution of Co-authors

We are grateful to Yujie Guo for his assistance with the Morphometric assay, Dr. Narendranth Reddy Chintagari for the image taking and analyzing, and Dr. Melanie Breshears for helping with evaluating the histopathology of $PTN^{-/-}$ mice. We thank Dr. T Muramatsu (Nagoya U) for kindly providing the $PTN^{-/-}$ mice. This work was supported by R01 HL-071628 (LL).

CHAPTER V

MICRORNA-150 REGULATES SURFACTANT SECRETION VIA P2X7 RECEPTORS

5.1 Abstract

P2X7 receptor (P2X7R) is a purinergic ion-channel receptor. Previously, we found that P2X7R could activate the surfactant secretion in AEC II by releasing ATP from AEC I. In this study, we determined whether miRNA regulates P2X7R-mediated surfactant secretion. We first used a dual-luciferase assay to screen the regulation of P2X7R 3'-UTR activity by miR-150, miR-186, miR-204 and miR-211. We found that miR-150 is a regulator of P2X7R in lung epithelial cells. The miR-150 regulation could be disrupted by site mutation of mature miR-150 or mutation of P2X7R 3'-UTR at miR-150 binding sites. Adenovirus expressing miR-150 significantly reduced the P2X7R protein expression in E10 cells. Furthermore, pre-treatment of E10 cells with adenovirus expressing miR-150 disrupted the surfactant secretion induced by E10 cell conditioned media. Our study is the first of its kind to demonstrate that miR-150 regulates P2X7R-mediated surfactant secretion.

Key words: P2X7R, miR-150, surfactant secretion

.

5.2 Introduction

P2X7 receptors (P2X7R) belongs to the P2X receptor family which are plasma membrane ligand-gated ion channels activated by ATP (16). P2X7R shares many similar properties with other P2X receptors. The binding of ATP causes P2X receptors to open within millisecond and stimulates cell depolarization by an influx of cationic ions, including Na^+, K^+ (normally through a Ca^{2+} activated K^+ channel), and Ca^{2+} ions (11). P2X7R was initially identified as a unique ATP-gated channel P2Z due to its low degree of structural homology compared with other family members. P2X7R has a less conserved and unusually long COOH terminus, which forms a large non-selective pore permeable to small molecules such as YO-PRO, Cl^-, Lucifer yellow and ethidium bromide (EB) (32). In comparation with other P2X receptors, the activation of P2X7R needs at least 10-fold higher ATP concentration due to its low affinity for ATP, but the desensitization of P2X7R is much slower compared to the other P2X receptors. Another unique property of P2X7R is that it mediates a reversible plasma membrane permeabilization. P2X7R activation also enhances the release of endogenous cytokines involved in the immune-response, such as interleukin-1beta (IL-1β) (25). However, sustained stimulation of P2X7R leads to membrane blebbing and programmed cell death (12; 30).

P2X7R mediates ATP release as well, which was first observed in rat astrocytes after stimulation with the P2X7R agonist, ([2'-3'-O-(4-Benzoyl-benzoyl) adenosine 5'-triphosphate or BzATP (2). Suadicani et. al further confirmed that P2X7R, but not Cx43 hemichannels mediated ATP release in human and mouse astrocytes (29). We have found that BzATP increases ATP release from alveolar epithelial cells via P2X7R (23).

The distal lung epithelium is lined with alveolar epithelial type I and type II cells (AEC I and AEC II). AEC I cover about 95% and AEC II occupy less than 5% of the alveolar surface area (22). AEC I are large squamous cells responsible for gas exchange, fluid transport and protection against oxidative stress (5; 6; 15; 27). AEC II are cuboidal and normally located in the corners of alveoli. AEC II also synthesize and secrete pulmonary surfactant, a lipoprotein complex that spreads on the surface of alveoli to form a thin lining layer and reduces the surface tension. Insufficient amount of pulmonary surfactant leads to abnormal lung functions(14; 34).

The molecular mechanism that regulates surfactant secretion is of great interest. The secretion of surfactant from AEC II can be regulated by many molecules, such as intracellular Ca^{2+}, P_2Y_2 receptor agonists (ATP and UTP), adenosine, platelet activating factor, and IL-1 etc (1). Of all these molecules, extracellular ATP is the most effective endogenous regulator. Through binding to P_2Y_2 receptors on the AEC II plasma membrane, ATP activates phospholipase C, which generates diacylglycerol (DAG) and inositol trisphosphate (IP_3), and subsequently activates protein kinase C (PKC) and increases cytoplasmic Ca^{2+} concentration (1).

MicroRNAs (miRNA) are naturally existed small non-coding RNAs that either cleave specific mRNAs or inhibit mRNA translation through complementary base pairing and subsequently silence target genes (19). They regulate diverse cellular processes such as proliferation, differentiation, apoptosis, and exocytosis. The processing of miRNA needs both Drosha and Dicer (31). In animals, miRNAs are first transcribed as primary transcripts (pri-miRNAs). The pri-miRNAs are cleaved by Drosha in the nucleus to release the loop structure and generate ~70nt pre-miRNAs (18). Pre-miRNAs are associated with Exportin 5-RanGTP, exported out of the nucleus and cleaved by Dicer in cytoplasm to yield 21-23 nt long mature miRNA (20; 36). One strand of miRNA is then loaded into the RNA-induced silencing component (RISC) (26). In mammals, the mature miRNA normally binds to the target mRNA with non-perfect base pairing and subsequently suppresses the mRNA translation.

MiR-150 is a miRNA highly expressed in the tumour cells surrounding the proliferation centres in the bone marrow and lymphoid tissues (35; 37). MiR-150 is also present in mature B and T cells. It blocks B cell development by silencing the expression of c-Myb (35). Recently, miR-150 and miR-186 are identified as potential miRNAs that target to P2X7R (38). However, whether these miRNAs regulate the P2X7R-mediated surfactant secretion is not known.

P2X7R is broadly expressed in multiple mammalian cells, including epithelial cells, endothelial cells, fibroblasts, and macrophages. P2X7R is specifically expressed in AEC I (8). Our preliminary studies have shown that the activation of P2X7R in AEC I stimulates surfactant secretion in AEC II (23).

In our study, we first used dual-luciferase assay to screen the possible miRNAs that regulate P2X7R expression. We further determined that the miR-150 inhibited endogenous P2X7R protein expression in lung cells. Then we characterized miR-150 expression in different organs and lung epithelial cells. Finally, we examined the effect of miR-150 in P2X7R-mediated surfactant secretion in primary cultured AEC II.

5.3 Materials and Methods

5.3.1 Cell Culture

E10 cell line was kindly provided by Dr. Mary Williams (Boston University). It was originally derived from explants of BALB/c female mouse lung and has AEC I characters. E10 cells were maintained in CMRL 1066 medium supplied with10% FBS and 0.5 mM L-glutamine. R3/1 cell is another AEC cell line and was kindly provided by Dr. Roland Koslowski (Dresden University of Technology, Germany). R3/1 cells were cultured in F12 medium supplied with 10% FBS. A549 is a human lung carcinoma cell line and was obtained from ATCC (Manassas, VA). A549 cells were cultured in Dulbecco's Modified Eagle Medium (DMEM) supplemented with 10% FBS.

5.3.2 miRNA viral vector construction

The pENTR/CMV-EGFP-pri-miRNA vector containing the primary transcript of human miRNA (pri-miRNA) was constructed as described previously (4; 13). Briefly, the pri-miRNA fragment (mature miRNA plus 200 base pairs at each end) was amplified from human genomic DNA (Clontech, Mountain View, CA) using primers listed in Table 1. The pri-miRNA fragment was digested with XhoI and EcoRI or BsaI, gel-purified and inserted into a modified pENTR/CMV-EGFP (Invitrogen, Carlsbad, CA) plasmid between enhanced green fluorescence protein stop coden and SV40 poly (A) terminal sequences. A plasmid that only expresses EGFP was used as a control vector.

The mutated miR-150 expression vector, pENTR/CMV-EGFP-pri-miRNA-150mut was constructed using overlapping PCR as shown in Fig.V.1. Two primers containing mutated mature miR-150 (miR-150mut Foward and reverse primers) were designed (Table 1). First, fragment 1 and fragment 2 were amplified from full length pri-miR-150 using primer pair miR-150 Foward/ miR-150mut Reverse and miR-150 Reveres/miR-150mut Foward. Then a second PCR was carried out using fragment 1 and fragment 2 as template and miR-150 forward and reverse primers. This PCR generated a pri-miR-150mut sequence which mutated the mature miR-150 from TTGGGAG to TTCCCAG. This pri-miR-150mut fragment was digested with XhoI and EcoRI and inserted into the pENTR/CMV-EGFP vectors as described above.

5.3.3 3'-UTR reporter vector construction

To construct the P2X7R 3'-UTR reporter vector, the full length P2X7R 3'-UTR sequence (23 to 1023) was amplified from human genomic DNA using the primers listed in Table 1. The amplified DNA fragment was digested using XbaI and PspOMI and inserted into the pRL-TK vector (Promega, Madison, WI), which contains a *Renilla* luciferase gene.

For the truncated P2X7R 3'-UTR which contain miR-150 binding sites or mutations, 2 pmol each of the two primers (Table 1) were annealed in 30 µl reaction system (0.1 M NaCl) for 30 min at room temperature, which results in a double-stranded fragment with sticky ends at both sides. The fragment was directly inserted into the pRL-TK vectors. The generated mutation vector of P2X7R 3'-UTR changed the miR-150 binding site from "TTGGGAG" to "TTCCCAG".

Table.V.1 Primers for pri-miRNA expression vector and P2X7R 3'-UTR reporter vector.

Vector	Foward Primer	Reverse Primer
miR-150	XhoI:5'-CACCTCGAGCGCGAGAGGCAGGTACAATA-3'	EcoRI:5'-GGCTCTAGAGTCTGTAATCCCAGCGCTTTCCCAG-3'
miR-150mut	5'-GGCCCTGTCT*GGG*AACCCTTGTACCAGTG-3'	5'-CAGCACTGGTACAAGGGTT*CCC*AGACAG-3'
miR-186	XhoI:5'-CACCTCGAGCCATGCTTATGCTACTGCACCA-3'	BsaI:5'-GGTTGGTCTCGAATTCCAGGTATATGGCACAGCAACAA-3'
miR-204	XhoI:5'-CACCTCGAGGCCTCCTGATCATTTACCCAC-3'	EcoRI:5'-GAGAATTCCTTCCTAATTCCAGAGCTGC-3'
miR-211	XhoI:5'-CACCTCGAGTCCTGGCGAATGGTCATTGG-3'	EcoRI:5'-GAGAATTCTGTGCAAAGCCCTGACCAGGAG-3'
Full P2X7 3' UTR	XbaI:5'-GGCTCTAGAGTCTGTAATCCCAGCGCTTTG-3'	PspOMI:5'-GTTGGGCCCTTGGTCTCCCAAAGTGCTG-3'
P2X7 3'-UTR 150-1	XbaI:5'-CTAGATGTAATCCCAGCGCTTTGGGAG-3'	PspOMI:5'-GGCCCTCCCAAAGCGCTGGGATTACAT-3'
P2X7 3'-UTR 150-1mut	XbaI:5'-CTAGACTCACGTCTGTAATCCCAGCGCTTT*CCC*AGGCCGAG-3'	PspOMI:5'-GGCCCTCGGCCT*GGG*AAAGCGCTGGGATTACAGACGTGAGT-3'
P2X7 3'-UTR 150-2	XbaI:5'-CTAGATGTAATCCCAGCACTTTGGGAGAG-3'	PspOMI:5'-GGCCCTCTCCCAAAGTGCTGGGATTACAT-3'
P2X7 3'-UTR 150-2mut	XbaI:5'-CTAGACACCTGTAATCCCAGCACTTT*CCC*AGACCAAG-3'	PspOMI:5'-GGCCCTTGGTCT*GGG*AAAGTGCTGGGATTACAGGTGT-3'

The restriction enzyme sites were underlined, the mutation sites were italic.

5.3.4 Dual-luciferase assay

E10 cells ($8X10^4$) were seeded in each well of 96-well plate. After 24 hours, 15 ng of 3'-UTR reporter vectors and 170 ng of miRNA expressing plasmids were co-transfected into E10 cells together with 15 ng of pGL-3 using Lipofectamine 2000 (Invitrogen, Carlsbad, CA). The pGL-3 expresses firefly luciferase and was used as a transfection control, Two days after transfection, the cells were harvested. The luciferase activities were determined using the Dual-Luciferase® Reporter Assay System (Promega, Madison, WI) and FLUOstar Optima (BMG Labtech Inc, Durham, NC).

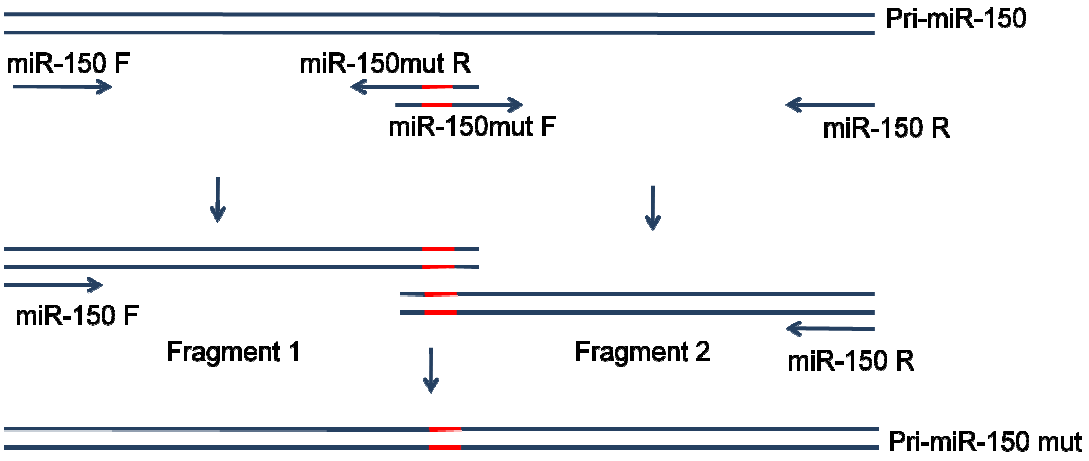

Fig.V.1 Overlapping PCR constructs the pri-miR-150 mutation expressing vector. At first, two fragments were generated using pri-miR-150 as template and the primer pair miR-150F/miR-150mutR and miR-150mutF/miR-150R. Then a second PCR were carried out using fragment 1 and fragment 2 as template and miR-150F/miR-150R primers.

5.3.5 Adenovirus production

The miRNA adenoviruses were produced as described (4). The CMV-EGFP-primiRNA sequences were transferred from pENTR/CMV-EGFP-primiRNA vector into pAd/PL-DEST by LR recombinant reaction using Gateway technology following the manufacturer's instructions (Invitrogen, Carlsbad, CA). The plasmid from the positive clone was digested with PacI, purified using MinElute PCR purification kit (Qiagen, Valencia, CA), and transfected into 293A producer cell line with Lipofectamine 2000 reagent (Invitrogen, Carlsbad, CA). The adenovirus-containing cells were harvested, and the generated virus was used to amplify the viral stock. The titer was determined by counting the GFP-positive cells.

5.3.6 Western Blot

E10 cells were tranduced with different doses of miR-150 or miR-186 expression adenoviruses for 4 days. Adenoviruses which only express GFP protein were used as a control. The cells were collected and lyzed in M-PER Mammalian Protein Extraction Reagent (Pierce, Rockford, IL) on ice. The protein concentration was determined using the Dc protein assay kit (Bio-Rad, Hercules, CA). Same amounts of proteins were separated by 10% SDS-PAGE and transferred onto a nitrocellulose membrane. The blot was stained by Ponceau S to check transfer efficiency. The membrane was blocked with 5% dry milk in Tris-buffered saline containing 0.05% Tween 20 (TTBS) for 1 hour, incubated with rabbit anti-P2X7R antibody (1:1,000, Sigma, St. Louis, MO) or mouse anti-β-actin antibody (1:1,000; Bio-Rad, Hercules, CA) overnight at 4℃. After being washed, the membrane was incubated with horseradish peroxidase-conjugated anti-

rabbit or anti-mouse IgG (1:2,000) for 1 hour. Finally, the membrane was developed with SuperSignal West Pico Chemiluminescent Substrate (Pierce, Rockford, IL) and exposed to X-ray film.

5.3.7 Real-time PCR

The cells or tissues were harvested and lyzed in the Lysis/Binding Buffer (Ambion Inc, Austin, TX). Total RNAs were isolated using the mirVana^{TM} miRNA Isolation Kit (Ambion Inc, Austin, TX) according to the manufacturer's instructions. RNase-free^{TM} DNase (Ambion Inc., Austin, TX) was used to remove the genomic DNA contamination. The RNAs were reverse-transcribed into cDNA using oligo dT and random hexamers (Promega, Madison, WI) and M-MLV reverse transcriptase (Invitrogen, Carlsbad, CA). The primers for real-time PCR were designed using Primer Express® software (Applied Biosystems, Foster City, CA). P2X7R: forward, 5'-ACCGTGCCAGTGTTGTTCTG-3', and reverse, 5'-AGCACCTGTGGTTGTTATTTTGT-3'; 18S rRNA: forward, 5'-ATTGCTCAATCTCGGGTGGCTG-3' and reverse, 5'-CGTTCTTAGTTGGTGGAGCGATTTG-3'. Real-time PCR was performed on 7500HT Fast Real-Time PCR System using SYBR Green I detection (Eurogentec, San Diego, CA) as previously described (33). After the amplification, a dissociation curve was generated to check the specificity of the amplification. 18S rRNA was used as an internal control.

The real-time for miR-150 was carried out as described (28). 5 µg of total RNA was polyadenylated using A-Plus™ Poly (A) Polymerase tailing kit (Epicentre Biotechnologies, Madison, WI) as described in the manufacture's instruction. The tailed RNA was purified using 1:1 phenol/Chloroform and precipitated with 75% ethonal. One µg poly(A) tailed RNA was reverse-transcribed into cDNA using oligo dT primers by M-MLV reverse transcriptase (Invitrogen, Carlsbad, CA). The target mature miRNA sequence (5'-CTGGTACAGGCCTGGGGGACAG-3') was used as the forward PCR primer and a universal primer (5'- GCGAGCACAGAATTAATACGACTCAC-3') was used as the reverse primer. Real-time PCR was performed as described above. U2 small RNA was used to normalize the data.

5.3.8 AEC II isolation

AEC II were isolated from Male Sprague-Dawley rats (180-200g) as previously described (3). Briefly, the lung was perfused, lavaged, and digested with elastase (3 units/ml) at 37°C. Then, the lung were chopped with a McIlwain tissue chopper (Brinkmann, Westbury, NY), and the cell suspension was further digested with 100 ng/ml DNase I and filtered through 160- and 37-µm nylon mesh once and 15-µm nylon mesh twice. The cells were seeded on rat IgG-coated plates twice for 45 and 30 min to remove macrophages. The final AEC II preparation normally has a purity of 90% and a viability of over 98%. AEC II were seeded onto 35-mm tissue culture-treated plastic dishes at a density of 1.0 X10^6 cells/dish in MEM with 10% FBS.

5.3.9 Surfactant Secretion

E10 cells were cultured in DMEM supplied with 10% FBS and transduced with 100 Multiplicity of Infection (MOI= ratio of infectious virus particles to cells) adenoviruses for 4 days. The cells were then treated with 25 μM BzATP for 2 hours. The media were collected as conditional media. The freshly isolated AEC II (1 X 10^6) were cultured overnight in the presence of [^{3}H] choline (0.6 μCi/10^6 cells). AEC II were incubated with or without the conditional media for 2 hours. Lipids in media and cells were extracted and surfactant secretion was performed according to Chintagari et al. (10). Surfactant secretion (%) was expressed as (dpm in medium/dpm in medium and cells) x100. A stimulation index was expressed as a ratio of stimulated secretion with a conditioned media to basal secretion without conditioned media.

5.4 Resutls

5.4.1 P2X7R is a direct target of miR-150

Based on the TargetScanHuman (V5.1) Target Database, there is only one conserved binding site of miR-204 and miR-211 on P2X7R 3'-UTR among mammals. Recently, miR-150 and miR-186 were reported as miRNAs that potentially target to P2X7R (38). To identify miRNAs that target P2X7R in alveolar epithelial cells, we constructed miRNA expression vectors (pENTR/CMV-EGFP-primiRNA) for miR-150, miR-186, miR-204 and miR-211. The pENTR/CMV-EGFP vector which only expresses EGFP was used as a control vector. Then we attached the full length 3'-UTR of P2X7R (23-1023) to *Renilla* luciferase (RL) gene. The resulted plasmid, RL-P2X7R, was co-transfected with a miRNA expression vector into E10 cells (a mouse AEC I cell line). As shown in Fig.V.2A, the pENTR expressing miR-150 significantly inhibited RL-P2X7R activity. However, all the other miRNAs had no effects on the RL-P2X7R activity. To assess the specificity of miR-150 regulation, we also constructed a plasmid which expressed a mutated miR-150. The mutation of miR-150 lost its inhibitory effect on RL-P2X7R activity (Fig.V.2B).

Similar inhibitory of RL-P2X7R by miR-150 was also observed in A549, a carcinoma human alveolar epithelial cell line, and R3/1, a rat lung type I cell line (Fig.V.2C). Our results demonstrated that the miR-150 regulation was conserved in different species and cells.

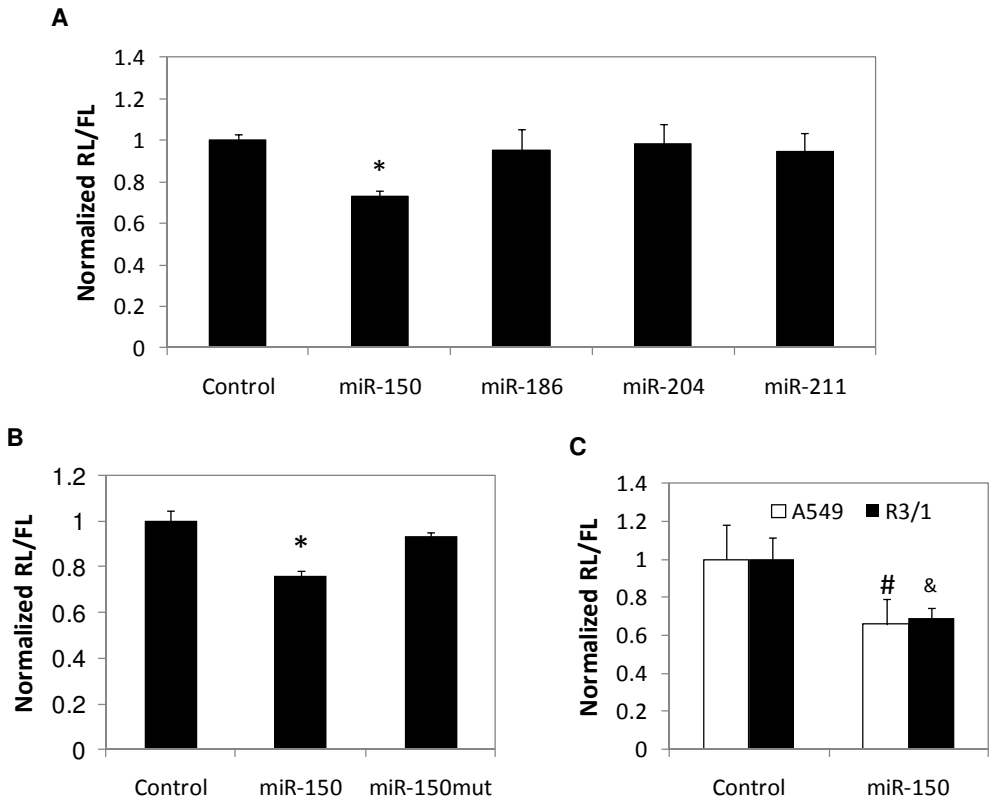

Fig.V.2 Screening of miRNAs regulating P2X7R 3'-UTR reporter activity. (A) To screen the miRNAs targeted to P2X7R, 170 ng pENTR/CMV-EGFP-primiRNA (Control vector, miR-150, miR-186, miR-204, or miR-211) were transfected into E10 cells together with 15 ng full-length P2X7R 3'UTR Renilla reporter construct (RL-P2X7R) and 15 ng pGL3 plasmid. 48 hours after transfection, the cells were haversted and the dual-luciferase activities were measured. (B) To examine the specificity of the miR-150 regulation of P2X7R 3'-UTR, mutation plasmids of miR-150 (miR-150mut) was constructed. 15 ng RL-P2X7R and 170 ng pENTR/CMV-EGFP-miR-150 or miR-150mut vectors were co-transfected into E10 cells with 15 ng pGL3. After two days, the dual-luciferase were determined. (C) 170 ng pENTR/CMV-primiRNA plasmids (miR-150 or control) and 15 ng P2X7R full length 3'UTR plasmids were cotransfected into A549 or R3/1 cells, along with 15 ng pGL3 plasmids for normalization. Luciferase activities were measured after 48 hours. Data were expressed as the ratio of Renilla reporter activity to Firefly reporter activity (Normalized RL/FL). The results shown were means ± S.E. (n=6 for panel A, and n=3 for others, * P< 0.05 *v.s.* control, # P<0.05 vs A549 control, & P<0.05 v.s. R3/1 control.)

TargetScan predicts that two miR-150 binding sites exist in the human P2X7R 3'-UTR. To determine which site miR-150 interacts with, we constructed truncated P2X7R 3'-UTR only containing the wild-type or the mutated miR-150 binding sites (RL-P2X7R-150B1, RL-P2X7R-

150B2, RL-P2X7R-150B1mut, and RL-P2X7R-150B2mut). MiR-150 down-regulated the luciferase activities of RL-P2X7R-150B2 but failed to inhibit the activities of RL-P2X7R-150B1 (Fig.V.3A and 3B). Mutation on miR-150 binding site 2 rescued the luciferase activity to control level (Fig.V.3B). Consistently, mutation of miR-150 failed to repress the reporter activities of RL-P2X7R-150B2.

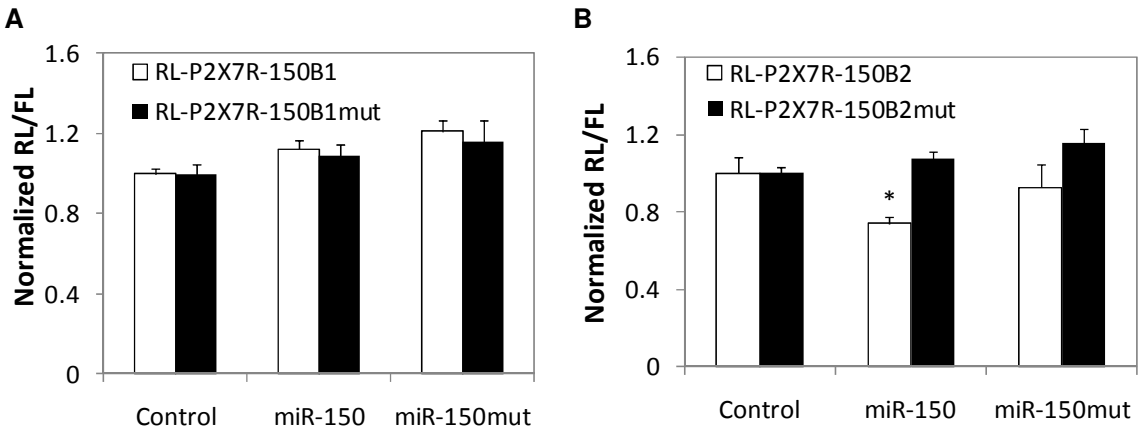

Fig.V.3 The binding site of miR-150 on P2X7R 3'-UTR. (A) 15 ng truncated P2X7 3'UTR plasmids containing wild-type or mutated miR150 binding site 1 (RL-P2X7R-150B1 and RL-P2X7R-150B1mut) (A), or truncated P2X7 3'-UTR plasmids containing wild-type or mutated miR-150 binding site 2 (RL-P2X7R-150B2 and RL-P2X7R-150B2mut) (B) were transfected into E10 cells with 170 ng pENTR/CMV-EGFP-primiRNA (control vector, miR-150 or miR-150mut) and 15 ng pGL3. The dual-luciferase activity was measured 48 hours after transfection. The results were normalized to Firefly luciferase activity. The data were means ± S.E. (n=3, *P< 0.05 *v.s.* control).

To determine whether miR-150 and miR-186 down-regulate endogenous P2X7R protein expression, we generated adenoviruses to overexpress miR-150 and miR-186. These viruses were used to transduce E10 cells for 4 days at a MOI of 50 or 100. As shown in Fig.V.4A, the P2X7R protein expression was not affected in the control and miR-186 expressing adenoviruses-treated cells. However, a significant decrease was observed in miR-150 expressing adenovirus-transduced cells. This decrease was virus dose-dependent. We also examined the P2X7R mRNA expression using real-time PCR. The control and miR-150 viruses had no effects on the P2X7R mRNA expression. MiR-186 viruses slightly increased the P2X7R level at both protein and mRNA levels. (Fig.V.4B).

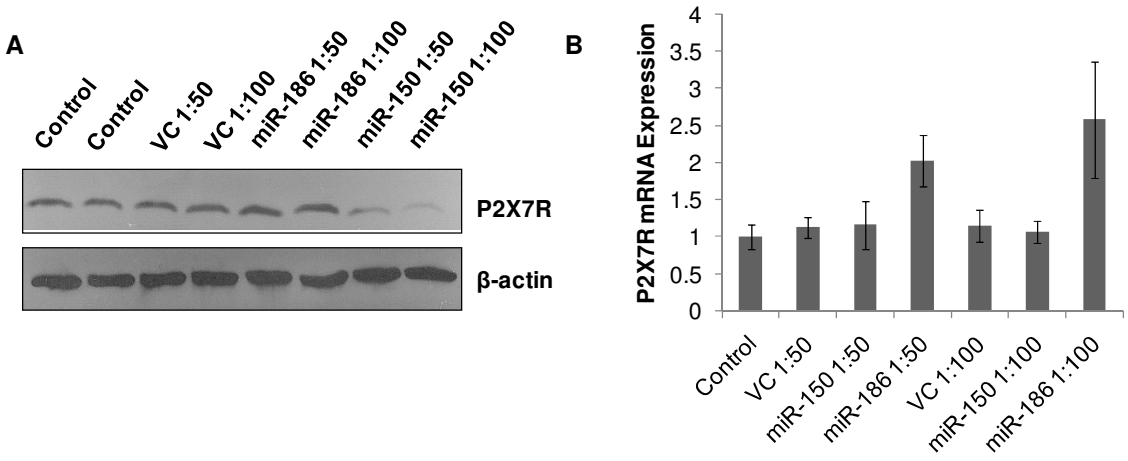

Fig.V.4 miR-150 silences the P2X7 protein expression. E10 cells were treated with different dose of miR-186 and miR-150 overexpressing viruses. A virus overexpressing GFP was used as a virus control (VC). Four days after treatement, protein (A) and mRNA (B) expression were examined using Western blot and Real-time PCR. β-actin were used as an internal control for western blot. 18S rR NA was used as an internal control for real-time PCR. For panel B, data are means ±S.E. (n=3 biological replicatios plus 2 technical replications).

5.4.2 Characterizaion of miR-150 expression

MiR-150 is highly expressed in lymph nodes, spleen, heart, and brain. However, its abundance in the lung is contradictory (35; 37). We first examined the expression of miR-150 in various organs by real-time PCR. As previously reported, miR-150 was highly expressed in spleen (Fig.V.5). Its expression in the lung was comparable to those in the heart and brain.

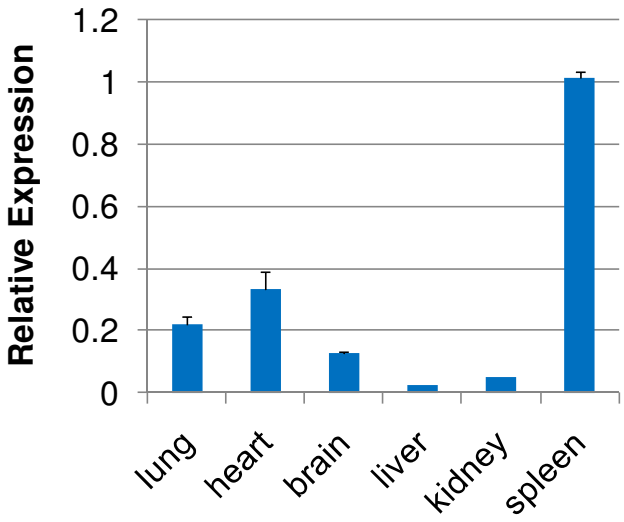

Fig.V.5 Expression level of miR-150 in organs. Total RNA were extracted from various organs, poly (A) tailed and reversed-transcripted into cDNA. Real-time PCR were used to examine the miR-150 level. The results were normalized to U2. The data were expressed as means ± S.E. (n=3 biological replications plus 2 technical replications)

MiR-150 expression level in type II cells was much higher than type I cells, which was inversely correlated with the P2X7R protein level (Fig.V.6A). MiR-150 was also highly expressed in the type I cell line, R3/1 that contained little P2X7R, in comparison with that in another type I cell line, E10 that contained a high level of P2X7R (Fig.V.6B). These results indicate that P2X7R may be a potential target of miR-150.

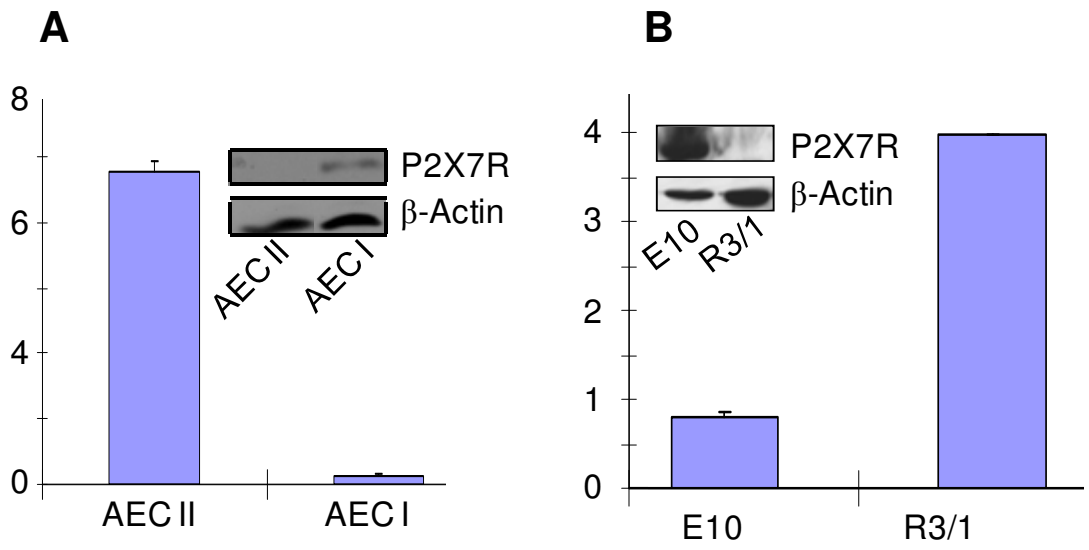

Fig.V.6 miR-150 and P2X7R expression in lung cells. Total RNA and proteins were extracted from AEC II (freshly isolated type II cells) and AEC I (trans-differentiated type I cells by culturing AEC II on plastic dishes for 5 days) (A), and E10 and R3/1 cells (B). miR-150 level was determined by real-time PCR. U2 was used as an internal reference. The results were expressed as means ± S.E. (n=6 except R3/1, n=2) P2X7R protein level was measured by Western blot and β-actin was used a loading control.

5.4.3 MiR-150 interrupted the P2X7R-mediated surfactant secretion

Previously, we found that BzATP activated P2X7R in AEC I, resulting in an increase in surfactant secretion in AEC II. We therefore examined whether miR-150 affects surfactant secretion. We pre-treated E10 cells with miR-150 or miR-186 overexpression viruses for 4 days and stimulated the E10 cells with BzATP for 2 hours. Then the conditioned media was used to

stimulate surfactant secretion in AEC II. As shown in Fig.V.7, miR-150 significantly decreased the surfactant secretion in AEC II. Interestingly, miR-186 also reduced surfactant secretion.

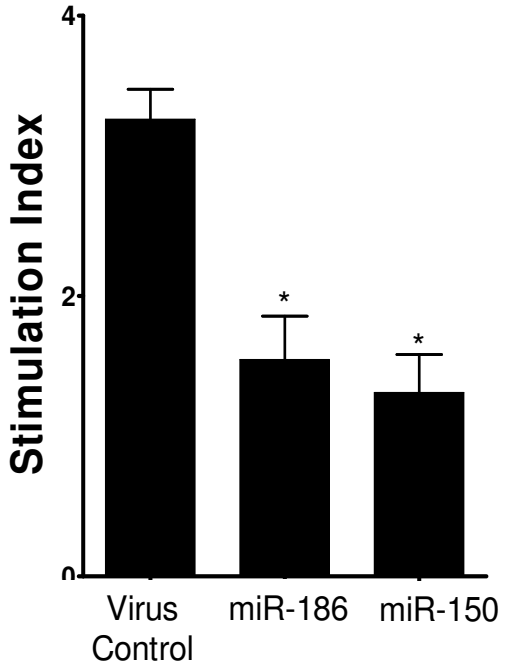

Fig.V.7 MiR-150 inhibits P2X7R-evoked surfactant secretion. (A) E10 cells were treated with 100 MOI of adenovirus expressing miR-150 or miR-186 for 4 days. Adenovirus only express EGFP was used as a control. E10 cells were stimulated for 2 hours with BzATP (25 μM). The E10 cell conditioned media were used to stimulate AEC II for 2 hours. PC secretion was measured. Data are means ± S.E. (n=3 student's t test, * P< 0.001 *vs*. control).

5.5 Discussion

The main purpose of this study is to identify miRNAs that regulate the P2X7R activity. Using dual-luciferase assay, we first explored the miRNAs which may target to P2X7R. Only miR-150 consistently inhibited the reporter gene expression. Next, we characterized the miR-150 expression in different cells. We found that miR-150 had much lower expression in P2X7R-enriched cells, such as AEC I and E10 cells, further supporting the miR-150 regulation of P2X7R. MiR-150 expressing adenovirus dramatically decreased the endogenous P2X7R expression in E10 cells. The conditioned media from miR-150 expressing virus treated E10 cells failed to stimulate surfactant secretion in AEC II. Our data suggests a possible role of miRNA-150 in surfactant secretion.

MiRNAs non-perfectly bind to the 3'-UTR of a target mRNA. In many cases, miRNAs only repress the mRNA translation by preventing the initiation of translation, disrupting the assembly of 80S ribosome (9) without degrading the mRNA, or by directly physical destruction of the mRNA (24). The features of the miRNA determine that it may have more than one target. Similarly, the mRNA can be regulated by several miRNAs. In addition, miRNA regulatory machinery changes with cell type and organisms.

Among the miRNAs tested, we found that only miR-150 significantly decreased the P2X7R 3'-UTR reporter expression in rat, mouse and human lung epithelial cells. Mutation of miR-150 lost the inhibitory effect on P2X7R expression. Our results indicate that the regulation of P2X7R by miR-150 is specific and conserved among different species. Consistent with the luciferase assay, we also showed that adenovirus expressing miR-150 down-regulated the P2X7R protein expression. MiR-150 failed to regulate the luciferase activities of the P2X7R binding site 1, indicating that the regulation of P2X7R by miR-150 was through the binding site 2. However, mutation of miR-150 could not regulate the mutated P2X7 3'-UTR. According to the mechanisms of miRNA processing: three crucial steps are needed: Drosha cleaves pri-miRNA into pre-miRNA; Dicer further cleaves pre-miRNA into 21-23 nt double-strand miRNA; and one strand of miRNA is loaded into RISC (17). One possible explanation is that mutated miRNA sequence affects the miRNA processing. For example, the miRNA cannot be cleaved properly, thus no mature mutated miR-150 is synthesized. Alternatively, the mature miRNA cannot be loaded into RISC.

According to our results, adenovirus expressing miR-150 decreased the endogenous P2X7R protein expression for more than 70%, the 3'-UTR reporter assay only showed around 25% decrease. There are two possible explainations. First, the transfection efficiency of E10 cells is only around 35%. It is possible that the miR-150 and P2X7 3'-UTR vectors were transfected into different cells. Thus not all the 3'-UTR plasmids are available for miR-150 inhibition. Second, E10 cells itself have a very high P2X7R expression. The endogenous P2X7R 3'-UTR may compete with the P2X7R 3'-UTR plasmids for miR-150.

The expression of miR-150 and P2X7R are consistent with their regulatory relationship. MiR-150 has relatively high expression in spleen, lung, brain, and heart, and a little in kidney and liver. P2X7R is initially identified in immune systems as a ion channel, and it mediates programmed cell death by releasing IL-1 beta from macrophages (7; 21). Similarly, miR-150 is highly expressed in the mature B and T cells. MiR-150 is a key regulator of the B cell maturation and differentiation. Overexpression of miR-150 in hematopoietic stem cells impairs the B cell development and differentiation by silencing the expression of c-Myb (35; 37). B cells produce antibodies against antigens and mediate a specific immune response. P2X7R is involved in the macrophage-mediated non-specific defense which helps to initiate the specific immune response. The high

expression of miR-150 in B cells may down-regulate the P2X7R expression and inhibit the subsequent non-specific cation influx and apoptosis.

Previously using a AEC I and AEC II mixed cell culture model, we found that P2X7R is involved in the ATP-induced surfactant secretion (23). E10 cell line is a mouse epithelial type I cell line which has high expression of P2X7R and low miR-150 expression. BzATP activates P2X7R and stimulates ATP release from E10 cells. The conditioned media from the BzATP-stimulated E10 cells increased the surfactant secretion of freshly isolated AEC II. If pre-treated the E10 cells with virus expressing miR-150 for 4 days, the P2X7R protein level in E10 cells were significantly decreased. As a result, surfactant secretion was reduced.

Pre-treatment of E10 cells with miR-150 and miR-186 overexpression viruses both significantly decreased the surfactant secretion from AEC II. However, miR-186 did not reduce the P2X7R protein level as miR-150 did, indicating that P2X7R is not a target of miR-186 in lung cells. Thus, the regulation of surfactant secretion by miR-186 must be via a different target. Since BzATP-stimulated conditioned medium was used for surfactant secretion, miR-186 may target a protein that regulates P2X7R-mediated release of a soluble factor.

In summary, miR-150 regulates the P2X7R expression and thus surfactant secretion. Our results verified that P2X7R is a target for miR-150 at protein level. Abnormal surfactant secretion may cause severe lung disease. Our results may provide new therapeutic strategies for lung diseases related to surfactant secretion.

5.6 References

1. Andreeva AV, Kutuzov MA and Voyno-Yasenetskaya TA. Regulation of surfactant secretion in alveolar type II cells. *Am J Physiol Lung Cell Mol Physiol* 293: L259-L271, 2007.
2. Ballerini P, Rathbone MP, Di IP, Renzetti A, Giuliani P, D'Alimonte I, Trubiani O, Caciagli F and Ciccarelli R. Rat astroglial P2Z (P2X7) receptors regulate intracellular calcium and purine release. *Neuroreport* 7: 2533-2537, 1996.
3. Bhaskaran M, Kolliputi N, Wang Y, Gou D, Chintagari NR and Liu L. Trans-differentiation of alveolar epithelial type II cells to type I cells involves autocrine signaling by transforming growth factor beta 1 through the Smad pathway. *J Biol Chem* 282: 3968-3976, 2007.
4. Bhaskaran M, Wang Y, Zhang H, Weng T, Baviskar P, Guo Y, Gou D and Liu L. MicroRNA-127 modulates fetal lung development. *Physiol Genomics* 37: 268-278, 2009.
5. Borok Z, Liebler JM, Lubman RL, Foster MJ, Zhou B, Li X, Zabski SM, Kim KJ and Crandall ED. Na transport proteins are expressed by rat alveolar epithelial type I cells. *Am J Physiol Lung Cell Mol Physiol* 282: L599-L608, 2002.
6. Chen J, Chen Z, Chintagari NR, Bhaskaran M, Jin N, Narasaraju T and Liu L. Alveolar type I cells protect rat lung epithelium from oxidative injury. *J Physiol* 572: 625-638, 2006.

7. Chen L and Brosnan CF. Regulation of immune response by P2X7 receptor. *Crit Rev Immunol* 26: 499-513, 2006.

8. Chen Z, Jin N, Narasaraju T, Chen J, McFarland LR, Scott M and Liu L. Identification of two novel markers for alveolar epithelial type I and II cells. *Biochem Biophys Res Commun* 319: 774-780, 2004.

9. Chendrimada TP, Finn KJ, Ji X, Baillat D, Gregory RI, Liebhaber SA, Pasquinelli AE and Shiekhattar R. MicroRNA silencing through RISC recruitment of eIF6. *Nature* 447: 823-828, 2007.

10. Chintagari NR, Jin N, Wang P, Narasaraju TA, Chen J and Liu L. Effect of cholesterol depletion on exocytosis of alveolar type II cells. *Am J Respir Cell Mol Biol* 34: 677-687, 2006.

11. Di VF, Chiozzi P, Falzoni S, Ferrari D, Sanz JM, Venketaraman V and Baricordi OR. Cytolytic P2X purinoceptors. *Cell Death Differ* 5: 191-199, 1998.

12. Garcia-Marcos M, Pochet S, Marino A and Dehaye JP. P2X7 and phospholipid signalling: the search of the "missing link" in epithelial cells. *Cell Signal* 18: 2098-2104, 2006.

13. Gou D, Narasaraju T, Chintagari NR, Jin N, Wang P and Liu L. Gene silencing in alveolar type II cells using cell-specific promoter in vitro and in vivo. *Nucleic Acids Res* 32: e134, 2004.

14. Hutchison AA. Respiratory disorders of the neonate. *Curr Opin Pediatr* 6: 142-153, 1994.

15. Johnson MD, Widdicombe JH, Allen L, Barbry P and Dobbs LG. Alveolar epithelial type I cells contain transport proteins and transport sodium, supporting an active role for type I cells in regulation of lung liquid homeostasis. *Proc Natl Acad Sci U S A* 99: 1966-1971, 2002.

16. Khakh BS and North RA. P2X receptors as cell-surface ATP sensors in health and disease. *Nature* 442: 527-532, 2006.

17. Kim VN. MicroRNA biogenesis: coordinated cropping and dicing. *Nat Rev Mol Cell Biol* 6: 376-385, 2005.

18. Lee Y, Ahn C, Han J, Choi H, Kim J, Yim J, Lee J, Provost P, Radmark O, Kim S and Kim VN. The nuclear RNase III Drosha initiates microRNA processing. *Nature* 425: 415-419, 2003.

19. Lee Y, Jeon K, Lee JT, Kim S and Kim VN. MicroRNA maturation: stepwise processing and subcellular localization. *EMBO J* 21: 4663-4670, 2002.

20. Lund E, Guttinger S, Calado A, Dahlberg JE and Kutay U. Nuclear export of microRNA precursors. *Science* 303: 95-98, 2004.

21. MacKenzie A, Wilson HL, Kiss-Toth E, Dower SK, North RA and Surprenant A. Rapid secretion of interleukin-1beta by microvesicle shedding. *Immunity* 15: 825-835, 2001.

22. McGowan SE and Synder JM. Development of Alveoli. In: The lung: development, aging and the environment., edited by Harding R, Pinkerton KE and Plopper CG. Academic Press, 2004, p. 55-73.

23. Mishra, A., Chintagari, N. R., and Liu, L. Purinergic P2X7 Receptor: A Pivotal Role in Surfactant Regulation. FASEB J. 22(931.4). 2008.
Ref Type: Abstract

24. Nilsen TW. Mechanisms of microRNA-mediated gene regulation in animal cells. *Trends Genet* 23: 243-249, 2007.

25. Pelegrin P, Barroso-Gutierrez C and Surprenant A. P2X7 receptor differentially couples to distinct release pathways for IL-1beta in mouse macrophage. *J Immunol* 180: 7147-7157, 2008.

26. Rana TM. Illuminating the silence: understanding the structure and function of small RNAs. *Nat Rev Mol Cell Biol* 8: 23-36, 2007.

27. Ridge KM, Olivera WG, Saldias F, Azzam Z, Horowitz S, Rutschman DH, Dumasius V, Factor P and Sznajder JI. Alveolar type 1 cells express the alpha2 Na,K-ATPase, which contributes to lung liquid clearance. *Circ Res* 92: 453-460, 2003.

28. Shi R and Chiang VL. Facile means for quantifying microRNA expression by real-time PCR. *Biotechniques* 39: 519-525, 2005.

29. Suadicani SO, Brosnan CF and Scemes E. P2X7 receptors mediate ATP release and amplification of astrocytic intercellular Ca2+ signaling. *J Neurosci* 26: 1378-1385, 2006.

30. Surprenant A, Rassendren F, Kawashima E, North RA and Buell G. The cytolytic P2Z receptor for extracellular ATP identified as a P2X receptor (P2X7). *Science* 272: 735-738, 1996.

31. Tomari Y and Zamore PD. Perspective: machines for RNAi. *Genes Dev* 19: 517-529, 2005.

32. Tsukimoto M, Harada H, Ikari A and Takagi K. Involvement of chloride in apoptotic cell death induced by activation of ATP-sensitive P2X7 purinoceptor. *J Biol Chem* 280: 2653-2658, 2005.

33. Weng T, Jin N and Liu L. Differentiation between amplicon polymerization and nonspecific products in SYBR green I real-time polymerase chain reaction. *Anal Biochem* 342: 167-169, 2005.

34. Wright JR and Clements JA. Metabolism and turnover of lung surfactant. *Am Rev Respir Dis* 136: 426-444, 1987.

35. Xiao C, Calado DP, Galler G, Thai TH, Patterson HC, Wang J, Rajewsky N, Bender TP and Rajewsky K. MiR-150 controls B cell differentiation by targeting the transcription factor c-Myb. *Cell* 131: 146-159, 2007.

36. Yi R, Qin Y, Macara IG and Cullen BR. Exportin-5 mediates the nuclear export of pre-microRNAs and short hairpin RNAs. *Genes Dev* 17: 3011-3016, 2003.

37. Zhou B, Wang S, Mayr C, Bartel DP and Lodish HF. miR-150, a microRNA expressed in mature B and T cells, blocks early B cell development when expressed prematurely. *Proc Natl Acad Sci U S A* 104: 7080-7085, 2007.

38. Zhou L, Qi X, Potashkin JA, bdul-Karim FW and Gorodeski GI. MicroRNAs miR-186 and miR-150 down-regulate expression of the pro-apoptotic purinergic P2X7 receptor by activation of instability sites at the 3'-untranslated region of the gene that decrease steady-state levels of the transcript. *J Biol Chem* 283: 28274-28286, 2008.

5.7 Acknowledgements

We are grateful to Dr. Amarjit Mishra for doing the surfactant secretion, Yujie Guo for amplifying the adenovirus for miR-150 and miR-186 and helping with some of the real-time PCR and western blot, and Yang Wang and Lijing Su for running the real-time PCR for miR-150. We thank Dr. Mary Williams (Boston U) for kindly providing the E10 cells and Dr. Roland Koslowski (Dresden U of Technology) for R3/1 cells. This work was supported by NIH grants R01 HL-083188 (LL).

CHAPTER V

DIFFERENTIATION BETWEEN AMPLICON POLYMERIZATION AND NONSPECIFIC PRODUCTS IN SYBR GREEN I REAL-TIME POLYMERASE CHAIN REACTION

6.1 Article

Real-time PCR is a well-established method for the quantification of gene expression levels in biological samples (4; 7; 9)]. The amount of PCR products (amplicons) can be detected in real time by measuring fluorescence (6)]. The mRNA levels of the unknown samples can be calculated from the cycle threshold (Ct) by either absolute or relative methods (1)]. SYBR Green I is a commonly used fluorescent dye to monitor PCR products based on its ability to emit a fluorescent signal upon binding to double-strand DNA (5; 12)]. This method sometimes is comprised by non-specific signals derived from non-specific amplifications or primer dimers. The effects of primer dimers can be eliminated by including a data acquisition step at a higher temperature than the annealing temperature (11)], although the latter sometimes may reduce the amplification efficiency. Non-specific amplification is mainly caused by non-specific primers, but sometimes also by a low annealing temperature and high concentrations of template DNA, Mg^{2+}, polymerase, or dNTPs (2)].

A melting curve is used to assess the specificity of the PCR products. A single peak is considered to be specific. Although in some cases, internal melting domains generate a complex melting curve (10)], the appearance of multiple peaks usually indicate non-specific amplifications. In this study, we observed that, for some genes, in addition to the amplicon peak, higher temperature peaks appeared at high copy numbers on the melting curve. We presented evidence that this is not due to non-specific amplification, but amplicon polymerization. We also provided a method to distinguish between amplicon polymerization and non-specific amplification.

.

The upstream and downstream primers of rattus norvegicus nasal embryonic LHRH factor (Nelf, NM_057190) and alcohol dehydrogenase 1 (Adh1, NM_019158) were located in two different exons to avoid the amplication from genomic DNA due to the contamination of the RNA samples; blast search indicated that they were specific to the respective genes. Aquaporin 8 (Aqp8) was used as a control to show non-specific amplifications and its forward primer was highly homogenous to another gene (Notch 1). The primer sequences are as follows: Nelf: forward, TTTGCCAAAGTGGAGAAGGAA, and reverse, CCCATGATGTGGATGACATTTG; Adh1: forward, CGGTTAGTGGATCCCTGTTCA, and reverse, TATCACCTGGTTTCACACAAGTCA; Aqp8: forward, AGAGTCTAGCGGACCAGTCTGAGT, and reverse, CCTTGATCTCACGTAGGTCCATACT. For Nelf and Adh1, the PCR products by conventional PCR were purified from agarose gel and used as templates. For Aqp8, the PCR products have multiple bands and different dilutions of adult rat lung tissue cDNA were used directly as templates. Real-time PCR was performed on an ABI 7500 system using SYBR Green I detection (Qiagen, Valencia, CA). The thermal condition was 95^{o}C for 15 min, followed by 40 cycles of 95^{o}C 20 sec, 60^{o}C for 30 sec, 72^{o}C for 30 sec, and data acquisition at 78^{o}C for 35 sec.

The melting curve of Nelf showed that there was peak at 79.6 ± 0.2℃ for all template concentrations (Fig.1B). All amplicons had one band of 100 bp on agarose gel (Fig.VI.1C). This represents a typical specific amplification. For Adh1, when template copy number was ≤ 100, a single peak was observed at 81.7ºC. As the template copy number increased, an additional peak appeared at higher temperatures. At ≥ 10^4 copy number, only the higher temperature peak remained (83.9 ºC) (Fig.VI.1E). On agarose gel, the amplicons from 10^4 to 10^7 copy numbers formed a smear, but the amplicons from 10 to 10^2 copy numbers had an expected single band of ~110 bp (Fig.VI.1F).

In order to figure out why there was a shift of Tm and why smears was formed in the PCR products of Adh1, we ran another real-time PCR for Adh1 under the same conditions for only 25 cycles, at which point, the reactions, containing the templates with 10^5 or lower copy numbers, were not saturated. Melting curve analysis showed that the Tm of 10^5 copy number template switched back to 81.7^{o}C from 83.9^{o}C (Fig.VI.1H). On agarose gel, the amplicons from 10^5 copy number template, which formed smears in the previous 40-cycle amplification, had only one band (~110 bp) for the 25-cycle amplification (Fig.VI.1I). Although the PCR products from 10^7 and 10^6 copy number templates still had multiple bands, they were not smears anymore. These additional bands from 10^7 and 10^6 copy numbers were ~220, ~330 and ~440 bp, respectively, which correspond to the sizes of dimers, trimers and tetramers of the specific amplicons. In order to further confirm that the additional bands are indeed due to the polymerization of the amplicons. 110 bp and 220 bp bands were purified from the agarose gel and cloned into the PCR®-Blunt (Invitrogen) through blunt ligation. After sequencing these PCR products, we found that the 110 bp band was the amplicon and 220 bp band was a dimer of the amplicon through three

nucleotides TGA. The hotstartTaq polymerase in the Quanti-tect SYBR Green kit can add extra A at the 3' end of the PCR products (in few cases other nucleotides), but has no proofreading 3' →5' exonuclease activities to remove the randomly filled nucleotides (3; 8)]; this may contribute to the polymerization of amplicons. The genes showing the amplicon polymerization mostly have 3 linked GC (4 of 6) at the 5' end of one of the primers, which possibly make it easier to add extra nucleotides at the end of the PCR products. The Tm shift derived from the PCR product polymerization can be distinguished from a real non-specific amplification. The non-specific amplifications have distinct peaks in the melting curves and different bands at all the template copy numbers (Fig.VI.1K and L), whereas the amplicon polymerization has a gradual shift of Tm and forms smears only at high template copy numbers (Fig.VI.1F).

Is the quantification from Adh1-like genes still reliable? Our answer is yes. Because real-time PCR uses Ct for quantification, which is always set in the exponential phase of the amplification and far away from saturation. Agarose gel and melting curve analysis are the end point analyses; even the polymerized PCR products appear at the end point, they do not interfere with the starting point (C_T) analyses. The standard curve of Adh1 has an R square of 0.99 and a slope of -3.4, indicating a 96.8% amplication efficiency. This is within the range of the acceptable slope (-3.0 to -3.9). In order to further confirm the reliability of the standard curve, we did series dilutions of new born rat lung tissue cDNA, which generate a single peak (81.7ºC) at all the dilutions in the melting curve because their low copy numbers of Adh1 in those samples, and quantitated the Adh1 expression. We found that $\log_{10}$ (copy number from the standard curve) vs $\log_{10}$ (cDNA concentration) generate a curve with an R square of 0.995 and a slope of 1.02. Furthermore, we compared the Adh1 expression quantitated from real-time PCR to those from DNA microarray, and found the fold changes from each pair of 6 samples having an 88% consistency between two methods. In our studies, we have run a total of 38 genes using real-time PCR. We found that 28 genes had a specific amplification, 6 genes amplicon polymerization, and 4 genes non-specific amplification.

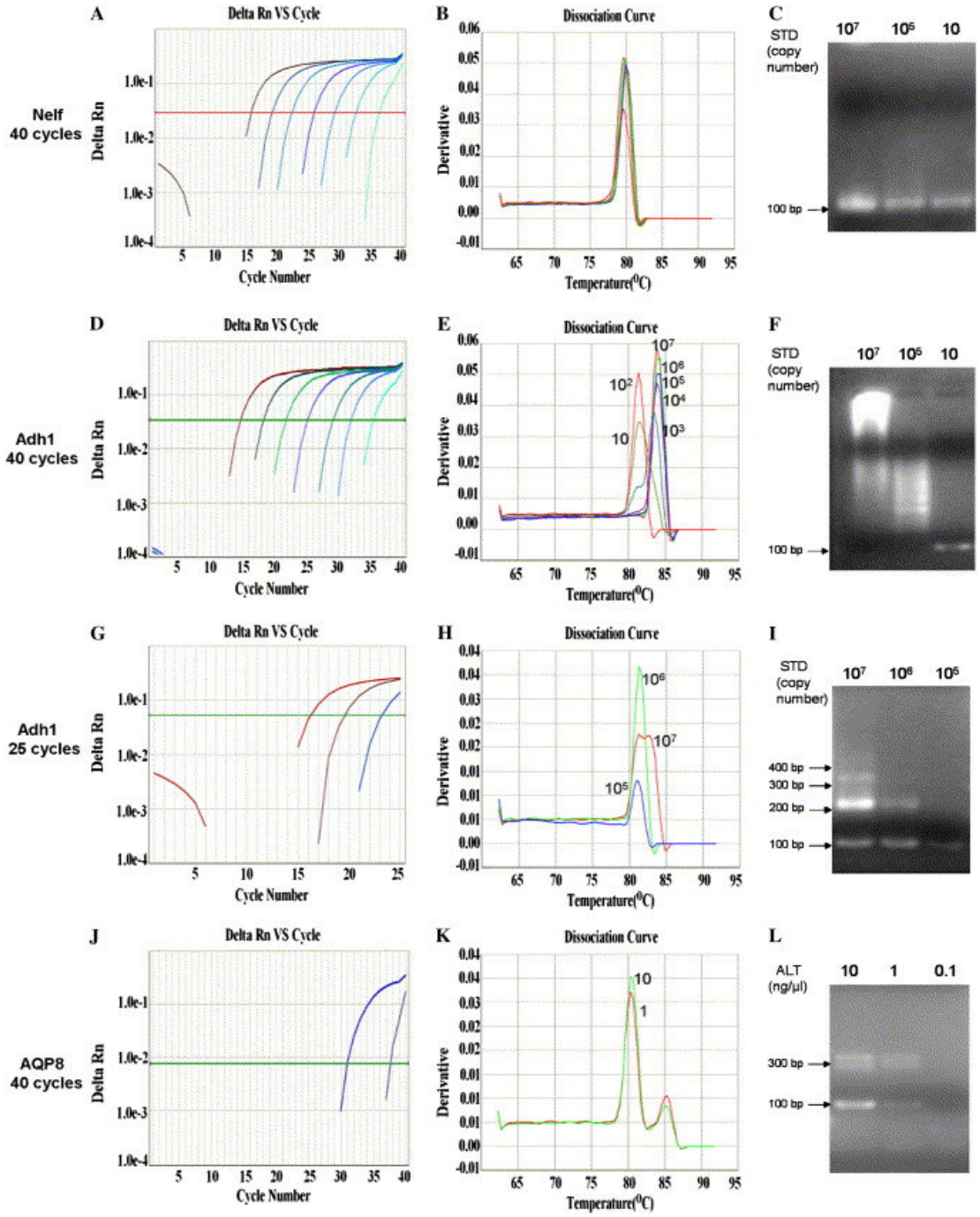

Fig.VI.1. Amplification, melting curve, and agarose gel electrophoresis of target genes. Nelf (A–C) and Adh1 (D–F) were amplified 40 cycles with series dilutions of PCR products as template (STD). (G and H). Real-time PCR for Adh1 was run with 25 cycle amplification under the same conditions as those in D–F. Aqp8 was run as a nonspecific control using series dilutions of adult lung tissue (ALT) cDNA as templates. The data collection temperature for real-time PCR was 78 ℃. The arrows represent DNA markers.

6.2 Reference List

1. Bustin SA. Absolute quantification of mRNA using real-time reverse transcription polymerase chain reaction assays. *J Mol Endocrinol* 25: 169-193, 2000.
2. Carbonari M, Sbarigia D, Cibati M and Fiorilli M. Optimization of PCR performance. *Trends Genet* 9: 42-43, 1993.
3. Clark JM. Novel non-templated nucleotide addition reactions catalyzed by procaryotic and eucaryotic DNA polymerases. *Nucleic Acids Res* 16: 9677-9686, 1988.
4. de Kok JB, van Balken MR, Roelofs RW, van Aarssen YA, Swinkels DW and Klein Gunnewiek JM. Quantification of hTERT mRNA and telomerase activity in bladder washings of patients with recurrent urothelial cell carcinomas. *Clin Chem* 46: 2003-2007, 2000.
5. Giglio S, Monis PT and Saint CP. Demonstration of preferential binding of SYBR Green I to specific DNA fragments in real-time multiplex PCR. *Nucleic Acids Res* 31: e136, 2003.
6. Holland PM, Abramson RD, Watson R and Gelfand DH. Detection of specific polymerase chain reaction product by utilizing the 5'----3' exonuclease activity of Thermus aquaticus DNA polymerase. *Proc Natl Acad Sci U S A* 88: 7276-7280, 1991.
7. Homey B, Dieu-Nosjean MC, Wiesenborn A, Massacrier C, Pin JJ, Oldham E, Catron D, Buchanan ME, Muller A, deWaal MR, Deng G, Orozco R, Ruzicka T, Lehmann P, Lebecque S, Caux C and Zlotnik A. Up-regulation of macrophage inflammatory protein-3 alpha/CCL20 and CC chemokine receptor 6 in psoriasis. *J Immunol* 164: 6621-6632, 2000.
8. Hu G. DNA polymerase-catalyzed addition of nontemplated extra nucleotides to the 3' end of a DNA fragment. *DNA Cell Biol* 12: 763-770, 1993.
9. Kubo A, Nishitani Y, Minamino N, Kikumoto K, Kurioka H, Nishino T, Iwano M, Shiiki H, Kangawa K and Dohi K. Adrenomedullin gene transcription is decreased in peripheral blood mononuclear cells of patients with IgA nephropathy. *Nephron* 85: 201-206, 2000.
10. Li W, Xi B, Yang W, Hawkins M and Schubart UK. Complex DNA melting profiles of small PCR products revealed using SYBR Green I. *Biotechniques* 35: 702-4, 706, 2003.
11. Morrison TB, Weis JJ and Wittwer CT. Quantification of low-copy transcripts by continuous SYBR Green I monitoring during amplification. *Biotechniques* 24: 954-8, 960, 962, 1998.
12. Ririe KM, Rasmussen RP and Wittwer CT. Product differentiation by analysis of DNA melting curves during the polymerase chain reaction. *Anal Biochem* 245: 154-160, 1997.

6.7 Acknowledgements

We are grateful to Dr. Nili Jin for her assistance with the real-time PCR and manuscript writing. This work was supported by NIH R01 HL-52146 and R01 HL-071628 (to L.L.). N.J. was supported by an AHA predoctoral fellowship (0315256Z).

CHAPTER VII

SUMMARY AND CONCLUSIONS

Fetal lung development is a complex and important biological process which includes the interactions among growth factors, transcription factors and extracellular matrix proteins. The maturation of AEC II and AEC I happens during the late stages of fetal lung development (Canalicular and Saccular stages). The differentiation of these two cells is crucial for normal lung function. The signaling pathways that regulate fetal lung development and AEC differentiation have been studied to some extent. However, whether there are additional signaling molecules which also regulate these processes is not known.

The present study was first designed to explore the genes which have expression changes during the late stages of fetal lung development. From there, we found that pleiotrophin (PTN) is a potential candidate. In the second part of the work, we studied the function of PTN including fetal AEC II proliferation, migration and trans-differentiation into AEC I. The signaling pathway of PTN was also examined. Next, *in vivo* studies were further carried out to examine the role of PTN in fetal lung development using $PTN^{-/-}$ mice. Since the regulation of surfactant secretion is an important aspect of lung development, we next carried out some studies on surfactant secretion. In the fourth part, we examined how microRNA-150 regulates surfactant secretion via P2X7R.

In our first set of studies, we want to screen genes which may regulate AEC II differentiation during fetal lung development. We used a loop-designed 10K DNA microarray to explore gene expression changes on embryonic day 18, 19, 20, 21, new born and adult. Statistical significance analysis of microarray (SAM) test identified 583 genes with >2 fold change between at least two time points and coefficient of variation less than 0.5. These genes were clustered into 7 clusters. One of these clusters was identified as a “developing” cluster, which only contains 10 known genes, but 7 of these 10 known genes are involved in development or cell proliferation. The expression of this group of genes increased from E18 to E20 and decreased after that time. Real-time PCR analysis of these 10 known genes showed an 88% consistency with the microarray data. We further examined the cellular localization of LIM homeodomain protein 3a (Lhx3), a transcription factor, and PTN, a Heparin-binding cytokine, using real-time PCR and immunohistochemistry. Lhx3 was mainly located in the developing airway epithelial cells, while PTN in the mesenchymal cells adjacent to the developing epithelium and endothelial cells. Using GenMAPP, we identified four regulatory pathways: transforming growth factor- 3 signaling, inflammatory response, cell cycle, and G protein signaling. We also identified two metabolic pathways: glycolysis-gluconeogenesis and proteasome degradation.

Since the expression pattern of PTN indicated that it may be involved in the epithelial-mesenchymal interactions, in the second set of studies, we examined the cellular localization of PTN receptor, protein tyrosine phosphatase receptor β/ζ (RPTPβ/ζ). RPTPβ/ζ was highly expressed in epithelial cells of the fetal lungs. Using isolated fetal alveolar epithelial type II cells, we demonstrated that human recombinant PTN increased wound healing of injured fetal AEC II monolayer, promoted fetal AEC II proliferation and arrested AECII trans-differentiation into AEC I. Silencing of PTN expression influenced lung branching morphogenesis in a fetal lung organ culture model. PTN signaling pathway through RPTPβ/ζ/β-catenin was also examined. PTN increased the tyrosine phosphorylation of β-catenin, promoted β-catenin translocation into the nucleus and activated TCF/LEF transcription factors. We also examined whether PTN regulates β-catenin downstream genes. These studies revealed that pleiotrophin/β-catenin pathway suppressed endogenous dlk1 expression. Promoter assay and chromatin immunoprecipitation further verified β-catenin as a potential regulator of dlk1. Our results demonstrated that PTN plays roles in fetal lung development by regulating AEC II migration, proliferation and differentiation through RPTPβ/ζ/β-catenin pathway.

In our third set of studies, we examined the lung morphology and marker gene expression during the development using PTN knockout ($PTN^{-/-}$) and wild-type ($PTN^{+/+}$) mice. No obvious difference was observed between $PTN^{-/-}$ and $PTN^{+/+}$ mouse lungs during the fetal and early postnatal stages when PTN expression was high. However, on postnatal day 15 and adult, HE staining showed that $PTN^{-/-}$ mice had hypercellular lungs with smaller alveoli and thicker septa in comparison with those of $PTN^{+/+}$ mice of the same age. These findings indicated that lungs of $PTN^{-/-}$ mice were less matured and developed. α-SMA, a myofibroblast makrer, had significantly higher expression in $PTN^{-/-}$ mice lungs on P15 and adult. Real-time PCR showed that SP-A, B, and C, and CCSP all significantly increased in adult $PTN^{-/-}$ mouse lungs, while P2X7R and T1-α expression decreased. Our data demonstrate for the first time that PTN may play an important role in the alveolarization that occurs during lung development.

In our forth set of studies, we determined whether miRNA regulates P2X7R-mediated surfactant secretion. The development of pulmonary surfactant system is a crucial part of the normal lung development. First, using a dual-luciferase assay, we screened the regulation of P2X7R 3'UTR activity by miR-150, miR-186, miR-204 and miR-211 in lung epithelial cells. Only miR-150 consistently suppressed P2X7R 3'UTR reporter activity. Site mutation of mature miR-150 or mutation of P2X7R 3'-UTR at miR-150 binding sites both disrupted the miR-150 regulation, indicating the specificity of miR-150 on P2X7R repression. We also constructed an *a*denovirus to express miR-150. This virus significantly downregulated the endogenous P2X7R protein expression in E10 cells, and subsequently disrupted the surfactant secretion stimulated by E10 cell conditioned media. Our study is the first of its kind to demonstrate that miR-150 regulates P2X7R-mediated surfactant secretion in AEC II.

The last set of studies is a by-product derived from this dissertation research. Real-time PCR is a potential tool to examine gene expression in cells and organs. In this study, higher temperature peaks were observed in additional to the amplicon peak on the melting curve. Agarose gel and following DNA sequencing indicated that this was due to amplicon polymerization instead of nonspecific amplification. We also provided a method to distinguish between amplicon polymerization and nonspecific amplification.

In summary, our results demonstrated for the first time that PTN plays an important role in fetal lung development. It regulates fetal type II cell proliferation, migration and differentiation at least partly through β-catenin pathways. *In vivo* studies further confirmed that PTN influences the lung alveolorization by regulating cell proliferation and differentiation. Finally, miR-150 was identified as a regulator of surfactant secretion by targeting to P2X7R.

The American Physiological Society
9650 Rockville Pike, Bethesda, MD 20814-3991, USA
Publications Department Phone: (301) 634-7070
Fax: (301) 634-7243

November 4, 2009

Tingting Weng, B.S.
Lundberg-Kienlen Lung Biology & Toxicology Laboratory
Department of Physiological Sciences
Oklahoma State University
Stillwater, OK 74078

Dear Tingting Weng:

The American Physiological Society grants you permission to use the following *American Journal of Physiology Lung Cellular and Molecular Physiology* article in your PhD thesis for Oklahoma State University:

Tingting Weng, Zhongming Chen, Nili Jin, Li Gao, and Lin Liu
Gene expression profiling identifies regulatory pathways involved in the late stage of rat fetal lung development
Am J Physiol Lung Cell Mol Physiol 291: L1027-L1037, 2006. First published June 23, 2006; doi:10.1152/ajplung.00435.2005

Copies of your thesis may be produced and sold on demand, but free internet downloads of the *Am J Physiol Lung Cell Mol Physiol* article may not be provided. You may make a free link from the APS Journal to a web site of your choice since the article is over twelve months from its print publishing date.

The American Physiological Society publication must be credited as the source with the words "used with permission" added when referencing the *Am J Physiol Lung Cell Mol Physiol* article.

Sincerely,

Rita Scheman

Ms. Rita Scheman
Director of Publications
The American Physiological Society

RS/pr

.

VITA

Tingting Weng

Candidate for the Degree of Doctor of philosophy

Thesis: The role of Pleiotrophin and microRNA-150 in fetal lung development and functions.

Major Field: Veterinary Biomedical Sciences (Physiology)

Biographical:

EDUCATION:

Bachelor of Science, University of Science & Technology of China, China, Sep. 1998-Jul.2003

Ph.D: Completed the requirement for Doctor of Philosophy degree with major in Veterinary Biomedical Sciences (Physiology) at Oklahoma State University, December, 2009.

EXPERIENCE:

Junior Research Fellow (Jan 2002-July 2003)

Research Associate (Aug 2003-Sep, 2009)

PROFESSIONAL MEMBERSHIPS:

American Physiological Society

American Association for Advancement of Science (AAAS)

Name: Tingting Weng Date of Degree: December, 2009

Institution: Oklahoma State University Location: Stillwater, Oklahoma

Title of Study: The role of pleiotrophin and microRNA-150 in fetal lung development and functions.

Pages in Study: 125 Candidate for the Degree of Doctor of Philosophy

Major Field: Veterinary Biomedical Sciences (Physiology)

Scope and Method of Study:

The present study was initiated to identify novel growth factors which regulate the fetal lung development. A loop-designed DNA microarray was used to examine the changed gene expression on embryonic day 18, 19, 20, 21, newborn and adult. From DNA microarray, we identified pleiotrophin (PTN) as a growth factor which is involved in AEC II differentiation during fetal lung development. Functional studies were carried out to examine the role of PTN on primary fetal AEC II proliferation, migration and trans-differentiation. The signaling pathway of PTN through RPTPβ/ζ and beta-catenin was also determined by measuring β-catenin tyrosine phosphorylation and nuclear translocation. PTN was silenced on fetal lung organ culture using RNA interference to check the role of PTN on lung branching morphogenesis. Furthermore, PTN knockout mice were used to examine the role of PTN on fetal lung development *in vivo*. P2X7R is previously identified to mediate surfactant secretion from AEC II. Finally, we examined how miR-150 regulates surfactant secretion via P2X7R.

Findings and Conclusions:

1. The expression of 583 genes were significantly changed during the fetal lung development with >2 fold changes between at least two time points and CV <0.5.
2. K-means cluster analysis identified 7 different expression patterns.
3. The gene expression of one cluster was verified using real-time PCR with 88% consistency with microarray data.
4. PTN was localized in the mesenchymal cells surrounding the developing epithelium and blood vessel.
5. PTN promoted the fetal AEC II proliferation and migration, but inhibited the fetal AEC II trans-differentiation into AEC I.
6. Silencing of PTN expression affects the lung branching morphogenesis on fetal lung organ culture.
7. PTN increased the tyrosine phosphorylation of β-catenin, promoted β-catenin translocation into the nucleus and activated TCF/LEF transcription factors.
8. The activation of PTN/β-catenin pathway decreased endogenous dlk1 expression, inhibited the Dlk1 promoter activity and the binding of β-catenin to the Dlk1 promoter.
9. $PTN^{-/-}$ mice had no abnormalities during fetal and early postnatal stages.
10. On postnatal day 15 and 35, the lungs of $PTN^{-/-}$ mice showed hyperplasia with smaller alveoli and thicker septa.
11. On postnatal day 15 and 35, the expression of SP-A, -B, -C, CC10 and α-SMA were upregulated in $PTN^{-/-}$ lung, while T1-α and P2X7R were downregulated .
12. 3'-UTR dual-luciferase assay identified miR-150 as a regulator of P2X7R in lung epithelial cells.
13. The regulation of miR-150 was disrupted by mutation of miR-150 or P2X7R 3'UTR at miR-150 binding site.
14. Pre-treating E10 cells with adenovirus expressing miR-150 disrupted the surfactant secretion stimulated by E10 cell conditioned media.

ADVISER'S APPROVAL Dr. Lin Liu